Onlay grafts for alveolar bone augmentation

Khadijeh Al-Abedalla

Faculty of Dentistry

McGill University, Montreal

Submitted: 15th of April, 2014.

Submitted to McGill University in partial fulfillment of the requirements for the degree of

Master of Sciences, Dental Sciences.

Dedicated to my family for their endless support, love, and encouragement.
Thank you all for giving me strength to chase my dreams.

"*Life isn't about waiting for the storm to pass; it's about learning to dance in the rain*."

Vivian Greene

Abstract

==========

Dental implants are a successful and predictable treatment for partially and fully edentulous patients. However, they require sufficient volume of healthy bone for stabilization and long-term success. Lack of bone volume prevents implant placement and it is usually due to many reasons such as tooth loss, trauma or diseases. A variety of surgical techniques are available for alveolar bone rehabilitation. However, bone onlay augmentation is the most reliable and commonly used one. Different bone grafts can be used for bone onlay augmentation. Autograft onlays are currently the gold standard onlay grafts because of their osteoinductive, osteoconductive, and osteogenic properties. However, due to their limitations and drawbacks, some of which are considered severe, alternative materials have been developed including allografts, xenografts, and alloplastic bone grafts. Although previous reports demonstrated high success rate of implants placed in bone augmented with allograft onlays, evidence based articles are still needed to prove these results. On the other hand, due to some concerns about the antigenicity of allografts and xenografts onlays, synthetic materials such as monetite onlays have been developed for bone augmentation *in vivo*. Nonetheless, these synthetic onlays were still inferior to autograft onlays. Therefore, this thesis has two main objectives. Firstly, to clinically assess the performance of freeze-dried allograft in bone augmentation and implant treatment. Secondly, to improve the capability of synthetic onlays in bone regeneration, then assess their performance in bone augmentation and implant treatment *in vivo*.

By conducting two cohort studies: clinical and histological, we proved that bone augmented with allograft onlays is similar to native alveolar bone in terms of bone quality and

quantity. Moreover, we showed that implants placed in bone augmented with allograft onlays have rates of success and survival similar to implants placed in either bone augmented with autograft onlays or native alveolar bone. We also demonstrated that customizing the morphology of monetite synthetic onlays according to the metabolic activity of the recipient site *in vivo* can enhance bone formation, monetite resorption, bone height and implant osseointegration.

Our results showed that allograft onlays could replace autograft onlays with similar clinical results. It was also observed that designing the macropore geometry according to the bone metabolic activity was a key parameter in increasing the volume of bone augmented within synthetic monetite onlays. However, further studies are needed to optimize the osteoconductivity of these synthetic onlays in order to be able to replace the autograft and allograft onlays in the future.

Résumé

==========

Les implants dentaires sont un traitement efficace et prévisible pour les patients partiellement et complètement édentés. Cependant, ils nécessitent un volume suffisant de l'os sain pour la stabilisation et le succès à long terme. Le manque du volume osseux empêchant la pose des implants est généralement dû à plusieurs raisons, telles que la perte des dents, des traumatismes ou encore à maladies. Une variété de techniques chirurgicales sont disponibles pour la réhabilitation de l'os alvéolaire. Cependant, l'augmentation osseuse onlay est la technique la plus fiable et aussi la technique la plus utilisée. Différentes greffes osseuses peuvent être utilisées pour l'augmentation osseuse onlay. Les autogreffes onlays sont actuellement les greffes de choix en raison de leurs propriétés ostéoinductrice, ostéoconductrice et ostéogéniques. Toutefois, en raison de leurs limitations ainsi que de leurs inconvénients parfois graves, d'autres matériaux ont été développés pour des allogreffes, xénogreffes et alloplastique greffes. Bien que des rapports précédents ont démontré un taux de réussite élevé pour les implants placés dans l'os augmenté avec les allogreffes onlays, il serait encore requis de se référer à des articles basés sur des preuves scientifiques pour appuyer ces résultats. D'autre part, en raison de certaines préoccupations concernant l'antigénicité des allogreffes et des xénogreffes onlays, des matériaux synthétiques tels que le monétite onlay a été développé pour l'augmentation osseuse in-vivo. Néanmoins, ces onlays synthétiques sont encore inférieurs à l'autogreffe onlay. Par conséquence, cette thèse a deux objectifs principaux. Le premier objectif est de cliniquement évaluer la performance de l'allogreffe lyophilisée en augmentation osseuse et en traitement implantaire. Le deuxième objectif est d'améliorer la capacité des onlays synthétiques dans la régénération

osseuse, et ensuite d'évaluer leur performance en augmentation osseuse et en traitement implantaire in-vivo.

En effectuant deux études de cohortes : une étude clinique et une étude histologique, nous avons démontré que l'os augmenté avec allogreffe est similaire à l'os alvéolaire natif en terme de qualité et de quantité osseuse. De plus, nous avons démontré que les implants placés dans l'os augmenté par allogreffes onlays ont des taux de réussite et de survie semblables aux implants placés dans l'os augmenté par onlay autogreffe ou à l'os alvéolaire natif. Nous avons également démontré que la personnalisation de la morphologie des onlays de type monétite synthétique en fonction de l'activité métabolique du site récipiendaire in-vivo, peut améliorer la formation osseuse, la résorption du monétite, la hauteur de l'os ainsi que l'ostéointégration de l'implant.

Nos résultats ont démontré que les onlays d'allogreffes pourraient remplacer les onlays autogreffes avec des résultats cliniques similaires. Il a été également noté que la conception de la géométrie des macropores selon l'activité métabolique des os était un paramètre clé dans l'augmentation du volume osseux à l'intérieur de l'onlay monétite synthétique. Cependant, d'autres études sont nécessaires pour optimiser l'ostéoconductivité de ces onlays synthétiques afin d'être en mesure de remplacer les autogreffes et les allogreffes onlays dans l'avenir.

Acknowledgement

==========

First and foremost, I have to sincerely give my thanks and appreciation to my supervisor, Professor Faleh Tamimi, for being a tremendous mentor and his continuous guidance and support throughout my academic studies, and for allowing me to grow as a researcher. I would also like to thank my committee members, Professors Jake Barralet, Samer Abi Nader, Veronique Benhamou for their support and brilliant comments and suggestions. Also, I would like to thank Professor Jesus Torres and Professor Nach Daniel for their help and guidance in performing the surgical work presented herein.

Special thanks to my lab members and friends, Xixi Wu, Mohammad Nur Abdalla, Hazem Eimar, Huifang Sun, and Cui Cui for their understanding and encouragement in my many moments of this journey. Your friendship made my life a wonderful experience, and words cannot express how grateful I am to you all.

I am grateful as well for my aunt and uncle, who were like a second family here in Canada, and for their support and encouragement that would never end. Finally, I would like to thank my family and grandparents, for their support, love, and giving me the chance to reach for the stars. No one could ask better loving family. Your prayer for me was what sustained me thus far.

Contribution of Authors

==========

A brief summary of the involvement of the candidate and the co-authors in each of these manuscripts is given below.

1. Bone augmented with allograft onlays is comparable to the native alveolar bone in terms of quality, quantity and implant success rate. Khadijeh Al-Abedalla, Arthur Cortes, Jesus Torres, Xixi Wu, Samer Abi Nader, Nach Daniel, Faleh Tamimi.

The candidate wrote the manuscript and performed the histological, histomorphometrical, statistical analyses, and collected the data. All her work was done under the supervision of Professor Faleh Tamimi, who provided laboratory and scientific guidance, and was the principal investigator of the study. All authors reviewed the manuscript. Professors Jesus Torres, Arthur Cortes, Samer Abi Nader, and Nach Daniel were the responsible for the surgeries, prosthetic rehabilitations, and follow-up of the patients. The PhD candidate Xixi Wu aided in data collection and supervised the statistical analysis.

2. Osseointegration of Dental Implants in 3D Printed Synthetic Onlay Grafts Customized According to Bone Metabolic Activity in Recipient Site. Faleh Tamimi, Jesus Torres, Khadijeh Al-Abedalla, Enrique Lopez-Cabarcos, Mohammad H. Alkhraisat, David C. Bassett, Uwe Gbureck, Jake E. Barralet.

The candidate wrote the manuscript and performed all the histomorphometrical analysis and the XRD mapping. All her work was done under the supervision of Professor Faleh Tamimi, who provided scientific and technical guidance throughout the time of this study. He also prepared the

histological sections. Professor Jake Barralet was the principal investigator who provided valuable knowledge and guidance. Professors Jesus Torres, Enrique Lopez-Cabarcos, and Mohammad H. Alkhraisat were responsible for the *in vivo* surgical procedures and animal care. Professor David C. Bassett generated the 3D designs of the onlays using the Computer Aided-Design technique. The monetite blocks were 3D-printed in Professor Uwe Gbureck's laboratory. All authors reviewed the manuscript.

Table of Contents

==========

List of Figures

==========

histomorphometrical analysis. **(e)** Results of the local histomorphometrical analysis of bone volume in each square in the grid. (*) Indicates that there is significant difference among the designs (p value < 0.05).

(a-h) Results of the local histomorphometrical measurements of bone infiltration in each row and column in the grid for each specific design (Figure 5.5). (*) Indicates that there is a significant difference between columns and rows of each design (p value < 0.05).

Interpolated maps of the histomorphometrical results in (Figure 5.5): **(a)** the averaged distribution of the newly formed bone in the onlays of the four designs. Red and orange colours show intense bone growth. Yellow and greens colours indicate moderate new bone formation, while blue and black indicate low bone formation in the onlays. **(b)** Distribution of the remained material within the onlays of the different designs. Red and orange colours show concentrated remaining material. Yellow and greens colours indicate moderate material, while blue and black indicate low material left in the onlays.

Local histomorphometrical measurements of the coronal histological cross sections in (Figure 5.5), using 8 x 1 computer generated grid adjusted to divide the area of the onlays into 8 smaller areas (1mm x 4mm), showing the average maximum height of bone growth within the onlays

Interpolated maps of the XRD phase analysis demonstrating the distribution of **(a)** apatite crystals (bone) and **(b)** monetite crystals across the onlays. The red and blue colours indicate high concentrations of material crystals, while the white colour indicates low concentration of both materials. **(c,d)** XRD patterns of the remaining material (apatite (bone) and monetite) within the onlay, demonstrating the materials intensity according to the diffraction angle 2θ

List of Tables

==========

Chapter one: Introduction

==========

1.1 Thesis outline

This thesis includes a literature review and 2 manuscripts, the first one entitled by "**Bone augmented with allograft onlays is comparable to the native alveolar bone in terms of quality, quantity and implant success rate"** is under preparation for publication, and the second one entitled by "**Osseointegration of Dental Implants in 3D Printed Synthetic Onlay Grafts Customized According to Bone Metabolic Activity in Recipient Site"** has been accepted for publication in the journal "Biomaterials".

1.2 Research Rationale

Onlay bone augmentation is the most predictable procedure for bone reconstruction prior to dental implant placement [1]. Bone grafts used with this method include autografts, allografts, xenografts, and alloplastic bone grafts. Although autograft onlays have high implant success rate, they also have high complication rate involving the bone harvesting procedures [2]. For this reason, bone substitutes are being developed to overcome autografts' limitations. Allograft onlays are commonly the second choice in situations where autografts cannot be used [3]. Despite the high success rate that was reported using these onlays, there is no evidence supporting the use of these materials as comparable substitutes to autografts [3-5].

The disadvantage of using allograft and xenograft onlays is their possible antigenicity that requires extensive processing and sterilization which lowers their mechanical properties [6, 7]. Therefore, a better alternative to autografts would be alloplastic bone grafts. Although many

studies have shown the efficacy of calcium phosphate based materials such as monetite in bone augmentation *in vivo*, they are still inferior to autograft onlays [8-10]. Thus, the properties of these bone substitutes in onlay bone augmentation need to be improved in order to replace autograft onlays.

Chapter two: Literature Review

==========

2.1 Implant osseointegration

Brånemark firstly described the term osseointegration as the direct structural and functional contact between living bone and an implant surface [11-13], after a healing period of 3-6 months [14]. This term usually applies to dental implants that have a root form connection or fixture [15]. There are three main biological phases that happen during osseointegration: haemostasis, inflammatory phase, and remodeling phase (details underneath) [16]. These phases are similar to bone repair mechanism that will be described later in the bone section [17-19].

2.1.1 Haemostasis

Haemostasis (exudative phase) begins with the surgical insertion of dental implants. The duration of this phase is minutes to hours. After implant placement, a layer of water molecules forms around the implant surface [20]. This layer facilitates protein absorption on the implant surface [21, 22], and continues till the implant surface is covered by a layer of extracellular matrix proteins. The composition of this protein layer depends upon the type of implant's surface [23]. Subsequently, through protein absorption, cells are able to attach to the implant surface initiating cellular adhesion, migration, and differentiation. This migration is a result of the released bone morphogenetic proteins (BMPs) in response to the surgical placement of the dental implants [16].

2.1.2 Inflammatory phase

The inflammatory phase begins approximately after 10 min and lasts from few hours to several days [24, 25]. This stage is mainly regulated by the extracellular matrix (ECM) proteins and growth factors [24, 25]. Multipotent mesenchymal cells are the first cells to migrate at the implant surface, then they differentiate into osteoblasts depending upon local oxygen tension [26], availability of nutrients, and local regulatory growth factors [27]. Oxygen concentration in the implant site has a critical role in cell migration. Broken capillaries in the surgical site might affect oxygen concentration which leads to local ischemia and necrosis [28]. Following the resorption of necrotic bone by the neutrophils and macrophages, matrix mineralization and remodeling occurs [29, 30]. One week after implant placement, the osseous matrix can be observed on the implant surface [30]. After 4 weeks, there will be an intimate contact between the implant surface and bone tissue.

2.1.3 Remodeling phase

The type of bone that initially forms is woven bone, and then during this remodeling phase, woven bone is removed by osteoclasts and replaced by lamellar bone [29]. Osteoclasts start to create space for new bone formation at the expense of removing primary bone implant contact. This phase can last several years until most woven bone and old bone from the primary bone contact is replaced by the newly formed lamellar bone.

2.2 Dental implants

Teeth may be lost due to many reasons such as dental diseases, trauma, surgery, or they can also be absent due to congenital reasons [31, 32]. Missing teeth can cause function, speech,

and aesthetics problems [2, 33]. The dental rehabilitation of single or multiple missing teeth with dental implants is often the best treatment option to restore oral aesthetics and function with predictable and reliable long-term results [34-36].

Osseointegration can retain implants placed in the alveolar bone allowing them to support dental prostheses. However, successful osseointegration requires implant stability [37]. Implant stability can be divided into two parts: primary and secondary [18]. Primary stability is mainly from the mechanical anchoring of the implants into the alveolar bone at the moment of surgery [38, 39]. Secondary stability gradually replaces the primary stability and it takes place as bone remodeling and osseointegration occurs during early wound healing [40, 41]. Therefore, Implants' long-term success is largely determined by the sufficient volume (quality and quantity) and location of residual alveolar bone to be stabilized at the recipient site [42-44].

Dental implants are available in different diameters, lengths, platforms, and surface modifications [45]. The materials used to fabricate dental implants include metals, alloys, ceramics, carbon, and polymers [46]; however, Titanium (Ti) or Ti-aluminum-vanadium alloys are currently the material of choice for dental implants.

Implant design is an important factor that can also affect their osseointegration and clinical performance in the oral cavity [47-50]. Implants' anchoring part was originally fabricated as cylindrical screws that turned out to be inappropriate for many clinical situations [51]. Therefore, tapered implants were developed to resemble the root form of natural teeth; this renders the implants more aesthetic and facilitates their placement between natural teeth [51]. Implants can have different surface morphologies, which can be either rough or machined (smooth or polished) [52]. Different processes can be used to fabricate rough implant surfaces such as acid etching, sandblasting, titanium plasma spraying, and hydroxyapatite coating [53].

Rough surfaces increase bone to implant contact by inducing bone growth and facilitating the attachment of cells on the implant's surface [54].

Implant success rate is described based on a combination of criteria, previously proposed by Albrektsson et al. in 1986, then updated by others such as Buser et al. in 1997 and Karoussis et al. in 2004 [34, 55, 56]. These criteria include:

- Absence of implants mobility [57].
- Absence of any continuous subjective complaints, including pain, foreign body sensation and/or dysaesthesia [57].
- Absence of recurrent infection surrounding the implant with suppuration [57].
- Absence of a persistent radiolucency around the implant [57].
- Pocket depth of no more or equal to 5mm [58].
- No bleeding on probing [58].
- A 1.5mm of vertical bone resorption is accepted during the first year of function, after that, the annual vertical bone loss should not exceed 0.2mm mesially or distally [34].

Studies have shown that the cumulative success of implants placed in the native alveolar bone ranges from 89% to 98.9% after follow-up periods of 3 to 15 years [1].

2.3 Bone

2.3.1 Bone structure and function

Bone is composed of both organic and inorganic material. The organic component compromises 30% of bone volume, and consists of collagen and non-collagen proteins, as well as bone cells [59]. The major constituent of the organic bone matrix is type I collagen, while remaining proteins include osteocalcin, osteonectin, fibronectin, osteopontin, and bone

sialoproteins [60]. All these proteins in the organic matrix have various functions in bone formation. The inorganic component compromises 60% of bone volume, and consist of mainly apatite calcium phosphate crystals [59]. Water compromises 10% of bone volume [59]. The inorganic phase also contains carbonate and small amounts of sodium, magnesium, and other trace elements [61]. The arrangement of these components provides bone with a hierarchical structure that contributes in making the high strength and self-repairing properties of bone [62].

Three major different cell types are found within bone tissue [63]:

1) Osteoblasts, which arise from multipotent mesenchymal stem cells [64], and produce bone matrix and regulate the osteoclasts' activity and differentiation [65].

2) Osteoclasts are large multinucleated cells (fused monocytes) that resorb bone tissue, and responsible of the turnover bone cycles [66].

3) Osteocytes account for 90% of bone cells in the adult skeleton. They are the imbedded form of osteoblasts, where they create an extensive interconnecting network of cellular communication [67].

The main functions of bone include support, movement, structure and protection [68]. Moreover, bone also plays a critical role in mineral and ion as well as in blood cell production [68]. Bone can be divided according to its structure into cortical bone, which is the outer dense part of bone, and cancellous bone (trabecular bone), which is the spongy inner part of bone.

2.3.2 Bone repair

Bone repair is a complex process where many factors contribute in its events such as cells, cellular signals, and extracellular matrix [69-71]. The cells that play major roles in this process are inflammatory cells, vascular cells, osteochondral progenitor cells, and osteoclasts

[72-74]. Other key players of these events include pro-inflammatory cytokines, growth factors, pro-osteogenic factors, and angiogenic factors [75]. In endochondral bone formation, bone repair consists of overlapped four histological stages: Inflammation, soft callus formation, hard callus formation, and bone remodeling. In intramembranous bone formation, there is no need for a cartilaginous tissue before bone formation, so the hard callus formation stage follows the inflammation stage directly.

2.3.2.1 Inflammation

The disruption of local tissues and normal vascular function leads to bleeding and the development of a hematoma. Following the production of a blood clot, inflammatory cells including macrophages, platelets, lymphocytes, and monocytes infiltrate the hematoma and start to fight against any infection by secreting cytokines and growth factors, [70, 71]. These factors and cytokines help in recruiting mesenchymal stem cells stimulating cells' growth and/or differentiation.

2.3.2.2 Soft callus (fibrocartilage) formation

Most healing sites are preceded by cartilaginous formation [71]. Fibroblasts and chondrocytes are mostly seen in this stage; where they build a soft callus tissue to primary stabilize the healing site. Growth factors stimulate chondrocytes to form ECM proteins particularly collagen type II. Consequently, the site is infiltrated by vascular endothelial cells forming large blood vessels.

2.3.2.3 Hard callus formation

This stage is also known as the primary bone formation stage [71], because it's the phase in which active osteogenesis occurs. This stage depends mostly on the vascular tissue that increases the level of oxygen allowing osteoblastic differentiation [76, 77]. Osteoblasts start the formation of mineralized bone matrix at the peripheral sites of the soft callus resulting in the formation of a hard callus that substitutes the degrading soft callus gradually.

2.3.2.4 Bone remodeling

This stage can also be termed as the secondary bone formation [71], and it involves converting the irregular woven bone callus into lamellar bone. Osteoclasts play a major role in this stage by resorbing the old woven bone [66, 78]. Eventually, the original geometry and function of the damaged tissue is restored.

2.3.3 Alveolar bone loss

Various reasons might lead to the loss or atrophy of alveolar bone as a result of trauma, surgical resection, denture-induced atrophy, tooth loss, congenital alveolar defects, or infectious diseases such as advanced periodontitis [79, 80]. The resorption pattern in the maxilla is usually different from the mandible [81], where in the maxilla, the buccal plate of the alveolar ridge tends to resorb faster than the labial wall, causing the atrophic residual ridge to be significantly palatal to the prosthetic tooth position. However, in the mandible, the lingual plate resorbs prior to the buccal one. In both situations, the horizontal dimension of the alveolar bone ridge is compromised earlier than its vertical one [82].

Alveolar bone loss results in inadequate alveolar ridge dimensions that might hinder dental implant placement or cause an unfavorable inter-arch relationship, which might affect the aesthetic and function of the dental treatment [34, 83]. Therefore, bone regeneration is often needed in order to restore the esthetics and function of the jaws.

2.3.4 Bone repair techniques

Numerous bone repair procedures have been described in the literature to reconstruct both the height and width of the alveolar ridge in order to achieve sufficient ridge volume for adequate implant placement and prosthodontic rehabilitation [84]. These techniques include distraction osteogenesis (DO), guided bone regeneration (GBR), bone block grafts, ridge splitting or expansion, osteotomies of the ridge or the jaws, or a combination of the above [85, 86]. Every surgical procedure has its advantages and disadvantages.

The choice of a particular technique should depend on the anatomical situation, the need for horizontal or vertical augmentation, the expected outcome and complication rate, the clinician or patient preference, and the type of prosthesis [87]. However, it is still not clear yet which procedure offers a better outcome for each particular clinical situation [85].

Bone repair techniques can be used to restore the alveolar ridge horizontally, vertically, or both. Vertical augmentation techniques were reported to have higher complication rates that ranges between 20 and 60% compared to horizontal augmentation methods [88, 89]. Several materials may be used in the aforementioned procedures, including autografts, allografts, xenografts, and alloplasts, as well as different barrier membranes, osteosynthesis materials or a combination of the above [84].

2.3.4.1 Distraction osteogenesis (DO)

Distraction osteogenesis is a technique that was developed by Llizarov and has been recently introduced to oral surgery and implantology [90, 91]. During this procedure, the bone is fractured into two bony segments. The two segments then gradually are moved apart during the distraction phase, allowing new bone to form in the gap.[90]. During the displacement of the fractured bony parts, a gap is filled with non-calcified immature bone tissue that matures later after a subsequent fixation period.

Implants placed in bone augmented with DO are associated with high implant survival rate (up to 100%) [88]. However, bone stability overtime is controversial and the rate of often severe complications might reach up to 75% [42, 92]. These complications vary from infection of the distraction chamber, fractures of the distractor, premature or delayed consolidation, fibrous non-union, resorption of the transported fragment, neurological alterations, deviations from the correct distraction vector, soft tissue dehiscence, and fractures of transported or basal [93, 94]. For these reasons, the use of intra-oral distraction osteogenesis is limited.

Although the highest vertical bone increase was documented using this method [95], sometimes it is impossible to use due to anatomical limitations such as the nasal cavity, the maxillary sinus, and the mandibular inferior alveolar nerve that may need bone grafting instead [96].

2.3.4.2 Guided bone regeneration (GBR)

In this technique that was first applied in dentistry early in the 1990s, membranes with or without bone grafts are used to protect defects from the ingrowth of soft tissue that can disturb or prevent bone healing [97]. The wide variety of membranes used in this technique is classified

into resorbable and non-resorbable [98]. Although, survival rate of implants placed along with this procedure is usually high, with an average of 92% in implants placed after horizontal bone augmentation and 98.9% in those placed after vertical bone augmentation, the complication rate can reach up to 45.5% [92, 99].

2.3.4.3 Inlay bone augmentation

Inlay bone augmentation (osteotomy) is a technique where a part of the jawbone is surgically separated into two bony sections then a bone graft material is placed (sandwiched) between the separated bony sections [100, 101]. This technique has high implant survival and success rate with low resorption rate [100, 102]. However, this technique cannot be applied for thin ridges and when the alveolar ridge height is less than 5 mm from the inferior mandibular nerve [103]. In addition this technique is associated with complications such as bone fracture and dissection of inferior alveolar never which the surgeon should consider before using this method for bone augmentation [103, 104].

2.3.4.4 Onlay bone augmentation

Onlay bone grafting is a reliable technique that can be used for the correction of both vertical and horizontal (less than 4 mm) alveolar bone defects with bone blocks to allow the placement of dental implants [82, 105]. In this procedure, after the surgical exposure of the defective area, the host bed is usually perforated with a small bur to improve the integration between the graft and recipient bed and to enhance the vascularization of the bone graft [106]. Subsequently, the onlay is fixed with screws (titanium or resorbable), plates, or dental implants [106]. Afterwards a barrier membrane can be used to reduce the resorption of block bone grafts

and improve graft integration, although the benefit of these barriers remains questionable [107]. Different studies have found that membranes could improve the graft healing while others showed that there is no difference in graft resorption whether covered by a membrane or not [108].

One unique advantage of onlay bone augmentation is that in some clinical situations it can be carried out simultaneously with implant insertion (one-stage procedure), whereas in the other techniques, a healing period of the alveolar ridge is often needed (two-stage procedure) [87]. Nonetheless, the two-stage procedure is usually preferred because the healing period ensures the stability of the augmented bone and the surrounding soft tissues, resulting in a higher implant survival rate [109, 110].

In addition, onlay bone augmentation is commonly used when there are anatomical limitations including the nasal and paranasal cavities (maxillary sinuses) in the maxilla and the inferior alveolar nerve in the mandible that contradict the use of other techniques [111]. Therefore, this technique can provide a safer option to place dental implants.

In the literature, it has been reported that high implant survival rate can be achieved using onlay bone grafting techniques ranging from 76% to 100%, and implant success rate that reaches 100% at 12 months and 89.5% at 5 years [112, 113]. On the other hand, complications seem to be substantially less frequent than with previously mentioned techniques, with a complication rate of 6%- 32% [114, 115]. Unfortunately, these studies have limited sample size are still and do not provide extensive information on the success rate of dental implants placed in bone augmented with onlay grafts and the associated risk factors.

2.4 Bone grafts

A bone graft is defined as any implanted biomaterial that promotes or facilitates bone healing [116]. Bone grafts can be incorporated in the modeling process of bone growth. These graft materials can promote bone healing through three different mechanisms: osteoconduction, osteoinduction, and osteogenesis [117].

- Osteoconduction: Osteoconduction means directing bone forming activity to a particular site or surface serving as scaffold for bone cells to attach and grow. In other words, these materials act as supporting scaffolds that facilitate bony ingrowth from the existing bone, but cannot induce bone formation. However, osteoconductive materials require the presence of bone or differentiated mesenchymal cells [118-120] and cannot produce bone if placed in soft tissues.
- Osteoinduction: osteoinduction involves the recruitment of mesenchymal stem cells to differentiate into mature bone cells. Osteoinductive materials are materials that can induce mesenchymal cells differentiation into osteoblasts or chondroblasts, thus, enhancing bone growth. This mechanism is dependent on some specific proteins such as bone morphogenic proteins (BMPs) [121].
- Osteogenesis: osteogenesis refers to the stimulation of osteoprogenitor cell proliferation and osteoblast biosynthetic activity. In other words, it refers to the ability of the graft to produce new bone. This process is dependent on the presence of living bone cells; therefore, osteogenic grafts are grafts that contain osteogenic cells such as osteoblasts or progenitor cells, thus, they are capable of forming bone directly from osteoblasts [121]. Grafts that have osteogenic potential can also be considered osteoinductive and osteoconductive.

2.5 Implant placement in bone grafts

Placement of dental implants can be performed either in combination with graft fixation (one-stage surgery) or in a later surgical stage after the healing period of the bone graft (two-stage surgery) [109, 110]. Although enough time should elapse for graft incorporation, implants should be inserted early enough to stimulate and maintain the regenerated bone. The implant site is often at the junction between the block and host bone; therefore, the surgeon should be careful not to displace the block from the ridge during implant placement [87].

2.6 Types of bone grafts onlays

2.6.1 Autograft onlays

Autograft bone onlays are bone grafts obtained from one anatomic site that are transferred to another site within the same subject [116], and they were first introduced to dentistry by Davis et al. to augment the alveolar ridge [122]. Similar to alveolar bone, autografts are composed of organic and inorganic structures that provide good mechanical properties. Autografts are osteoinductive, osteoconductive and have osteogenic potential because they contain osteoblastic and predecessor cells that are capable of forming new bone; therefore, they are considered the gold standard of bone grafts [123].

Bone augmented with autografts heals during three overlapping phases [121]. The first phase one lasts for 4 weeks, and includes the formation of osteoid tissue by the surviving cells in the graft (osteogenesis) [121]. The second phase is the osteoinduction phase that starts 2 weeks after the surgical grafting. At this stage blood vessels and host tissues invade the bone graft, leading to new bone formation and graft resorption [68, 118]. The BMPs, released from the bone graft as it resorbs, mediate this second phase [121]. The third phase is similar to osteoconduction

mechanism, where inorganic component of the graft acts as a source of minerals for bone formation [121].

Onlay bone augmentation using autogenous bone grafts is a predictable, reliable, and commonly used technique that allows implant placement in atrophied alveolar ridges [2]. Success rate of implants placed in bone augmented with autogenous onlays ranges between 73 to 97% for follow-up periods of up to 10 years [1]. The most frequent complications with autograft onlays are soft tissue dehiscence and graft resorption with an overall complication rate that ranges between 9-21% [2]. The resorption rate is higher during the first three years after function and might reach up to 40%, but becomes stable afterwards [124].

Autograft onlays can be either harvested from extraoral (the calvaria, iliac crest, tibia, ulna and radius bones) or intraoral (the symphysis and ramus of the mandible) sites. Intraoral donor sites can be used in situations where small-sized grafts are required, and extraoral sites, such as the iliac bone, are used when larger sized grafts are required. Since the harvesting procedure from the donor sites requires an additional surgery, this causes many complications that limit the use of autogenous bone grafts [87]. These drawbacks include limited availability of bone to harvest and donor site morbidity [87]. The complications that should be considered when using this type of bone graft include injury to local nerves, pain, pulpal injury, wound healing problems, blood loss, altered facial contour, and bone fracture [87]. Therefore, patients often prefer other bone substitute to the autograft onlays [2].

2.6.2 Allograft onlays

Allogeneic bone grafts are homografts harvested from cadaveric sources, and are successively processed and stored in different ways. Their main advantage as alternatives to

autografts is that they eliminate the need of the harvesting surgery, and the drawbacks that come with it. Allografts are available as cortical, cancellous, or corticocancellous grafts [125], and according to their processing techniques, there are three main types of allografts: frozen, freeze-dried (lyophilized), and demineralized freeze-dried bone grafts [126, 127]. Besides the above-mentioned techniques allografts can also undergo additional processing in order to reduce their antigenicity such as gamma radiation, ethylene oxide, or hydrogen peroxide. Although these processing techniques can ensure the safety of allograft usage, they still affect the mechanical and structural properties of these materials. Despite all these procedures to reduce the allograft antigenicity, they still raise some concerns regarding their risk of disease transmission, especially with the fresh type of these grafts [128, 129].

Allografts are mainly osteoconductive. They provide structural support and allow bone ingrowth within their scaffolds, and consequently they achieve good integration with the host recipient bone [130]. However, depending on their processing methods they can also be osteoinductive as well [131, 132]. Indeed, bone augmented with allograft onlays can undergo regeneration through both intramembranous ossification and de novo apposition, indicating their osteoinductivity [133]. Complications with allograft similar to autografts [4] and include graft fracture, lack of integration with surrounding peripheral bone, and infection [134, 135], although the main complication is usually soft tissue dehiscence [4]. Below we describe in details the main types of allografts:

2.6.2.1 Fresh frozen onlays

Frozen allografts are homografts prepared by immediate freezing to -80C° [136]. The use of fresh-frozen bone allograft has been accounted for about one third of the bone grafts used in

dentistry and orthopedics in the United States [137]. Fresh frozen allografts can achieve good integration and vascularization throughout the onlays [7, 138]. The use of fresh-frozen onlays provides an adequate treatment method for atrophied alveolar ridges [7, 138]. Nonetheless, even with the development of bone banks, harvesting guidelines, and screening methods, the antigenicity of this material is still debatable and more long-term and histological studies are needed to confirm their safety in bone augmentation procedures [138-140].

2.6.2.2 Demineralized freeze-dried bone allografts

Demineralization of allografts was performed to allow the BMPs to stimulate bone growth [141]. *In vivo* studies have shown that demineralized freeze-dried bone allografts have osteogenic potential [142, 143]. Bone formation in demineralized freeze-dried bone allografts appears to be age dependent, since it is higher in younger animals compared to older ones [144, 145]. This type of allografts has been used clinically for bone augmentation; however, similar to fresh frozen allograft, these onlays also present some histological evidence of inflammatory infiltration [146].

2.6.2.3Freeze-dried onlays

Freeze-dried allografts are prepared by freezing, and then dehydrating bone allografts to approximately 5% of water content. Although freeze-dried forms of allografts are prone to microfracture and are weak after rehydration, the use of these materials has recently increased [147]. This is the material of interest in our clinical study, because compared to other allografts, freeze-dried allografts have several advantages such as longer shelf life and less antigenicity [148, 149].

Currently freeze-dried allograft blocks or onlays are widely used in the orthopedic surgery, and have recently been introduced for maxillofacial surgery [4, 150]. High implant success rate can be achieved in bone augmented with allograft onlays[151-155]. However, the quality of bone augmented with these onlays, as well as the long-term success rates of subsequently inserted implants is not well known [4]. Therefore, the clinical performance of these onlays compared to autografts is still questionable.

2.6.3 Xenografts

Xenografts are grafts derived from a different species (animals). Currently, the two main sources of xenografts are bovine or porcine [156]. Xenografts can be either used alone or with other types of bone grafts [157, 158]. They are only osteoconductive; therefore, they act only as a scaffold allowing the ingrowth of osteoblasts [159, 160]. Xenografts present a slow resorption rate compared to other grafting materials that might reach up to 4 years [161, 162].

Although these materials have reported a successful clinical performance in bone regeneration and sinus left procedures [163, 164], there is still a controversy in the literature about their osteoconductivity. This might be because of their low resorption rate that causes the graft material to be encapsulated by connective tissue and achieve low bone volume [165]. In addition to the before-mentioned limitations, there have been concerns regarding their histocompatibility mismatch and disease transmission between human's native alveolar bone and xenografts [166, 167]. However, long-term studies are needed for further investigation regarding their performance and safety [165].

2.6.4 Alloplastic onlays

These are osteoconductive synthetic materials that allow bone formation by providing a physical framework for bone ingrowth [130, 168]. In addition, depending on the type of the synthetic material and its chemical composition, they can also be osteoinductive [130, 168]. They come in a variety of shapes, sizes, and texture, and vary greatly in their resorption properties [130, 168].

Patients prefer synthetic bone replacement materials to autologous bone grafts, because they can be pre-fabricated to fit the defect areas of the alveolar ridges and provide reproducible results. Underneath we describe the most relevant alloplastic materials:

2.6.4.1 Polymers:

A polymer is a large molecule, or macromolecule, composed of many repeated subunits, known as monomers. Several natural or synthetic polymers have been used in medicine and dentistry [169, 170]. Synthetic polymers can be used in form of scaffolds for bone and cartilage regeneration [169, 171, 172]. There are various types of synthetic polymers that can be either resorbable or non-resorbable materials.

Resorbable polymers have been used clinically as growth factors for delivering scaffolds or they can be manufactured into various forms to fit deficient or fractured bones, such as poly (lactide-co-glycolide) (PLGA) [169, 173, 174]. PLGA is the most popular biodegradable polymer, because it has higher mechanical properties and adjustable degradation rates compared to other polymers [175-178]. However, there are many disadvantages that limit their usage in bone augmentation including their rapid resorption rate that affects their mechanical properties

[116]; therefore, they cannot be utilized for load bearing applications [179, 180]. In addition, they can induce foreign body reactions due to their degradation products [181, 182].

The clinical use of non-resorbable synthetically produced polymers started in the 1960s as disposable equipments, such as syringes and catheters [183]. Compared to metallic or ceramic materials, the advantages of non-resorbable polymers are their reasonable cost and their availability in a wide range of physical and mechanical properties [183]. Non-resorbable synthetic polymers such as polymethylmethacrylate (PMMA) can also be used as acrylic bone cements for implant fixation and as a filling material [183]. However, their exothermic polymerization reaction might damage the adjacent tissues [183].

2.6.4.2 Bioactive glasses

Bioactive glasses are made from calcium salts, phosphate, sodium salts, and silicon. They are a unique graft material because they actually bind to the host bone tissue through the development of a surface layer of carbonated apatite [184-186]. After their exposure to body fluids, a double layer formed of calcium phosphate-rich and silica gel covers the bioactive glass materials and promotes the adsorption of proteins [187]. These proteins are utilized by osteoblasts to form a mineralized extracellular matrix [187]. Although these materials might promote osteogenesis, and rapid bone formation [188], in some clinical situations they showed low performance in bone healing, due to connective tissue encapsulation of the graft material [189, 190].

2.6.4.3 Calcium Sulfate

Generally known as Plaster of Paris, or gypsum. Calcium sulfate was firstly used for bone regeneration by Dreesman [191], and has been used for more than 100 years as a filling material for osseous defects [3, 192]. Calcium sulfates are osteoconductive materials that present good clinical performance in bone regeneration [193, 194], and are commercially available either alone or mixed with other materials. However, they have a high resorption rate, which may cause an imbalance between the material resorption and bone formation. In addition, they have low mechanical properties compared to other calcium phosphate compounds [3].

2.6.4.4 Apatites

There are many types of apatite materials that differ by their chemical and physical characteristics. One of the commonly used apatite in bone regeneration is hydroxyapatite ($Ca_{10}(PO_4)_6(OH)_2$) , which is a calcium phosphate mineral with a calcium-to-phosphorus ratio of 10:6 [195, 196]. Hydroxyapatite is osteoconductive, but not osteogenic nor osteoinductive [195, 196]. Synthetic apatites do not induce any foreign body response and have been successfully used clinically for bone augmentation [157, 197-202]. However, depending on the manufacturing process, apatites can be either nonresorbable [203, 204] or resorbable with a low resorption rate [118, 195, 196], which limits their clinical applications.

2.6.4.5 Tricalcium phosphate (TCP)

Tricalcium phosphate ($Ca_3(PO_4)_2$) is a bioceramic that has a calcium to phosphorus ratio of 3:2 which is similar to cancellous bone [205]. TCP materials are very sensitive to heat and sterilization, because these processes affect their chemical structure and change their properties

[206]. There are three types of TCP, β-TCP, α-TCP, and Amorphous–TCP. They can be either osteoinductive or osteoconductive. Although TCP have also shown their efficacy in bone augmentation without inducing immunological reactions [157, 197, 198], their clinical results are not always predictable [207-211]. A portion of TCP converts to HA *in vivo*; however, it still resorbs faster than synthetic HA, which makes it more suitable as a scaffold for bone formation [212] .

2.6.4.6 Brushite

Dicalcium phosphate dihydrate (brushite) is an osteoconductive and partially resorbable bioceramic material that has been used as filler for bone augmentation [213]. It is highly soluble; however, after a period of time its resorbability slows down, and brushite starts to precipitate into unresorbable HA crystals [214]. Therefore, its usage is limited in onlay bone augmentation [215].

2.6.4.7 Monetite

Dicalcium phosphate anhydrous (CaHPO) is a biocompatible and biodegradable bioceramic material that is produced by the hydrothermal conversion or dehydration of Brushite [216]. Although Monetite is slightly less soluble than brushite, its structure in general contains high microporosity; therefore, it dissolves faster compared to brushite, without transforming into HA crystals [214].

This is the material of interest in our *in vivo* study, because it has been recently shown that it is an osteoconductive and osteoinductive bone graft material [8, 217]. In addition, clinical and *in vivo* studies showed that these bone grafts cab achieve high yield of bone augmentation

volume [9, 10, 218, 219]. Monetite can be produced as blocks using 3D-printing techniques for vertical bone augmentation [9, 10, 218]. 3D-printed monetite blocks have a compressive strength that is lower than cortical bone (22 MPa), but is similar to that of spongy bone (9.4–25.2 MPa) [9, 214].

Chapter three: Hypothesis and objectives

==========

3.1 Hypothesis

The general hypothesis of this thesis is that bone substitutes can replace autografts in onlay bone augmentation procedure. This global hypothesis involves two implications:

1) Bone augmented with allograft onlays can be comparable to native alveolar bone in terms of quality and quantity. In addition, the success rate of implants placed in bone augmented with allograft onlays can be comparable to the ones inserted in bone augmented with autograft onlays and native alveolar bone.
2) Modifying the geometry of synthetic onlays according to the metabolic activity of the recipient site would enhance bone augmentation within the onlays and implant osseointegration.

3.2 Objectives

In order to test our hypothesis, the overall objectives of the thesis were to assess the capability of allografts onlays in achieving comparable results to autograft onlays, and to improve the osteoconductivity of the synthetic bone grafts in order to overcome their limitations. The specific objectives were:

1) Histological and histomorphometric comparison between bone augmented with allograft onlays and native alveolar bone.
2) And compare the clinical success rate of implants placed in bone augmented with allograft and autograft onlays, as well as native alveolar bone.

3) To assess the metabolic activity of the calvarial bone as a recipient site for monetite onlays *in vivo*.
4) Develop new onlay designed with different morphological features according to the first objective and test these onlays *in vivo*.
5) Histological, histomorphometric, and XRD assessment of bone augmented with the customized monetite onlays *in vivo*.

This thesis includes a literature review and two manuscripts, providing a thorough clinical and histological assessment of the behavior of allograft onlays in alveolar bone augmentation. The thesis provides new insight to the metabolic activity of the calvarial bone *in vivo*, and the capability of customized monetite onlays in bone augmentation *in vivo*. This work was accomplished by the candidate between January 2012 and March 2014 under the supervision of Dr. Faleh Tamimi in the Faculty of Dentistry, McGill University.

Chapter Four: Allograft Onlays

==========

4.1 Bone augmented with allograft onlays is comparable to native alveolar bone in terms of quality and implant success rate.

4.2 Abstract

Bone allograft onlays have great potential for bone augmentation of deficient alveolar ridges. However, the quality of bone augmented with these materials and the success rate of the implants placed in it have not been thoroughly assessed. This study had two objectives. Firstly, to analyze the quality and quantity of bone augmented with allograft onlays in comparison to native alveolar bone. Secondly, to assess the success rate of Ti dental implants placed in bone augmented with allograft onlays in comparison with autografts onlays and the host native bone. Two cohort studies were performed: a bone histological and histomorphometric study on 46 patients and a clinical study on 369 patients. In the first study, 21 patients with insufficient alveolar bone volume received 68 allograft onlays prior to implant placement, while 25 patients with sufficient bone volume had their implants placed without bone grafts. Upon implant placement, bone samples were retrieved using trephine burs and submitted for undecalcified histological analysis. For the second study, 345 patients received dental implants without bone augmentation, 43 patients received autograft onlays and 16 patients received allograft onlays. Onlay and implant success rates were assessed at the end of the follow-up period.

The histological study revealed that there were no significant differences (P=0.33) between the volume of the newly formed bone in the allograft onlay group (61.0±13.3%) and the native bone group (65.5±17.9%). The clinical study revealed that the implant success rate in the

control group (95.7%), autograft group (96.4%), and in the allograft group (96.8%) were similar to each other. The quantity and quality of bone augmented with allograft onlays is similar to the host native alveolar bone. Success rate of implants placed in bone augmented with allograft onlays are comparable to those placed in either the autograft onlays or native alveolar bone.

4.3 Introduction

Dental implants have become an essential treatment modality with a high success rate upon rehabilitation of lost dentition [31, 220]. However, inadequate bone volume to support dental implants can compromise the functional and esthetic outcome of the treatment [221-228]. A variety of surgical techniques for improving bone volume have been presented in the literature to facilitate implant placement [229, 230]. Among these techniques, alveolar bone augmentation can be used to increase the length, diameter, and number of implants that can be placed in deficient alveolar ridges [85, 231, 232], with a highly predictable clinical performance [92, 233].

Autograft onlays are the most predictable and successful bone graft material used for alveolar bone augmentation [108, 234-236]. However, these grafts have many drawbacks, which might limit patient's acceptance to these onlays in clinical practice, including their limited availability, high resorption rate, as well as the need for a harvesting surgery that is associated with bleeding, morbidity, and possible nerve injury [229, 237]. Therefore, other materials have been used to overcome the above limitations, such as xenograft, synthetic bone grafts, allograft, or a combination of more than one material [229]. Among these various bone grafts, allograft is highly biocompatible with lower complication rate compared to other grafting materials [151, 152].

Bone allografts were introduced in the 1970s [238], but only recently they have been

used as onlays for alveolar augmentation [153, 239-241]. These grafts include mainly fresh-frozen, freeze-dried, or demineralized freeze-dried bones that are all harvested from cadaveric sources, processed and stored with different techniques [242, 243]. Allografts are osteoconductive, and even osteoinductive depending on the type of material and the processing technique [244, 245].

Although some studies reported immunological reactions using some types of allografts [246, 247], freeze-dried allografts are unlikely to induce sensitization response in the host tissue [248]. Freeze-dried allografts are the most commonly used grafting material for inter-body fusion of the cervical, thoracic, and lumbar spines [150, 249]. Among these graft cortico-cancellous blocks was that these types of block grafts are the most frequently used [250-252], because they combine the properties of both the cancellous bone that allows vascular infiltration, and the cortical bone that provides rigid fixation and resistance to resorption [151, 152, 251, 253].

Clinical studies suggested that predictable results could be obtained with implants placed in bone augmented with allograft onlays, achieving a success rate of 90% after at least 1 year follow-up [147, 254-256]. However, these studies were limited to maxilla and cancellous type of allografts with different treatment modalities [246]. In addition, the quality of bone augmented with these materials, and the success rate of implants placed in the augmented bone have not been thoroughly assessed.

We hypothesize that the quality of bone augmented with allograft onlays is sufficient to allow high implant success rate. Therefore, the objective of this study was to analyze the quality and quantity of bone augmented with allograft onlays, as well as the success rate of Ti dental implants in it.

4.4 Materials and Methods

To achieve our objective we performed two cohort studies, one to assess the quality of bone augmented with allograft onlays, and the second one to investigate the success rate of implants placed in allograft-augmented bone.

4.4.1 Quality of bone augmented with allograft onlays

4.4.1.1 Study design

The first cohort study was performed to assess bone histological and histomorphometric features of bone augmented with allograft group and compare it to the native alveolar bone. Ethical approval from the Committee for Clinical Trials of "San Carlos" University Hospital [no. (P-07/151), Madrid, Spain] following the Spanish legislation for clinical research was obtained. All patients received an informed written consent explaining the study objectives, surgical techniques and possible side effects.

Partial-edentulous patients who came seeking dental implant treatment from January, 2009 to September, 2013 were enrolled in the first cohort study. These patients were divided into two groups according to the bone volume of pre-implanted sites. Patients with sufficient bone volume had their implants placed in native alveolar bone without any bone grafting procedure (control group). On the other hand, patients with insufficient alveolar bone volume (< 5mm vertically and/or <4 mm horizontally) [257-259] preventing the placement of a regular size implant received cortico-cancellous allograft onlays (Tutogen Medical GmbH, Neunkirchen am Brand; Germany), prior to dental implant placement.

Patients with severe systemic disease (American Society of Anaesthesiology III or IV) were excluded from the study. In addition, patients who were pregnant, or patients with diseases affecting bone, such as Paget's disease, osteomalacia, vitamin D deficiency, alcoholism, hyperthyroidism cancer (excluding non-melanoma skin cancer), or osteoporosis as well as those on medications that might affect bone metabolism, such as bisphosphonates, corticosteroids or antiepileptic medicaments were also excluded [107].

4.4.1.2 Intervention

4.4.1.2.1 Surgical procedures

4.4.1.2.1.1 Bone augmentation

All patients were assessed clinically and radiographically with CT-scans and periapical radiographs. Patients with sufficient alveolar ridge volume went through implant placement directly as described underneath, and patients with insufficient alveolar bone went through a bone augmentation procedure before implant placement. Prior to the surgery, all patients rinsed their mouth with 15 ml 0.12% chlorhexidine digluconate for 1 minute, and then povidone- iodine 10% solution was applied to the peri-oral skin. During the surgery, 4 mg of Dexamethasone was given to the patients intramuscularly. A full thickness flap was raised to provide a full visualization of the alveolar ridge. In the allograft group, the cortico-cancellous bone blocks were rehydrated in saline solution before fixation, allowing their temperature to decrease gradually (Fig 4.1.A). Bone blocks were trimmed in length and height to fit the defects under abundant sterile saline solution irrigation and blocks were fixed with the cancellous bone side facing the host bone using osteosynthesis screws (AO/ASIF 4.0 self-drilling screws; Synthes, Synthes GmbH&Co, Umkirch, Germany) (2 mm Ø, 12 mm length). Then, the flaps were

repositioned to cover the bone grafts completely, and were closed with 4–0 nylon sutures (Fig 4.1.B). The onlays were left to heal and evaluated 6 months after placement. Patients were then again assessed clinically and radiographically with CT-scans and periapical radiographs. Both onlay bone augmentation and implant placement procedures were performed by the same surgeon.

4.4.1.2.1.2 Implant placement

Implants were placed following the manufacturer instructions (Fig 4.1. C&D). During implant installation surgery, bone samples were taken perpendicular to the superior surface of the alveolar bone ridge or allograft onlay, using a trephine burr (internal Ø = 2.0, and length of 10.0 mm). Bone biopsies were then submitted for histological and histomorphometric analysis.

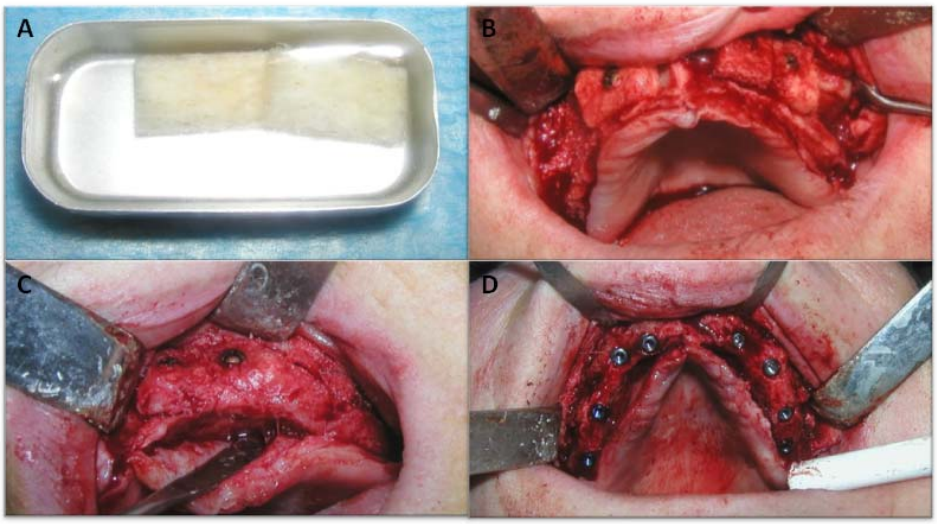

Figure 4.1. Photographs showing: **A)** the allograft blocks prior to surgical implantation; **B)** surgical placement of allograft onlays (first surgery); **C)** Reopening of the onlay augmented surgical sites for retrievement of bone samples and implants placement (second surgery) **(D)**.

4.4.1.2.2 Post-operative

Postoperatively, Amoxicillin 750mg t.d.s was prescribed for 7 days, Ibuprofen 600mg t.d.s. for 4 days, and Chlorhexidine 0.20% mouth rinse t.d.s. for 10 days. Prosthetic restorations were delivered and patients were regularly followed-up. CT-scans and periapical radiographs were taken again after the final treatment. Implant failure was defined as implants that are characterized or associated with one or more of the followings: pain on function, mobility, radiographic bone loss (1/2 length of the implant), uncontrolled exudates, no longer available in the patient's mouth [260].

4.4.1.3 Histological and histomorphometric procedures

Using the undecalcified histological technique, bone samples were fixed in 10% formaldehyde, and then dehydrated in ascending concentrations of alcohol (70–100%). After dehydration, samples were embedded in 2-hidroxyethyl-methacrylate (resin monomer) (Technovit; Leica Microsystems GMBH; Wetzlar, Germany), and then polymerized into cylindrical blocks. Longitudinal histological sections crossing the center of the polymerized cylindrical biopsies were taken using a micro-saw (SP1600 Leica Microsystems GmbH, Wetzlar; Germany), and stained with methylene blue/basic fuchsine for histological and histomorphometric analysis. Pictures of histological sections were taken by Zen 2012 software (Carl Zeiss, Oberkochen, Germany) using a Zeiss Imager.M2 colored camera (Carl Zeiss, Oberkochen, Germany) installed on a light microscope (Axio Imager.M2; Carl Zeiss Microscopy, S.L., Oberkochen; Germany). In each histological section, the percentage of newly formed bone was calculated by dividing the area occupied by the newly formed bone over the total area of the biopsy using Image J software (ImageJ 1.46r; Wayne Rasband, National

Institutes of Health, Maryland). In addition, Image J was also used to measure the thickness of cortical bone of both native alveolar bone and allograft-augmented bone.

4.4.2 Success rate of implants placed in allograft-augmented bone

A second cohort study was performed to assess the success rate of implants placed in bone augmented with allograft onlays and compare it to implants placed in bone augmented with autograft onlays, as well as native alveolar bone. The ethical approval (12-321 GEN) to conduct this part of the study in the private dental clinic "East Coast Oral Surgery" (Moncton, New Brunswick, Canada) was obtained from the Ethical Committee for Clinical Trials of McGill University following the legislation for clinical research in private clinics.

Partial-edentulous patients who came seeking dental implant treatment from January, 2009 to September, 2013 were enrolled in the second cohort study. Based on the clinical screening and X-ray examination, patients who needed implant placement were divided into three groups according to the amount of bone volume available to support implant placement. First group consisted of patients who had sufficient alveolar bone and went through dental implant treatment without bone augmentation procedure (control group). Patients with insufficient bone volume (< 5mm vertically and/or <4 mm horizontally [257-259]) received bone augmentation treatment prior to implant placement with either allograft onlays (second group) or autograft onlays (third group). The second and third groups were divided depending on patients' preference. In the autograft group, cortico-cancellous bone blocks of adequate size according to defect dimensions were harvested from the either the patients' iliac crest or chin. Allograft bone augmentation, implant placement, and post-operative interventions were done as described in the above-mentioned first cohort study.

4.4.3 Statistical analysis

In the histological cohort study, the volume of living bone was compared between the two groups (allograft and control) using student t-test, and the statistical significance was set at $P < 0.05$ (two-sided). In addition, the patient and implant-based demographic differences between the implants placed in the native alveolar bone and those placed in the allograft augmented bone were assessed. T-test was used for normally distributed-continuous variables, Mann-Whiteny U test for abnormally distributed-continuous variables, and Chi^2 test for binary variables (Table 4.1).

In the success rate assessment cohort study, Cohen's f^2 test sample size indicated that a minimum of 543 implants was required to detect a difference of failure rate of 9.9% between the groups, with a power of 0.8 at an effect size ($f2$) of 0.02, 3 predictors and a probability level of 0.05 [261]. Relative risk with 95% confidence intervals (CIs) was performed to investigate the effect of the confounders on implant success in each group. Multiple logistic regression, generalized estimating equation (GEE), and Cox regression were adjusted for possible confounders, and were used to assess if there is a significant difference in implant success rate between the three groups. Adjusted confounders included gender, age, implant length, implant torque, and implant loading time (Table 4.3). Kaplan-Meier and Cox regression analyses were used to assess for significant differences in implant success rate between the three groups through the whole follow-up period. Post-hoc power calculation was done using Cohen's f^2. All statistical analyses were performed using the software SPSS 17.0 (SPSS Inc., Chicago, IL, USA) and Origin 7.0 (Origin 7.0, Origin Lab Co.; Northampton; MA).

4.5 Results:

4.5.1 Quality of bone augmented with allograft onlays

4.5.1.1 Clinical outcome

A total of 46 patients met both our inclusion and exclusion criteria, twenty-five patients (13 females and 12 males; 60.0±11.4 years old) with sufficient bone volume had their implants placed without any type of bone graft (Table 4.1), and twenty-one patients (18 females and 3 males; 54.7±12.8 years old) with insufficient alveolar bone volume received 68 cortico-cancellous allograft onlays (Table 4.1), prior to implant placement Clinical observations revealed that all allograft onlays were successfully integrated to the alveolar bone except one that was lost because of soft tissue dehiscence, yielding a success rate of 98.5%. Each patient received 1 to 6 onlay blocks and 1-8 implants. A total of 79 dental implants were inserted in bone augmented with allograft onlays, and 31 implants were placed in the control group (Table 4.1). All implants remained clinically osseointegrated and stable and none was lost, reflecting a 100% success rate at the end of the follow-up examination. Table 4.1 demonstrates the comparison between patients and implants in both the allograft and native alveolar bone groups in terms of dental and demographic conditions. Only the gender, implant length, and cortical thickness were significantly different between the two groups. There were significantly more female patients in the autograft group than in both the native alveolar bone ($P = 0.03$), and implants placed in the allograft group were longer than those placed in both the native alveolar bone group ($P=0.001$). The cortical bone of the native alveolar bone was significantly thicker than that of the allograft-augmented bone ($P=0.01$). Other factors were similar and showed no significant differences between the two groups.

Table 4.1. Comparison of patient-related and implant-related factors between the allograft and native alveolar bone groups for the histological and histomorphometric cohort study.

	Allograft	Native bone	P-value
Patients	21	25	-
Implants	86	31	-
Age (years)	54.7± 12.8	60.0 ± 11.4	0.14[a]
Gender			
Male	3	12	0.03*[b]
Female	18	13	
Implant Diameter (mm)	4.04 ± 0.18	4.1	0.27[c]
Implant length (mm)	10.57 ± 1.3	10.0	0.001*[c]
Follow-up (months)	22.9 ± 9.8	21.9 ± 10.4	0.64[a]
Bone volume (%)	61.0 ± 13.3	65.5 ± 17.9	0.33[a]
Cortical bone thickness (mm)	0.45±0.1	0.8±0.7	0.01* [a]

*Statistically significant (P<0.05).
[a] Indicates that a student t-test has been used for this variable to assess the difference between the two groups.
[b] Indicates that odds ratio risk analysis (CI 95%) has been used for this variable to assess the difference between the two groups. Odds ratio = 5.5 (CI = 1.3-23.7)
[c] Indicates that Mann-Whitney non-parametric test has been used for this variable to assess the difference between the two groups.

4.5.1.2 Histological and histomorphometric results

Histological analysis of the bone specimens from the allograft group demonstrated a mixture of newly formed bone and residual bone graft in all biopsies (Fig. 4.2.). Both groups (control and allograft) showed similar characteristic of mature and vital bone osseous tissue. A clear lamellar pattern and multiple appositions of newly formed bone were noticed in both the allograft and control groups (Fig. 4.2. C&F). However, analysis showed that the cortical bone thickness was different between the two groups, the cortical bone of the native alveolar bone was significantly thicker than that of the allograft augmented. The residual non-vital allograft bone was identified by the empty osteocyte lacunae (red arrows); however, there was no evidence of inflammatory infiltrations within or around the specimens (Fig. 4.2. C). The vital bone was characterized by the presence of vital osteocytes in the bone lacunae (Fig. 4.2. C).

Histomorphometric analysis showed that the mean average of vital bone volume was 65.0±17.9% in the sections taken from the control group, and 61.0±13.3% in the allograft group.

The remaining volume of the specimens was occupied by the residual bone graft and connective tissue. No statistically significant differences were found between the two groups (P = 0.33).

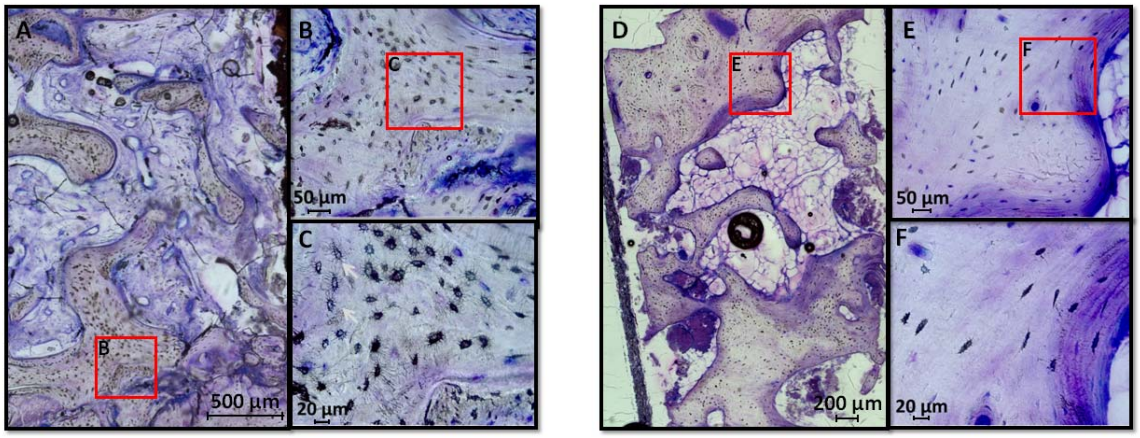

Figure 4.2. A) Histological section from the allograft group, original magnification x2.5. **B)** A magnified section of Figure 4.A showing newly formed bone within the allograft material, original magnification x10. **C)** A magnified section of Figure 4.B showing the lamellar pattern of the newly formed bone, the living osteoblasts, and the empty lacuna of the graft's cells (red arrows), original magnification x20. **D)** Histological section from the control group, original magnification x2.5. **E and F)** Magnified sections of Figure 4.D showing the lamellar pattern of the original alveolar bone and the living osteoblasts, original magnification x10 and x20 respectively.

4.5.2 Success rate of implants placed in allograft-augmented bone

Out of 578 patients screened for this study only 369 met our inclusion and exclusion criteria (Fig. 4.3). Three hundred and ten patients (117 male and 171 female patients) with an average age of 56.8±14.6 years received a total of 575 implants (Torque 35.4±10.7 Ncm) without

bone graft. These implants had an average length of 11.9±2.2 mm and diameter of 4.2±0.5 mm, and were loaded 4.8±1.5 months after placement. On the other hand, 43 patients received autograft onlays (7 male and 36 female patients, 48.3±12.5 years old), and 16 patients received allograft onlays (9 male and 7 female patients, 58.6±9 years old).

In the group where bone was augmented with autograft onlays, 83 implants were placed with an average length and diameter of 11.3±2.1 mm and 4.2±0.5 mm respectively (Torque 30.0±10.2 Ncm), and loaded after 5.5±0.9 months. In the group where bone was augmented with allograft onlays, 63 implants were placed with an average length and diameter of 11.4±1.4 mm and 4.2±0.4 mm respectively (Torque 25.1±8.7 Ncm), and loaded after 5.7±0.7 months. The mean follow-up periods were 33.7±26.4 months in the allograft group, 40.4±23.4 months in the autograft group, and 30.0±11.3 months in the native alveolar bone group, respectively. Twenty-four implants failed in the control group (4.2%), 3 in the autograft onlays group (4.1%), and 2 in the allograft onlays group (3.2%) yielding a success rate of 95.8%, 96.4%, 96.8%, for each group respectively. The rest of the implants remained clinically osseointegrated at the end of the follow-up examination (30.3±26.4 months) and received prosthetic rehabilitation.

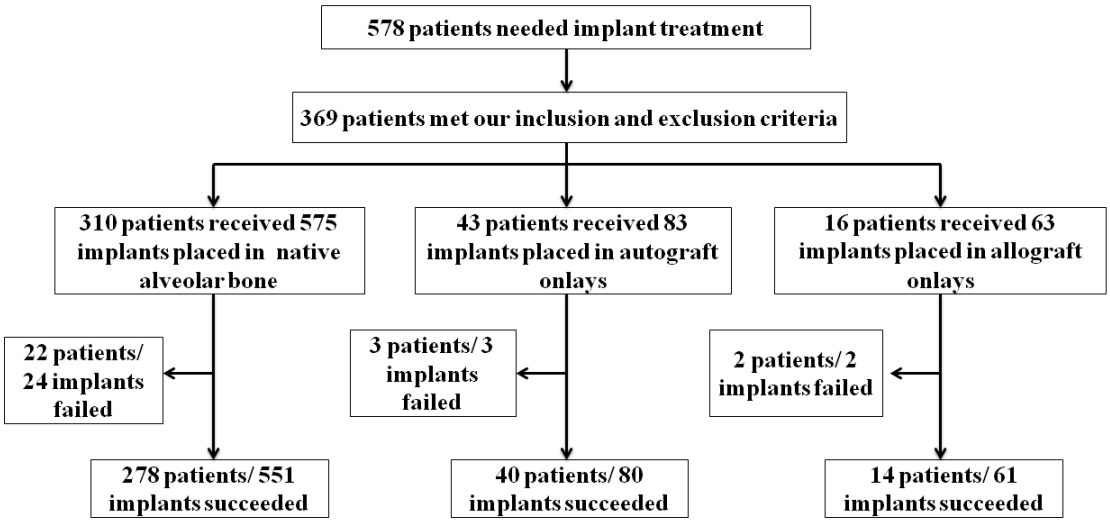

Figure 4.3. Flow diagram of the number of participants and implants those were included in the second part of the study.

4.5.2.1 Risk analysis

Tables 4.2.A and B present the results of risk analysis of both implant-related and patient-related factors on the implant success rate in each group. Risk analysis of the groups treated with allograft or autograft onlays could not identify any risk factor associated with higher risk of implant failure. In the native alveolar bone group, only smoking ($P < 0.001$) showed a negative association with implant success rate.

Table 4.3 demonstrates the comparison between the three groups in terms of implant-related and patient-related factors. There were significantly more female patients in the autograft group than in both the native alveolar bone ($P = 0.001$) and allograft groups ($P = 0.01$). Patients in the autograft group were younger than in both native alveolar bone ($P = 0.001$) and allograft groups ($P = 0.03$). Implants placed in the allograft group were longer than those placed in both the autograft ($P = 0.01$) and native alveolar bone groups ($P = 0.02$). Higher torque was needed to

place dental implants in native alveolar bone compared to autograft ($P = 0.001$) and allograft groups ($P < 0.001$). In addition, implants needed lower torque to be placed in the allograft group compared to the autograft group ($P < 0.001$). Implant loading was delayed significantly more in the allograft and autograft groups, compared to the native alveolar bone group ($P < 0.001$). No significant differences were found between the three groups in terms of smoking and alcohol habits, follow-up period, as well as their systemic health conditions.

4.5.2.2 Implant success rate assessment

Table 4.4 shows the results of multiple logistic regression, GEE, and Cox survival model analyses for comparisons between the native alveolar bone, autograft, and allograft groups in terms of implant success rate. After adjusting these models to the possible confounders that were identified in Table 4.3, no significant differences between the three groups were observed, and the post-hoc power analysis revealed that there is sufficient statistical power to support our results. Power analysis for multiple regression showed that the post-hoc power was 0.91 between native alveolar group and autograft group, 0.98 between native alveolar group and allograft group, and 0.89 between the autograft and allograft groups. In addition, the Kaplan-Meier algorithm (Fig. 4.4) and Cox survival analyses confirmed that the survival functions in the three groups are similar throughout the whole follow-up period.

Table 4.2 A. Patient-based risk factor assessment of implant failure in the three groups.

Factor	Native Alveolar bone				Autograft onlays				Allograft onlays			
	N Success (%)†	N Failure (%)†	OR (CI)	P-value	N Success (%)†	N Failure (%)†	OR (CI)	P-value	N Success (%)†	N Failure (%)†	OR (CI)	P-value
Gender												
Female	171 (94)	11 (6)	1	-	34 (94)	2 (6)	1	-	6 (86)	1 (14)	1	-
Male	117 (91)	11 (9)	1.5 (0.6-3.5)	0.50	6 (86)	1 (14)	2.8 (0.2-36.4)	0.42	8 (89)	1 (11)	0.8 (0.04-14.6)	1.00
Age												
<60	172 (94)	12 (7)	1	-	35 (95)	2 (5)	1	-	8 (89)	1 (11)	1	-
≥ 60	116 (92)	10 (8)	1.2 (0.5-3.0)	0.66	5 (83)	1 (17)	3.5 (0.3-46.1)	0.37	6 (86)	1 (14)	1.3 (0.1-25.9)	1.00
Smoking												
No	265 (95)	14 (5)	1	-	37 (93)	3 (8)	1	-	14 (93)	1 (7)	1	-
Yes	23 (74)	8 (26)	6.5(2.5-17.3)	<0.001*	3 (100)	0	0.9 (0.9-1.0)	1.00	0	1 (100)	2.0 (0.5-8.0)	0.13
Alcohol												
No	147 (93)	11 (7)	1	-	21 (96)	1 (5)	1	-	8 (80)	2 (20)	1	-
Yes	141 (93)	11 (7)	1.0 (0.4-1.9)	1.00	19 (91)	2 (10)	2.2 (1.9-26.4)	0.61	6 (100)	0	0.6 (0.4-0.9)	0.50
Hypertension												
No	231 (94)	16 (7)	1	-	35 (95)	2 (5)	1	-	11 (92)	1 (8)	1	-
Yes	57 (91)	6 (10)	1.5 (0.6-4.1)	0.41	5 (83)	1 (17)	1.0 (0.9-1.0)	1.00	3 (75)	1 (25)	3.7 (0.2-77.6)	0.45
Asthma												
No	268 (93)	19 (7)	1	-	39 (95)	2 (5)	1	-	13 (87)	2 (13)	1	-
Yes	20 (87)	3 (13)	2.1 (0.6-7.8)	0.22	1 (100)	0	0.9 (0.7-1.1)	1.00	1 (100)	0	0.9 (0.7-1.1)	1.00
Allergies or hives												
No	238 (92)	20 (8)	1	-	35 (95)	2 (5)	1	-	11 (85)	2 (18)	1	-
Yes	50 (96)	2 (4)	0.5 (0.1-2.1)	0.55	5 (83)	1 (17)	3.5 (0.6-46.1)	0.37	3 (100)	0	0.9 (0. 7-1.1)	1.00
Thyroid disease												
No	268 (93)	21 (7)	1	-	37 (93)	3 (8)	1	-	11 (85)	2 (18)	1	-
Yes	19 (95)	1 (5)	0.6(0.09-5.3)	1.00	3 (100)	0	0.9 (0.9-1.0)	1.00	3 (100)	0	0.9 (0.7-1.1)	1.00
Depression												
No	270 (94)	18 (6)	1	-	36 (95)	2 (5)	1	-	13 (87)	2 (13)	1	-
Yes	18 (82)	4 (18)	3.3(1.0-10.9)	0.06	4 (80)	1 (20)	4.5 (0.3-61.4)	0.32	1 (100)	0	0.9 (0.7-1.1)	1.00
Nervous Anxiety												
No	264 (93)	21 (7)	1	-	37 (93)	3 (8)	1	-	12 (86)	2 (14)	1	-
Yes	24 (96)	1 (4)	0.5(0.07-4.1)	1.00	3 (100)	0	0.9 (0.9-1.0)	1.00	2 (100)	0	0.9 (0.7-1.1)	1.00
Allergic to Medication												
No	218 (92)	18 (8)	1	-	34 (97)	1 (3)	1	-	10 (91)	1 (9)	1	-
Yes	70 (95)	4 (5)	0.7 (0.2-2.1)	0.61	6 (75)	2 (25)	11.3 (0.9-145.5)	0.08	4 (80)	1 (20)	2.5 (0.1-50.4)	1.00

*Statistically significant (P<0.05)
†Total percentages might not equal 100 due to rounding or missing information
N: Sample number
CI: Confidence interval
OR: Odds ratio

Table 4.2 B. Implant-based risk factor assessment of implant failure in the three groups.

	Native Alveolar bone				Autograft onlays				Allograft onlays			
Factor	**N Success (%)†**	**N Failure (%)†**	**OR (CI)**	**P-value**	**N Success (%)†**	**N Failure (%)†**	**OR (CI)**	**P-value**	**N Success (%)†**	**N Failure (%)†**	**OR (CI)**	**P-value**
Implant Diameter												
≥ 4 mm	465 (96)	21 (4)	1	-	72 (96)	3 (4)	1	-	58 (96.7)	2 (3.3)	1	-
< 4 mm	61 (95)	3 (5)	0.92 (0.3-3.2)	0.75	8 (100)	0	1.0 (1.0-1.1)	1.00	3 (100)	0	0.9 (1.0-1.1)	1.00
Missing	25 (100)	0 (0)	1.8 (0.2-14.0)	1.00								
Implant Length												
< 9 mm	69 (99)	1 (1)	1	-	13 (93)	1 (7)	1	-	2 (100)	0	1	-
≥ 9 mm	458 (95)	23 (5)	3.5 (0.5-26.1)	0.34	67 (97)	2 (3)	0.4 (0.03-4.6)	0.43	59 (96.7)	2 (3.2)	1.0 (1.0-1.1)	1.00
Missing	24 (100)	0 (0)	2.9 (0.4-21.5)	0.50								
Torque												
< 30 Ncm	123 (98)	3 (2)	1	-	33 (97)	1 (3)	1	-	41 (97.6)	1 (2.4)	1	-
≥ 30 Ncm	320 (95)	16 (5)	2.1 (0.6-7.2)	0.30	38 (97)	1 (3)	1.1 (0.1-14.4)	1.00	11 (100)	0	0.9 (0.9-1.0)	1.00
Missing	113 (96)	5 (4)	1.0 (0.4-2.5)	1.00	9 (90)	1 (10)	0.2 (0.01-4.2)	0.37	9 (90)	1 (10)	0.9 (0.7-1.1)	0.48
Loading Time												
≤ 4 months	280 (97)	9 (3)	1	-	19 (95)	1 (5)	1	-	10 (100)	0	1	-
> 4 months	197 (93)	15 (7)	0.4 (0.2-1.0)	0.06	57 (97)	2 (3)	0.7 (0.1-17.5)	1.00	51 (96.2)	2 (3.8)	1.0 (0.9-1.0)	1.00
Missing	74 (100)	0 (0)	0.9 (0.3-3.5)	1.00	4 (100)	0 (0)	0.9 (1.0-1.2)	1.00				
Follow-up												
≥ 12 months	335 (96)	14 (4)	1	-	69 (97)	2 (3)	1	-	31 (94)	2 (6)	1	-
< 12 months	216 (96)	10 (4)	0.90 (0.4-2.1)	0.83	11 (92)	1 (8)	3.1 (0.03-3.8)	0.38	30 (100)	0 (0)	0.96 (0.98-1.10)	0.49

*Statistically significant (P<0.05)

†Total percentages might not equal 100 due to rounding or missing information

N: sample number

CI: Confidence interval

OR: odds ratio

Table 4.3. Comparison of patient-related and implant-related factors between the three groups. Raw numbers are in Table 4.2 A&B.

	Native Alveolar Bone	Autograft		Allograft	
Factor	**OR (CI)**	**OR (CI)**	**P-value**	**OR (CI)**	**P-value**
Gender					
Male/ Female	1	0.28 (0.12-0.64)	0.001*	1.83 (0.66-5.04)	0.30
	-	1	-	0.53 (0.29-12.61)	0.01*
Age					
< 60/ ≥ 60	1	0.24 (0.1-0.58)	0.001*	1.14 (0.41-3.13)	0.80
	-	1	-	0.40 (0.39-17.56)	0.03*
Smoking					
No/ Yes	1	0.68 (0.20-2.31)	0.78	0.60 (0.77-4.70)	1.00
	-	1	-	0.9 (0.11-11.68)	1.00
Alcohol					
No/ Yes	1	1.00 (0.52-1.88)	1.00	0.62 (0.22-1.76)	0.45
	-	1	-	0.96 (0.16-5.96)	0.56
Implant Diameter					
≥ 4 mm/< 4 mm	1	1.24 (0.57-2.68)	0.71	2.6 (0.8-8.6)	0.13
	-	1	-	0.47 (0.12-1.84)	0.35
Implant Length					
≥ 10 mm/ < 10 mm	1	0.72 (0.38-1.34)	0.30	4.4 (1.1-18.56)	0.02*
	-	1	-	6.3 (1.4-25.1)	0.01*
Torque					
≥ 35 Ncm/ < 35 Ncm	1	0.43 (0.26-0.71)	0.001*	0.1 (0.05-0.20)	<0.001*
	-	1	-	0.23 (0.10-0.51)	<0.001*
Loading Time					
≤4 months/ >4 months	1	0.25 (0.15-0.43)	<0.001*	0.14 (0.07-0.28)	<0.001*
	-	1	-	0.56 (0.24-1.30)	0.22
Follow-up					
≥ 12 months/ < 12 months	1	0.63 (0.32-1.23)	0.18	0.71 (0.42-1.20)	0.22
	-	1	-	0.76 (0.34-1.66)	0.56
Hypertension	-				
No/ Yes	1	0.64 (0.26-1.57)	0.41	1.31 (0.41-4.19)	0.75
	-	1	-	0.49 (0.12-2.02)	0.44
Asthma	1				
No/ Yes	-	0.30 (0.04-2.3)	0.33	0.83 (0.11-6.58)	1.00
	1	1	-	0.36 (0.02-6.08)	0.47
Allergies or hives	-				
No/ Yes	1	0.81 (0.32-2.0)	0.83	1.15 (0.32-4.16)	0.74
	-	1	-	0.70 (0.15-3.22)	0.69
Thyroid disease	1				
No/ Yes	-	1.08 (0.31-3.81)	0.75	3.34 (0.88-12.7)	0.09
	1	1	-	0.33 (0.06-1.81)	0.33
Depression	-				
No/ Yes	1	1.7 (0.62-4.82)	0.35	0.87 (0.11-6.92)	1.00
	-	1	-	0.51 (0.21-18.33)	1.00
Nervous Anxiety	1				
No/ Yes	-	0.86 (0.25-2.96)	1.00	1.63 (0.35-7.57)	0.63
	1	1	-	0.53 (0.08-3.48)	0.61
Allergic to Medication	-				
No/ Yes	1	0.73 (0.32-1.64)	0.56	1.45 (0.49-4.31)	0.55
	-	1	-	0.50 (0.14-1.86)	0.31

*Statistically significant (P<0.05)
OR: Odds ratio
CI: Confidence interval

Table 4.4. Comparison between the three groups in terms of adjusted odds ratio, Cox regression, and generalized estimating equation

	Groups		
Type of Analysis	**Native alveolar bone**	**Autograft**	**Allograft**
AOR (CI; p-value; power)	1	1.40[a] (0.30-6.52; 0.67; 0.91)	1.72[b] (0.20-14.81; 0.62; 0.98)
	-	1	2.63[c] (0.15-46.53;0.51; 0.89)
Cox (CI; p-value)	1	2.49[a] (0.50-12.41; 0.27)	2.30[b] (0.28-18.95; 0.44)
	-	1	2.84[c] (0.17-46.99; 0.47)
GEE p-value	1	0.68[a]	0.60[b]
	-	-	0.43[c]

[a] Covariets: gender, age, implant torque, implant loading time.
[b] Covariets: implant length, implant torque, implant loading time.
[c] Covariets: gender, age, implant length, implant torque.
AOR: Adjusted odds ratio.
GEE: Generalized Estimating Equation.
CI: Confidence interval

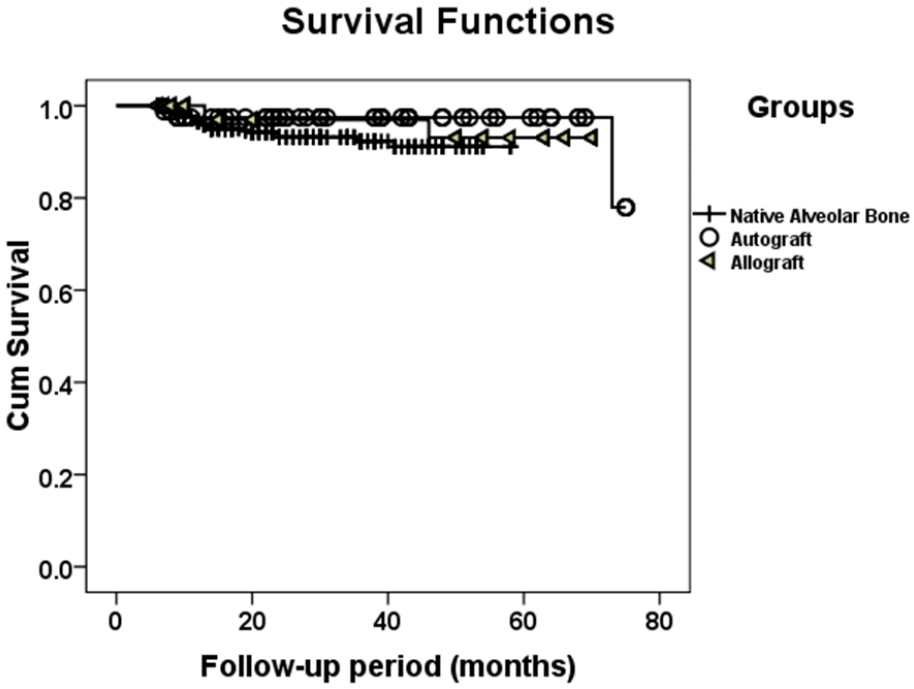

Figure 4.4. Kaplan – Meiers charts representing the survival function (success rate through the follow-up period) of the three groups: native alveolar bone, autograft, and allograft groups.

4.6 Discussion

This study confirmed our hypothesis by demonstrating for the first time that the vital bone augmented with allograft onlays was similar to the native alveolar bone regarding the histological architecture and bone volume. In addition, we were able to demonstrate that the success and success rates of implants placed in bone-augmented allograft onlays were similar to the ones placed in either bone augmented with autograft onlays or native alveolar bone. Underneath we discuss each of our specific finding in details.

4.6.1 Volume and architecture of bone augmented with allograft onlays

The histological and histomorphometric results demonstrated that bone augmented with allograft onlays was comparable to the native alveolar bone in terms of quality and quantity. Both patient and implant-related factors of the allograft and native alveolar bone groups were also similar in terms of age, gender, implant dimension, and follow-up period.

Bone quality and quantity had been assessed both in native and allograft separately in different studies [147, 254-256]. However, this is the first study to perform a direct comparison between allograft onlays and native alveolar bone. The results of this study revealed that 6 months after onlay bone augmentation using cortico-cancellous allograft bone blocks**,** 61.0±13.3% of the biopsies volume was vital bone, which is almost similar to previous reports [256]. On the other hand, the percentage of bone volume in the biopsies from the native alveolar group reached 65.0±17.9%, and there were no significant differences between the allograft and native alveolar bone groups. These

histological and histomorphometrical results allow us to expect similar success rate of implants placed in either bone augmented with allograft onlays or native alveolar bone.

Although histological studies showed that fresh frozen allograft could induce inflammatory reaction in patients [139, 140, 262, 263], in our study we did not register any clinical or histological signs of inflammatory reaction within freeze-dried allograft onlays. This is probably because these types of allografts undergo rapid resorprtion compared to the other types leaving behind small remains of the graft material [264, 265].

4.6.2 Implant success rate

Different factors might affect the success rate of implants placed in both native alveolar bone and augmented bone [266]. Among these various factors, it is believed that the strongest predictor of the implant success outcome especially in the augmented area is bone quality [266]. The histological part of this study has demonstrated that bone augmented with allograft onlays was similar quantitatively and qualitatively to the native alveolar bone. Other factors that might affect implant success rate include implant-related and patient-related factors [267], which have not been addressed thoroughly in the previous literature on onlay bone grafts.

This is the first study that assesses the implant success rate between allograft onlays, autograft onlays and native alveolar bone in the same study. Our results demonstrated that the success rate of implants placed in bone augmented with allograft onlays was similar to those placed in either bone augmented with autograft onlays or native alveolar bone (95.8% in the native alveolar bone, 96.4% and 96.8% in bone augmented with autograft and allograft onlays respectively). For multiple regression, Cox

survival, and GEE analyses, possible confounders were adjusted to overcome the cohort limitation "confounding by indication" since these confounders were significantly different between the three groups including gender, age, implant length, implant torque, implant loading time. These analyses were done to assess implant success rate between the native alveolar bone, autograft, and allograft groups, and they all showed no significant differences between each other, with a high post-hoc power.

Survival function was used to measure the success rate of implants throughout the follow-up period. Kaplan-Meiers algorithm analysis confirmed that the success rate of implants placed in bone augmented with allograft onlays was similar to the success rate of implants placed in bone augmented with autograft onlays and native alveolar bone through the whole follow-up period that reached more than 40 months.

The findings of our study showed that the success rate of implants placed in bone augmented with allograft onlays can reach up to 96.8% for an average follow-up of 33.7±26.4, which was similar to previous studies [154, 246]. Although, our findings might represent a lower success rate than those with shorter follow-up periods, our results are still within the criteria established by the National Institute of Health [268]. On the other hand, implant success rates in the autograft and native alveolar bone groups were also similar to the ones that have been previously documented in the literature [223, 269-271].

4.6.3 Smoking

Our results indicated that smoking had a negative effect on the success rate of implants placed in native alveolar bone. This was expected because it has been proven in

the literature that smoking affects the healing of both bone and mucosa, thus affecting the success rate of implants placed in both native alveolar bone and augmented bone [31, 220, 223]. This negative association was not seen in the other groups (autograft and allograft), which is probably because the number of smokers were lower in these two groups compared to native alveolar bone group.

4.6.4 Patients' age and gender

Risk analysis showed that patients' age and gender had no association with implant success rate in native alveolar bone, autograft, or allograft groups, respectively. This was also seen in previous studies with implants placed in native alveolar bone [223]. However, our results in the clinical cohort study showed that patients treated with autograft onlays were predominantly females compared to patients treated with allograft onlays as well as those who did not require bone augmentation.

On the other hand, patients treated with autograft onlays were mainly young patients (<60 years old), where as patients treated with allograft onlays as well as those who did not require bone augmentation were mainly older patients (>60 years old).This female and young age predominance in patients receiving autologous bone grafts has been reported previously [222]. The reason behind it is probably because females and younger patients can tolerate the graft harvesting procedure and the associated morbidity, whereas older patients might be frail and have limited availability of bone for harvesting [222]. Therefore, they were treated with allograft onlays instead.

4.6.5 Implant length

Our study showed that implant length was not associated with the success rate of implants placed in each of the three groups (native alveolar bone, autograft, and allograft groups). In the literature, there is a controversy about the effect of implant length on success rate of dental implants [272]. Studies have shown that shorter implants might be associated with higher risk than longer implants, and others showed that there is no association at all [272]. However, implant length should not be considered as a solely risk factor, because other factors which are related to implant length should be considered as well, such as the implant surface, quality of the patient's bone, the practitioner's surgical capabilities, anatomical limitations, and implant primary stability [272]. In addition, this study considered short implants those that had <9 mm implant length, while previous studies had different parameters, where they considered implants that are <8 mm or <13 mm as short implants [272]. Therefore, further studies are needed to investigate implant's length as solely risk factor for implant success rate in bone augmented with allograft onlays.

On the other hand, those two cohort studies showed that implants placed in bone augmented with either autograft or allograft onlays were longer compared to the ones placed in native alveolar bone. This was expected since onlay bone augmentation allows the placement of longer and wider implants in deficient alveolar ridges [85, 231, 232]. In addition, our analysis showed that implants placed in bone augmented with allograft onlays were even longer than those placed in bone augmented in autograft onlays. This is probably because of the vertical bone resorption that occurs in autograft onlays during the

first year of onlays placement [273], although further clinical studies are needed to investigate the difference of onlay graft resorption between autograft and allograft onlays.

4.6.7 Implant loading time

In the autograft and allograft groups, implants loading was delayed for a longer period of time from the time of implant placement (>4 months) compared to the native alveolar bone. This might be because a longer period of time is needed to allow for sufficient osseointegration of implants placed in bone augmented with onlay bone grafts [12, 274-276]. However, implant loading time had no significant effect on implant success rate in bone augmented with either autograft or allograft onlays. Loading time of implants placed in bone augmented with onlay grafts is still controversial in the literature, and systemic reviews showed that implants are usually loaded three months after surgical placement of implants in bone augmented with autograft onlays [277, 278]. In addition, loading time did not affect the success rate of dental implants placed in native alveolar bone, which is in agreement to what was reported in the previous literature [279, 280].

4.6.8 Implant torque

Implants placed in native alveolar bone required higher torque compared to implants placed in the augmented bone. Previous studies showed similar results, indicating that the cutting torque values revealed an inverse linear relation to the Lekholm and Zarb bone quality index [281]. Therefore, significantly lower cutting torque values were seen in grafted bone than in native alveolar bone [281]. Although our histological and histomorphometrical part of this study showed that bone augmented with

allograft onlays was similar to the native alveolar bone in quantity and quality, the thickness of the cortical bone is different between the two groups (Figure 4.3). In the literature, it was shown that higher torque values are needed in thicker cortical bone to ensure implant stability [282, 283]. Despite all that, our results showed no association between the torque value and implant success rate in any of the groups, which is similar to other previous studies that have found no differences in the success of implants placed at both high and low torques [282, 284].

4.7 Limitations

In order to achieve our objectives, this study included two cohort studies. Cohort study design has its own advantages and disadvantages; one of the limitations that cohort studies might be subjected to is "confounding by indication". However, in this study we adjusted our statistical analysis for possible confounders to overcome these limitations, and the power analysis showed that we have enough power to support these data. Nonetheless, randomized clinical trials will be needed to confirm the above-mentioned results and overcome the limitations of observational studies.

4.8 Conclusion

Within the limits of our study, we can conclude that bone augmented with allograft onlays is comparable to the host native alveolar bone in terms of histological features and bone volume. For this reason, the success rate of implants placed in bone augmented with allograft onlays is comparable to the success rate of implants placed in either bone augmented with autograft onlays or even native alveolar bone.

4.9 Acknowledgement

The authors acknowledge the staff of “Clinica Dental Alcala”, the staff of “East Coast Oral Surgery continuing education Center” for their help and support. We wish to confirm that there are no known conflicts of interest associated with this publication, and there has been no significant financial support for this work that could have influenced its outcome.

Chapter Five: Synthetic Onlays.

==========

5.1 Osseointegration of Dental Implants in 3D Printed Synthetic Onlay Grafts Customized According to Bone Metabolic Activity in Recipient Site.

5.2 Abstract

Onlay grafts made of monolithic microporous monetite bioresorbable bioceramics have the capacity to conduct bone augmentation. However, there is heterogeneity in the graft behaviour *in vivo* that seems to correlate with the host anatomy. In this study, we sought to investigate the metabolic activity of the regenerated bone in monolithic monetite onlays by using positron emission tomography–computed tomography (PET-CT) in rats. This information was used to optimize the design of monetite onlays with different macroporous architecture that were then fabricated using a 3D-printing technique. *In vivo*, bone augmentation was attempted with these customized onlays in rabbits. PET-CT findings demonstrated that bone metabolism in the calvarial bone showed higher activity in the inferior and lateral areas of the onlays. Histological observations revealed higher bone volume (up to 47%), less heterogeneity and more implant osseointegration (up to 38%) in the augmented bone with the customized monetite onlays. Our results demonstrated that it is possible to achieve osseointegration of dental implants in bone augmented with 3D-printed synthetic onlays. It was also observed that designing the macropore geometry according to the bone metabolic activity was a key parameter in increasing the volume of bone augmented within monetite onlays.

5.3 Introduction

Dental implants are currently the preferred treatment option for replacement of teeth lost due to disease, trauma, surgery or congenital problems, because they are highly successful and maintain the integrity of the surrounding tissues [31, 32]. Successful implant placement requires sufficient alveolar bone volume in order to ensure implant stability and osseointegration [31, 92]. In severe cases of disease or trauma, alveolar bone must be restored before or in combination with implant placement. Although established procedures are highly successful for horizontal bone, vertical bone augmentation remains a major challenge due to anatomical limitations and technical difficulties [92, 229].

There are three major surgical approaches for alveolar ridge restoration: guided bone regeneration, bone augmentation and distraction osteogenesis [229]; however, each of these techniques has its own limitations when used in cases with severe alveolar bone loss [285]. Bone augmentation using onlay bone grafts, harvested from either intraoral or extraoral sites is currently the most reliable technique with the highest success rate [105, 286]. However, the use of autografts as onlays has many drawbacks such as the high morbidity and blood loss at the donor site, the need for multiple surgical sites, high resorption rate of the graft, and limited bone availability [103, 286, 287]. Not surprisingly, previous studies have reported that patients prefer a bone substitute block over an autograft block harvested from the iliac crest [285].

Synthetic bone substitutes, such as calcium phosphates, are being developed to eliminate the need of autologous grafts and to overcome their limitations [8]. Among these materials, dicalcium phosphate anhydrous (monetite) is of special interest because it

is a resorbable, osteoconductive and osteoinductive biomaterial [8, 217]. Moreover, monetite onlays could be suitable for vertical bone augmentation, and can be produced in customized designs using 3D-printing [10, 218].

The *in vivo* osteoconductivity of synthetic bone substitutes is dependent on several properties including morphology, chemical composition and geometry at both the macro- and micro-scale. Biomaterials pore size, distribution and interconnectivity can significantly influence the exchange of fluids and hence the delivery of ions, nutrients and cells within and through the bone substitute [288-293]. On the other hand, porosity can increase the biodegradation of the implant material by increasing the surface area in contact with body fluids, which may enhance the osteoinductive potential of the material [290], but may also mechanically weaken the material, so a fine balance must be found.

Dental implants can be successfully placed in onlays when the newly formed bone occupies 30-40% of the total volume of the onlay [157]. Previously we have shown that monetite onlays used for vertical bone augmentation could be infiltrated by new bone *in vivo*, occupying up to 43% of the graft volume after 8 weeks implantation [9]. However, these onlays were still inferior to autologous grafts and featured heterogeneous bone growth distribution across their medial-lateral and inferior-superior axes, where higher bone volume was observed in the lateral and inferior areas of the onlays, which matches the distribution of blood vessels in the recipient site.

Therefore, we hypothesized that the anatomy of the recipient site could influence the bone metabolism within monetite onlays, and therefore accordingly, modifying the design of the synthetic onlays using 3D-printing technique by adding geometrical

features that would facilitate and enhance the blood perfusion within the onlays could improve the bone growth in these onlays *in vivo*.

Previous studies proved that PET analysis could be used as a tool to assess bone viability in autogenous and allogeneic bone grafts [294, 295]. Compared to other techniques, PET can detect early-mineralized bone formation and provide insight into the bone metabolic activity that occurs at specific sites of the skeleton [296, 297].

Accordingly, the first aim of this study was to evaluate bone metabolic activity within monolithic monetite onlays *in vivo* using positron emission tomography-computed tomography (PET-CT). The second aim was to assess to what extent the customization of the onlay designed according to the anatomy and metabolic activity of the recipient site could affect the amount of bone formed in monetite onlays and its ability to osseointegrate with Ti dental implants.

5.4 Materials and Methods

5.4.1 Ethical Approval

In vivo experiments were approved by the ethical committee for animal experiments of the Rey Juan Carlos University of Madrid, Spain. Experiments were performed according to the guidelines described by the European Community Council Directive of 24 November 1986 (86/609/EEC), and adequate measures were taken to minimize pain and discomfort to the animals.

5.4.2 Assessment of bone metabolic activity in onlays

The aim of this part was to evaluate the metabolic activity within monolithic

monetite onlays using PET analysis.

5.4.2.1 Onlays fabrication and Three Dimensional-printing (3D-printing)

A previously described 3D-printing technique (Z-Corporation, Rock Hill, SC) was used to prepare dicalcium phosphate dihydrate (DCPD) onlays [214]. Briefly, a 2:1 molar ratio mixture of dicalcium phosphate anhydrous ($CaHPO_4$, monetite) (Merck, Darmstadt, Germany) and calcium carbonate ($CaCO_3$, calcite) (Merck, Darmstadt, Germany) was heated at 1400 °C for 7 h to synthesize α/β-tricalcium phosphate (α/β-TCP). After quenching to room temperature, the sintered mixture was crushed using a pestle and mortar, and then passed through a 160μm sieve. Finally, a planetary ball mill (PM400, Retsch, Germany) was used for milling β-TCP for 10 min. Brushite onlays were printed with a 3D-powder printing system (Z-Corporation, Rock Hill, S.C) using 20% of diluted phosphoric acid (H_3PO_4) and β-TCP powder (Merck, Darmstadt, Germany).

After being printed, the samples were retrieved from the powder bed, and cleaned from residual unreacted β-TCP powder. To increase the degree of reaction to DCPD, the samples were stored in 20% H_3PO_4 for 3 × 60 s, and the onlays were then concurrently dehydrated into monetite and sterilized by autoclaving (121 °C; humidity 100%; 30 min). The final onlays were composed of the samples was approximately 63% monetite and 37% unreacted β-TCP with a total porosity of 44% [10, 21]. Monetite monolithic blocks were prepared without any geometrical modifications using CAD software (Alibre design Xpress 10.0, Alibre Inc., Rock Hill, S.C). These blocks were cylindrical in shape (Ø 5.0 mm, 5.0 mm thick), and had a central hole (Ø 1.0 mm) for fixation with osteosynthesis screws (Mozo Gar, Valladolid; Spain).

5.4.2.2 Surgical procedure

Six monolithic onlays were placed on the calvarial bone of 6 female Wistar rats (0.2 – 0.4 kg weight). The rats were anaesthetized and the head was shaved. The cutaneous surface was disinfected with povidone iodine solution prior to the operation. A ~2cm long full depth incision was made on the linea media of the calvaria and the periosteum was separated from the bone surface with a periosteal elevator. The monolithic monetite blocks were secured with osseosynthesis titanium screws. The incision was closed with a silk 4-o suture and the animals were left to heal for 8weeks before being sacrificed with an overdose of sodium pentobarbital (Dolethal;Vetoquinol, France).

5.4.2.3 Computed tomography (CT) and Positron emission tomography (PET)

Computed tomography (CT) and positron emission tomography (PET) scanning were performed after 8 weeks of healing period using PET-CT Albira Ars machine (Oncovision, Valencia; Spain). The live animals were anesthetized and placed in a supine position. Consequently, they received an injection of 18F-NaF tracer (the dose was 15MSv per rat), and simultaneously they were introduced into the PET-CT scanning machine for 20 minutes. PET and CT images were taken in three sections (coronal, sagittal and horizontal) and processed by using the software PMOD 2.95 (PMOD technologies, Zurich University, Zurich; Switzerland) (Figure 5.1. a-i).

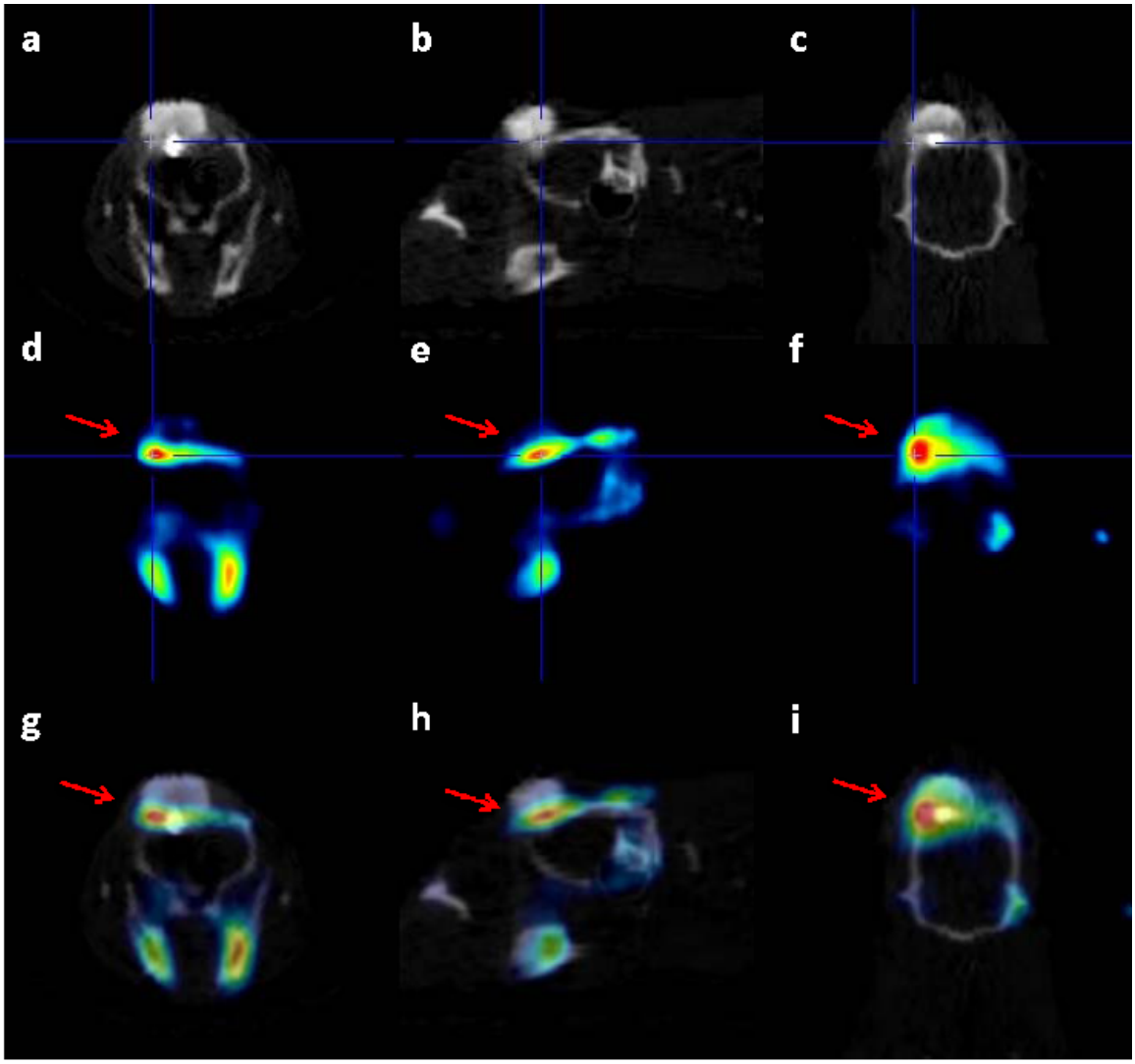

Figure 5.1: (a-c) CT scans of the onlays fixed with screws on the rats' calvaria bone in coronal, sagittal and horizontal sections respectively. **(d-f)** PET images, taken in a coronal, sagittal and horizontal sections respectively, demonstrating the low and high (red arrows) regions of bone metabolic activity. **(g-i)** Superimposed images of PET and CT scans, demonstrating that the high bone metabolic activity was in the lateral region of the onlays (red arrows) compared to the medial region.

5.4.3 Customizing onlays with different designs

5.4.3.1 Designs Fabrication

According to the findings of PET analysis for bone metabolic activity, onlays were designed to allow blood flow and bone formation from areas of high metabolic rate to areas of low metabolic rate. Therefore, different designs were created using CAD software (Alibre design Xpress 10.0, Alibre Inc., Rock Hill, S.C). All designs were cylindrical in shape (Ø 9.0 mm, 4.0 mm thick), and had a central hole (Ø 0.5 mm) for fixation with osteosynthesis screws (AO/ASIF 4.0 self-drilling screws, Synthes GmbH&Co, Umkirch, Germany) (Figure 5.2.a-c). The onlays were then printed as described earlier.

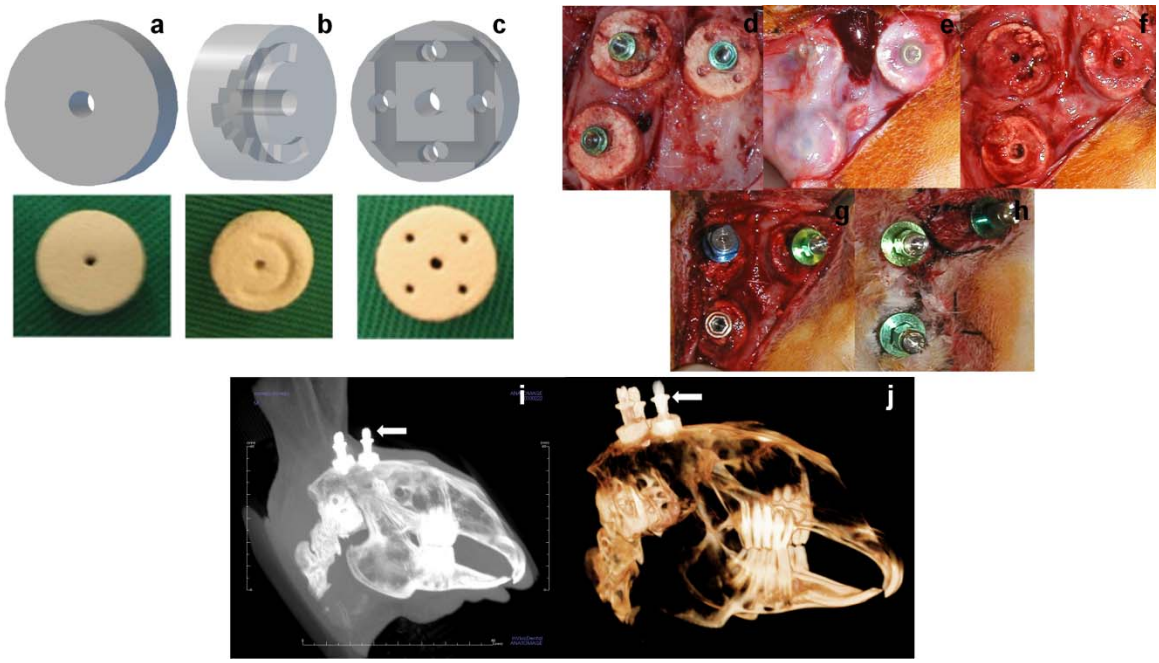

Figure 5.2: (a-c) CAD images of the onlay designs (top) compared with photographs of the 3D-printed monetite bioceramics (bottom): **(a)** Design A, monolithic without any surface modifications; **(b)** Designs B and C had a C-shaped groove either on the superior

surface of the onlay facing the periosteum (Design B) or on the inferior surface of the onlay facing the bone (Design C); **(c)** Design D had 8 interconnected channels (4 vertical and 4 horizontal) opened into all the surfaces of the onlay. All designs possessed a central hole to allow placement of osteosynthesis screws. **(d-h)** Photographs depicting the surgical procedure: **(d)** onlay placement fixation with osteosynthesis screws; **(e)** Opening of the surgical sites after 4 weeks, **(f)** and removal of the osteosynthesis screws; **(g)** Implant placement in the holes left be the removed screws; **(h)** Suturing of the surgical site. **(i,j)** CT scan and cone beam in a lateral view of the skull showing the Ti implants (arrows) in the monetite onlays following placement on the rabbit calvaria respectively.

5.4.3.2 Surgical Procedure

Sixteen New Zealand rabbits (3.5–4.0 kg) were used to test the customized onlays *in vivo*. The animals were anesthetized and their heads were shaved before disinfecting the cutaneous surface with povidone iodine solution prior to the surgery. A full depth incision (~5 cm) was made on the linea media of the calvaria, and then the periosteum was separated from the bone using a periosteal elevator. Onlays were placed on the calvarial bone and fixed with osteosynthesis titanium screws. After a healing period of 8 weeks, a second surgery was performed to expose the onlays and place the Ti dental implants after four weeks from the initial placement of the onlays (3.35 mm Ø, 8.5mm length; NobelBiocare, Kloten, Switzerland) (Figure 5.2.e-h) and then the incisions were closed with a silk 3-0 suture. Computed tomography (CT scan) and Cone beam images were taken in a lateral view of the rabbits' skull 4 weeks after Ti-implant placement,

followed by sacrificing the rabbits. After that, implant samples from surgical sites were collected for histological analysis (Figure 5.2. i and j).

5.4.3.3 Histological preparation

Histological examinations were performed on dehydrated and resin embedded sections as described previously [9, 10]. Shortly, the explants were fixed in 2.5% glutaraldehyde solution followed by dehydration in ascending concentrations of ethanol. The samples were then infiltrated and embedded in resin for 24 h before final polymerization (Technovit, Leica Microsystems GmbH, Wetzlar, Germany). Coronal histological sections crossing the centre of the onlays were taken using a micro saw (SP1600 Leica Microsystems GmbH, Wetzlar, Germany), and the samples were stained with methylene blue (MB) and basic fuchsine (BF).

Pictures of histological sections were taken by Bioquant Nova Prime software (BIOQUANT Image Analysis Corporation, Nashville, TN) using a ProgRes C14 digital camera (Jenoptik, Jena, Germany) installed on a Leica DMR light and fluorescence microscope (Leica DMR microscope type 020-525.024, Leica Microsystems, Wetzlar, Germany). Prior to analysis, the individual pictures were stitched using the software PTGui (New House Internet Services B.V., Rotterdam; The Netherlands) (Figure 5.3).

5.4.3.4 Histomorphometrical analysis

Images of the histological coronal sections crossing the centre of the blocks were used to perform the histomorphometrical analysis of the implanted area [9, 10]. For each histological section, the area occupied by the remaining unresorbed graft material, as well

as the bone growing around and within the onlays was identified and measured. These values were used to calculate the percentage of bone volume, and remaining material within the onlay, as well as the bone height and Ti implant osseointegration (Figure 5.4).

In each image section, the augmented bone area was divided into 24 smaller squares (1mm x 1mm) using a 6 column x 4 row computer generated grid which was adjusted to cover the entire onlay in the image, and localized histomorphometrical analysis was performed for each square (supplementary) [9, 10]. The localized histomorphometrical values of each square were interpolated in order to generate a statistical map of the distribution of bone and remaining monetite within the onlays using the Renka-Kline model [298] (Origin 7.0; Origin Lab Co., Northampton, MA) (Figure 5.5). The monetite resorption was quantified by subtracting the area of remaining monetite in the histological sections (after 8 weeks) from the original cross-sectional area of each onlay divided by the original cross-sectional area of each onlay adjusted to the original microporosity (44%).

To evaluate the bone height gained within the onlays during implantation, histological sections crossing through the dental implants at the centre of the onlays were evaluated. Vertical bone height was measured by calculating the distance between the original calvarial surface and the maximum bone height gained in the onlays. To assess the maximum bone height distribution within the onlays, the augmented bone area was divided into 8 smaller columns (1mm x 4mm) using the same computer generated grid described above, and maximum bone height in each column was measured (Figure 5.8). The software Image J (ImageJ 1.46r; Wayne Rasband, National Institutes of Health, Maryland) was used to assess the percentage of bone-to-implant contact ratio.

Kruskal-Wallis one-way analysis was used to evaluate any significant differences among the four designs, and Mann-Whitney test was used to evaluate head-to-head differences between the designs (SPSS 19, IBM Corp.; New York; USA). The statistical significance was set at a value of $P < 0.05$.

5.4.3.5 X-Ray Diffraction analysis (XRD)

X-ray diffraction (XRD) was used to analyze the crystallographic composition of the implanted onlays in the polymerized blocks using the X-ray diffraction spectroscopic machine (D8 DISCOVER/GADDS, Bruker, Karlsruhe, Germany) with a two-dimensional detector (50mm, HI-STAR, Bruker, Karlsruhe, Germany). XRD patterns were collected at 40kV and 40mA Cu Kα monochromatic radiation, and from 2θ= 20°-45° scanning angle with a step size of 0.02° and a normalized count time of 1s/step. The International Center for Diffraction Data references were used to check for α-TCP (PDF Ref. 09- 0348), β-TCP (PDF Ref. 09-0169), monetite (PDF Ref. 09-0080), brushite (PDF Ref. 09-0077) and hydroxyapatite (PDF Ref. 09-0432) using a DIFFRACplus EVA software (AXS, Bruker, Karlsruhe, Germany) that analyzes the data obtained from each XRD spectrum (Figure 5.9. a and b). To demonstrate the distribution of the HA and monetite crystals within the onlays, multi-target scan was run to record patterns of different points across the onlay. This multi-target scan was used to generate interpolated maps of the XRD patterns by using Origin program (Origin 7.0; Origin Lab Co., Northampton, MA).

5.5. Results

5.5.1 Bone metabolic activity

5.5.1.1 PET-CT analysis

None of the monolithic onlays grafted on rats calvaria were lost or showed any signs of inflammation. CT and PET imaging were performed 8 weeks after the grafting procedures, and CT images of the onlay in different sections showed that the onlays were well integrated to the calvarial bone (Figure 5.1. a-c). PET analyses showed that the bone metabolism was significantly higher in the lateral and inferior areas of the onlay compared to other areas (Figure 5.1. d-f). PET and CT scan were superimposed on each other to display the increase of bone metabolic activity that is shown in the PET images on the anatomical structure that could be seen in the CT images (Figure 5.1. g-i).

These results were used to construct the second objective of the study, where onlays with different geometry were designed to facilitate an equal distribution of the bone metabolic activity across the onlay.

5.5.1.2 Monetite onlays with different designs

The geometrical modification of the onlays was aimed to increase bone formation and blood flow in the medial and superior areas, hence they showed low bone metabolic activity according to the PET-CT analysis. Therefore, four designs were fabricated: Design A, monolithic without any modifications as a control group (Figure 5.2.a). Design B included a C-shaped groove with a hill-like depth profile on the superior surface of the onlay facing the overlain periosteum. The length of the groove equals half the circumference of the cylinder's surface, where the groove sloped inside the onlay (Figure

5.2.b). When implanted, the deepest part of the groove is the most inferior surface of the slope facing the midline suture of the calvarial bone, and the shallowest part is at the ends of the groove (Figure 5.2.d).

Design C was the same as Design B, but the C-shaped groove was placed on the inferior surface of the onlay facing the periosteally stripped bone, where the deepest part of the groove would be the most superior surface of the slope (Figure 5.2.b). Designs B and C were fabricated to assess the influence of adding macroporosity in different regions of the onlay.

Design D included 8 interconnected channels open at all the surfaces of the onlay. Four vertical channels open on the superior and inferior surfaces of the cylinder, and four horizontal channels open on the sides of the cylinder (Figure 5.2.c) to allow blood diffusion from the high metabolic areas (lateral and inferior) to low metabolic areas (medial and superior). The final phase composition of the samples was approximately 63% monetite and 37% unreacted β-TCP. All design features were discernable at the resolution of printing with a total microporosity of 44% and a micropore diameter of 10–20 μm [8].

5.5.2 Bone augmentation with customized onlays

5.5.2.1 Surgical observation

During the two surgical procedures and the post-operative phase, no complications were noticed. Upon implant retrieval, no signs of rejection were observed in all the onlays and they all appeared to be integrated and vascularised. Moreover, no loosening of the Ti implants or onlays was observed (Figure 5.2. i and j).

5.5.2.2 Histological observation

Histological observations revealed that the onlays were well integrated with the calvarial bone (Figure 5.3). In addition, no inflammatory cell infiltration was found around or within the onlays (Figure 5.3). Bone infiltration and blood vessels formation occurred throughout the monetite onlays of all designs (Figure 5.3), although it was more pronounced inside the holes of Design D and grooves of Design C (Figure 5.3.d and c).

Abundant soft tissue formation and scarce bone infiltration was observed on the superior areas of the groove in Design B; however, the inferior part of the groove showed more bone formation in comparison to the other parts of the same groove (Figure 5.3.c). The Ti implants appeared to be osseointegrated with the new bone formed in the onlays, as it can be inferred from the close contact observed between the infiltrated bone and the surface of the Ti implants (Figure 5.3).

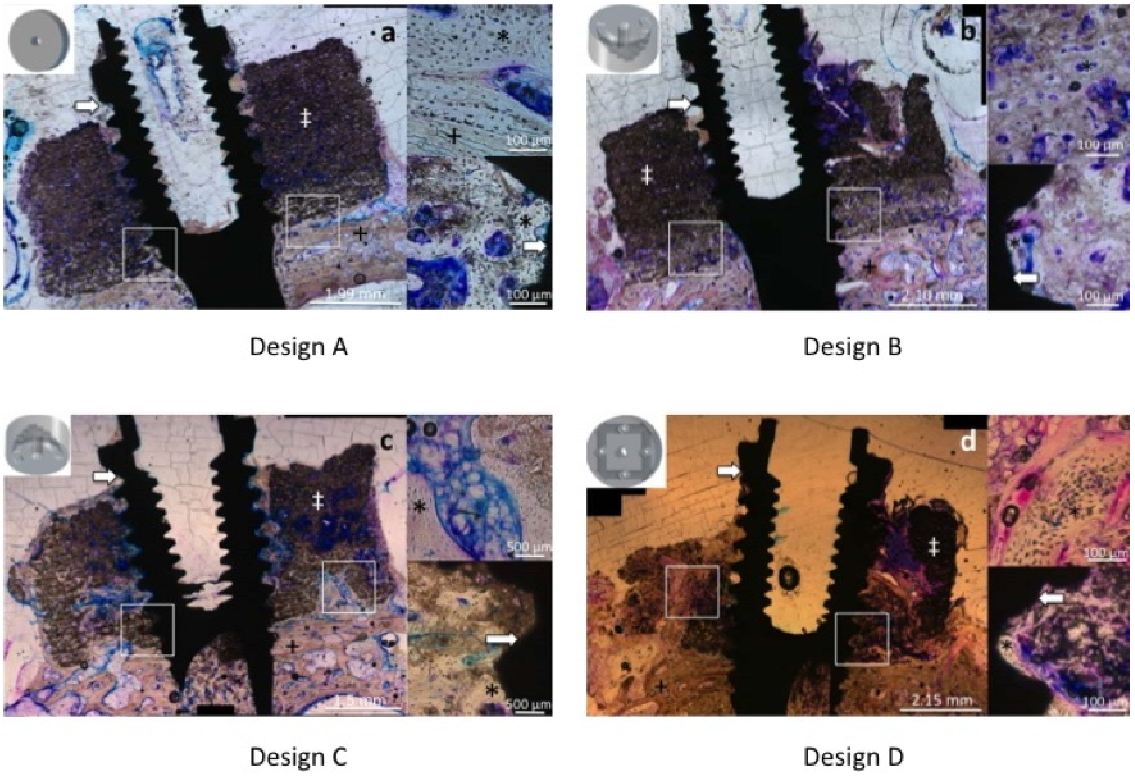

Figure 5.3: Histological micrograph sections taken from: Design A **(a)**, Design B **(b)**, Design C **(c)**, and Design D **(d)** showing bone infiltration within the monetite onlays (‡) grafted on the calvarial bone in rabbits (+), and Ti dental implant (arrow). Original magnification x2.5. Inserts show magnified sections of images (a, b, c and d) showing the osseointegration interface between the newly formed bone (*) in the onlays and the Ti implants (arrow), and the integrated area between the calvarial bone (+) and the bone infiltrated in the onlays (*), original magnification x20.

5.5.2.3 Histomorphometrical analysis

5.5.2.3.1 Bone augmentation within onlays

Histomorphometric analysis revealed that the percentage of new bone formed in the onlays ranged between 35.7 ± 9.8 % (Design A) to 46.9 ± 5.7 % (Design D) of the

total onlay area (Figure 5.4.a). Although Kruskal-Wallis test did not show any significant differences among the designs, Mann-Whitney test showed that there was a significant head-to-head difference between designs A and D (P=0.047), as well as between designs B and D (P=0.028) (Figure 5.4.a). The interpolated maps of the histomorphometrical analysis for the distribution of augmented bone within the onlays revealed that more bone formed in the lateral and inferior areas of all the onlays as well as inside the holes and grooves, and less bone formed in the superior and medial areas (Figure 5.5, Figure 5.6, and Figure 5.7.a).

In the areas close to the calvarial bone (inferiorly), designs A and C showed more bone formation in the lateral side compared to the medial side. However, designs B and D showed almost equal amount of bone infiltration in both sides (Figure 5.5, Figure 5.6, and Figure 5.7.a). In the superior areas close to the periosteum, all designs showed more bone formation in the lateral areas than the medial areas (Figure 5.5, Figure 5.6, and Figure 5.7.a).

The groove in both designs B and C showed more bone formation in the inferior and lateral areas compared to the superior and medial ones (Figure 5.5, Figure 5.6, and Figure 5.7.a). In addition, Design D showed more bone formation inside the holes compared to the other areas (Figure 5.5, Figure 5.6, and Figure 5.7.a), and more bone formation was observed in the inferior areas of the holes compared to the superior areas (Figure 5.5, Figure 5.6, and Figure 5.7.a).

5.5.2.3.2 Effect of customized macroporous geometry on bone formation

Although the heterogeneity of bone distribution was noticeable in Design A, the other designs showed more uniformly bone distribution along the medial-lateral and superior-inferior axes. In areas close to the periosteum, designs C and D showed higher bone formation in the lateral side compared to designs A and B (Figure 5.5, Figure 5.6, and Figure 5.7.a). However, all designs showed little or no bone formation in the most superior-medial area.

The groove in Design C showed more bone formation and no soft tissue infiltration compared to Design B (Figure 5.5, Figure 5.6, and Figure 5.7.a). In addition, designs B and C showed high bone formation in the area around the implant compared to designs A and D, where Design D showed more bone formation in the sides of the onlay compared to the centre area (Figure 5.5, Figure 5.6, and Figure 5.7.a).

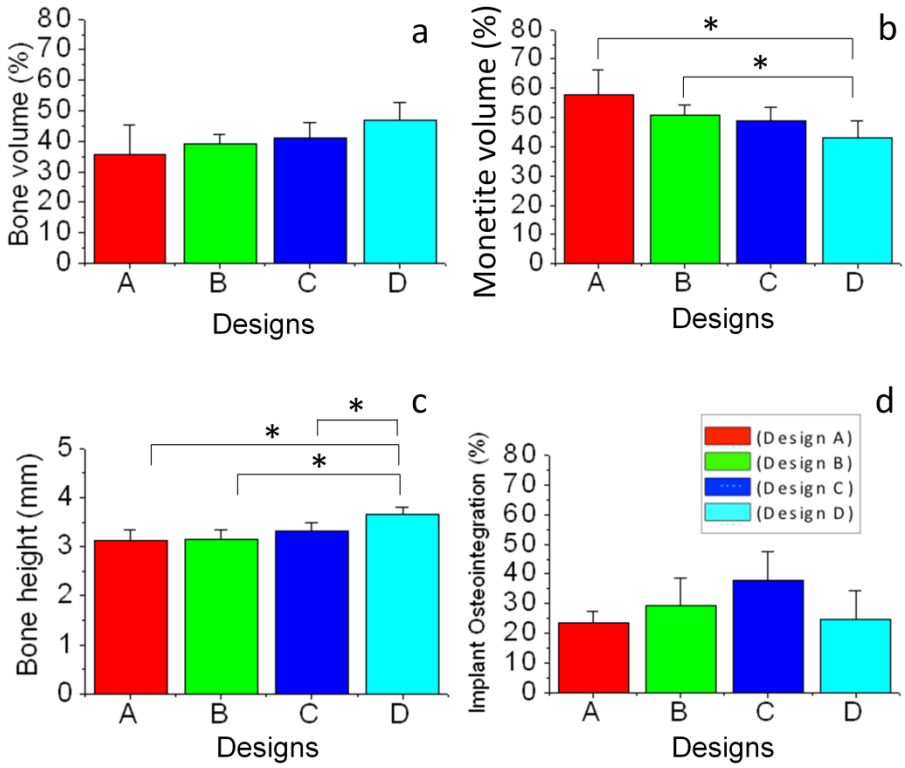

Figure 5.4: Graphs of the histomorphometrical analysis representing: **(a)** Bone volume percentages and **(b)** monetite percentage in the different onlay designs. **(c)** Ti implant osseointegration, **(d)** bone height gained in the different onlay designs (*) Indicates that there is significant difference between the designs (P value < 0.05).

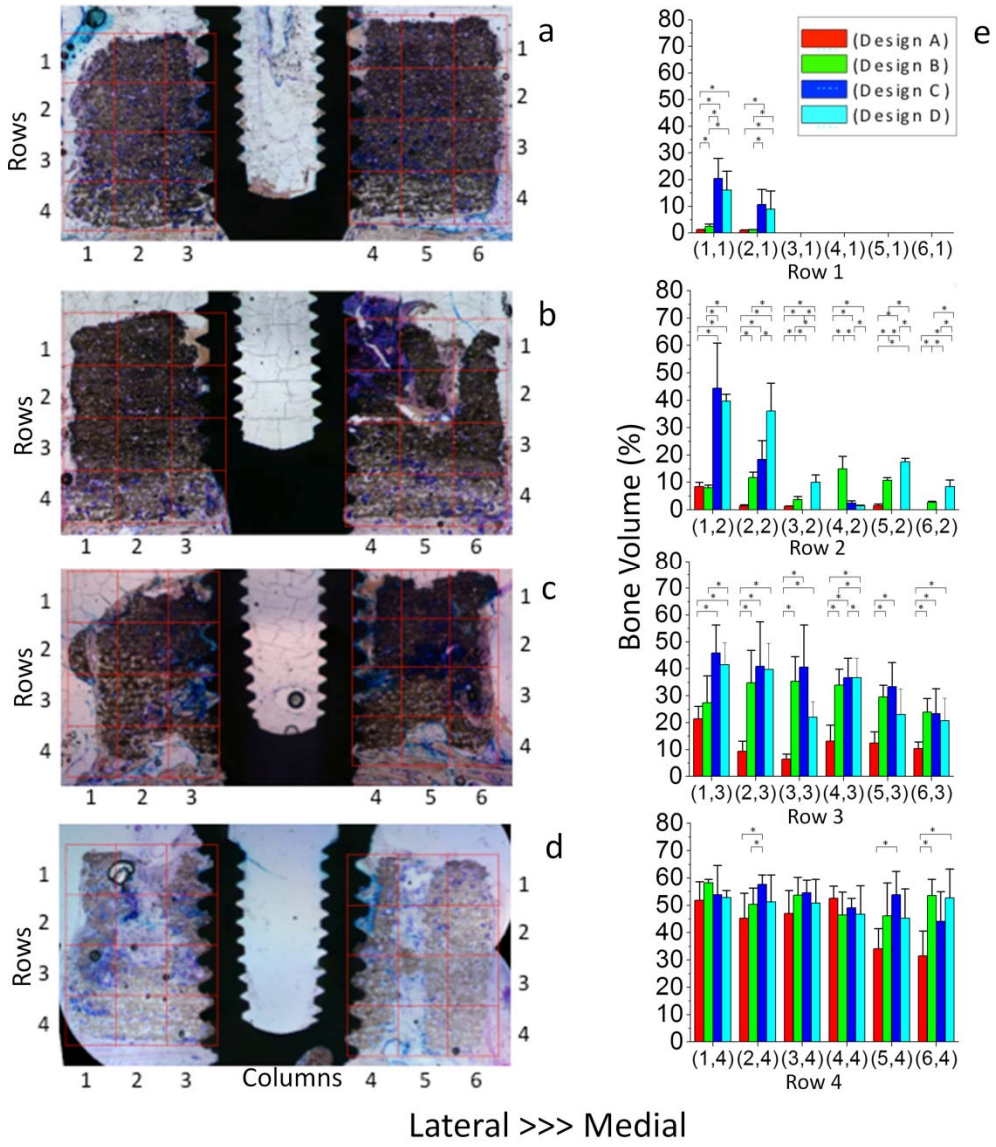

Figure 5.5: Coronal histological cross sections of Design A (the control design), Design B (the design with upper groove), Design C **(**the design with lower groove), and Design D (the design with 8 interconnected holes). The area occupied by the onlay in the micrograph was divided into 24 squares (1mm x 1mm) using a 6 column x 4 row grid to fit the onlay site for local histomorphometrical analysis. **(e)** Results of the local histomorphometrical analysis of bone volume in each square in the grid. (*) Indicates that there is significant difference among the designs (p value < 0.05)

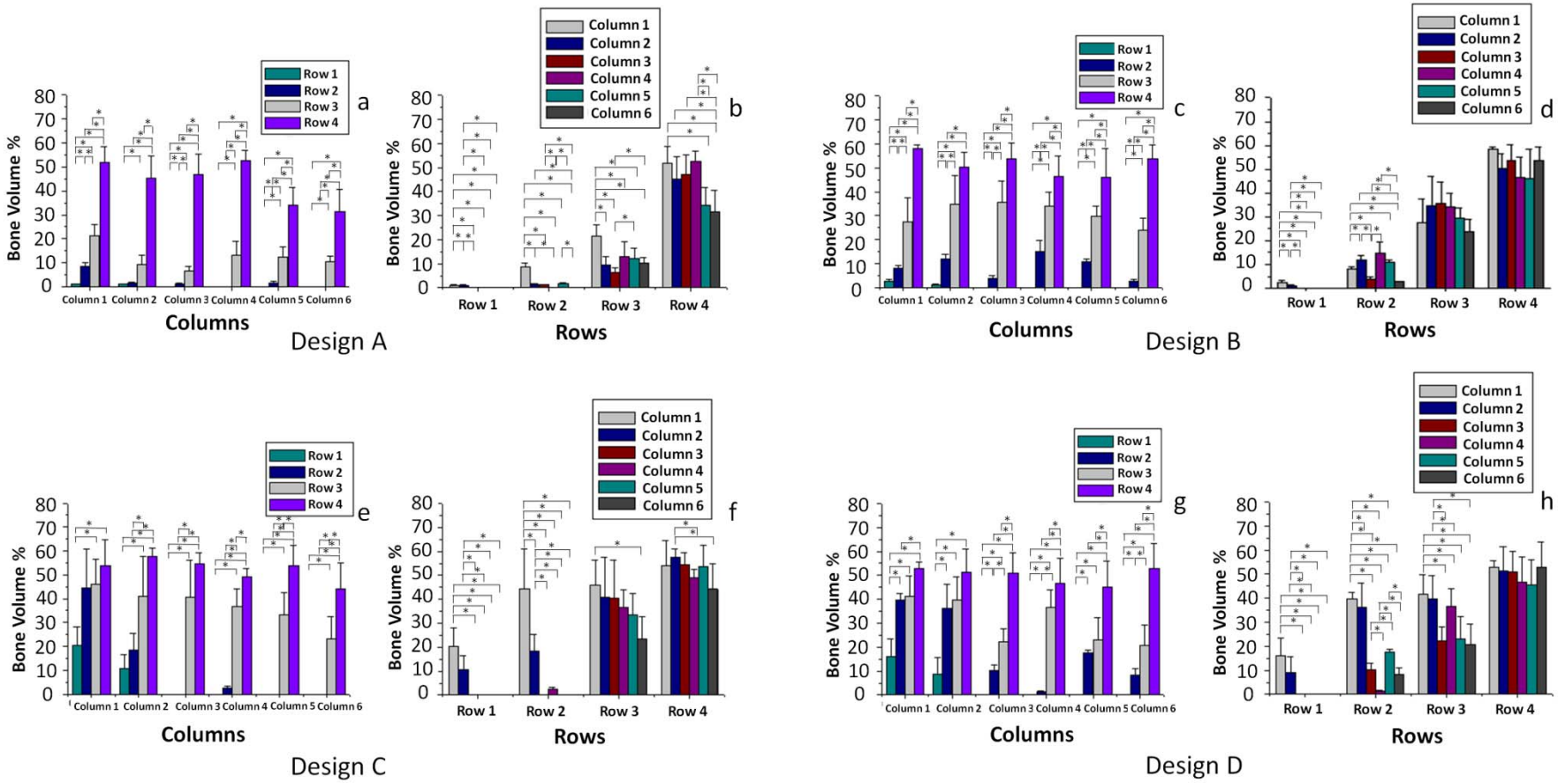

Figure 5.6: (a-h) Results of the local histomorphometrical measurements of bone infiltration in each row and column in the grid for each specific design (Fig. 5.5). (*) Indicates that there is a significant difference between columns and rows of each design (p value < 0.05).

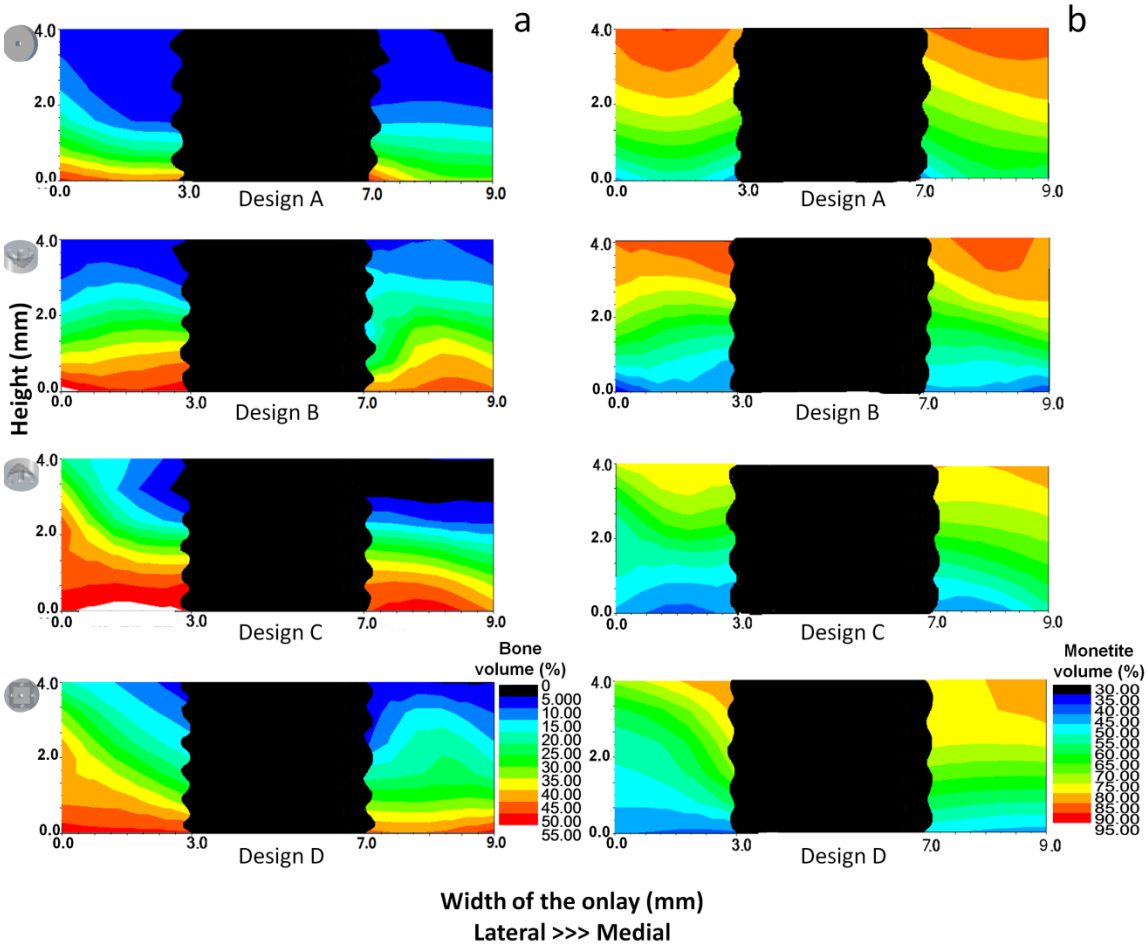

Figure 5.7: Interpolated maps of the histomorphometrical results in (Figure 5.5): **(a)** the averaged distribution of the newly formed bone in the onlays of the four designs. Red and orange colours show intense bone growth. Yellow and greens colours indicate moderate new bone formation, while blue and black indicate low bone formation in the onlays. **(b)** Distribution of the remained material within the onlays of the different designs. Red and orange colours show concentrated remaining material. Yellow and greens colours indicate moderate material, while blue and black indicate low material left in the onlays.

5.5.2.3.3 Bone height gained

The average bone height gained in the monetite onlays ranged from 3.1±0.2 mm in Design A to 3.7±0.1 mm in Design D. The Mann-Whitney test showed that there were significant differences between the designs A and D (P=0.021), B and D (P=0.021), C and D (P=0.021) (Figure 5.4.c). All onlays gained more bone height in the lateral area compared to the medial area (Figure 5.8). According to the Kruskal Wallis test, there were no significant differences between the medial areas of the designs. However, the Mann-Whitney test showed that designs C and D gained significantly more bone height in comparison to the other designs.

In the medial area close to the implant, a significant difference in bone height was found between designs D and B (P=0.021), as well as designs D and C (P=0.021) (supplementary). In the centre of the medial area, there were significant differences between designs D and A (P=0.021), designs D and B (P=0.021), designs D and C (P=0.043), as well as between designs A and C (P=0.021), and designs B and C (P=0.021) (Figure 5.8). In addition, the most medial side of the onlay showed a significant difference between designs A and C (P=0.043), as well as designs A and D (P=0.021).

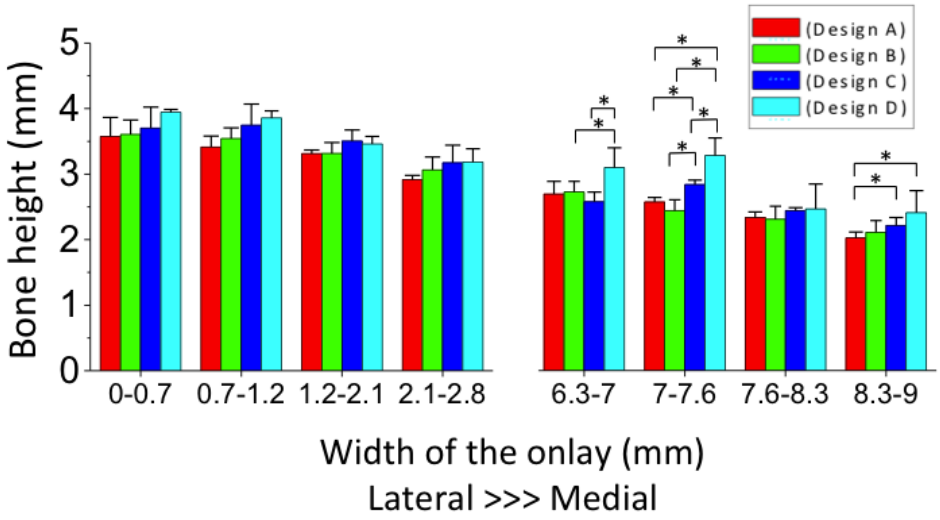

Figure 5.8: Local histomorphometrical measurements of the coronal histological cross sections in (Figure 5.5), using 8 x 1 computer generated grid adjusted to divide the area of the onlays into 8 smaller areas (1mm x 4mm), showing the average maximum height of bone growth within the onlays

5.5.2.3.4 Monetite resorption

The percentage of remaining unresorbed monetite ranged between 43.1 ± 5.7 % (in Design D) and 57.7 ± 8.5 % (in Design A) of the total onlay area, with significant differences between designs A and D (P =0.037), as well as between designs B and D (P=0.037) (Figure 5.4.b). The interpolated maps of the remaining monetite distribution showed that a scarce amount of monetite remained in the inferior areas of all the onlays, and a greater amount remained in the medial and upper areas of designs A and B compared to designs C and D (Figure 5.7.b.). The monetite resorption in Design A reached 42.2 ± 8.9%, and reached 47.9 ± 6.9% and 51.0 ± 8.1% in designs B and C respectively, and 56.5 ± 7.4% in Design D. The monetite resorption in Design D was

significantly higher than in Design A, with a significant difference between Design A and D (P=0.047).

XRD pattern analysis confirmed the histological observations and demonstrated that the crystals of the remaining material were composed of monetite and β-TCP only (Figure 5.9. c and d). XRD interpolated maps of Design B demonstrated that bone (apatite crystals) was more concentrated in the lateral and inferior regions of the onlay compared to the medial and superior ones where monetite crystals were more concentrated (Figure 5.9. a and b).

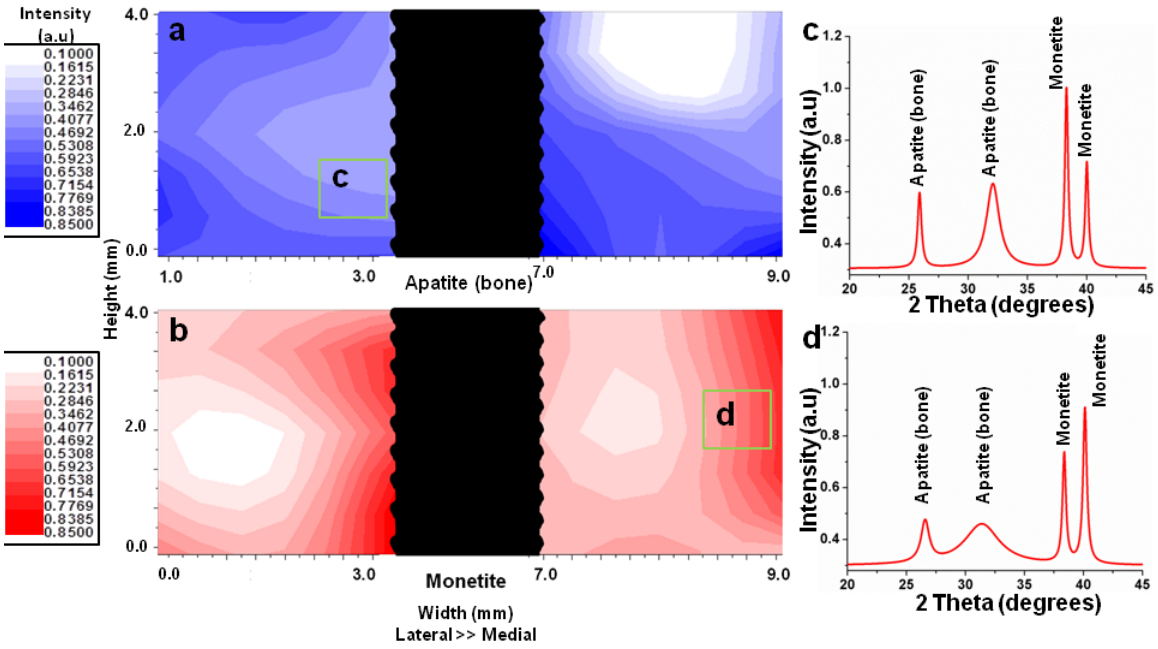

Figure 5.9: Interpolated maps of the XRD phase analysis demonstrating the distribution of **(a)** apatite crystals (bone) and **(b)** monetite crystals across the onlays. The red and blue colours indicate high concentrations of material crystals, while the white colour indicates low concentration of both materials. **(c,d)** XRD patterns of the remaining material (apatite (bone) and monetite) within the onlay, demonstrating the materials intensity according to the diffraction angle 2θ.

5.5.2.3.5 Implant osseointegration

The surface of the Ti-implants placed in the onlays was partially osseointegrated (20.9 ± 9.7% - 37.8 ± 9.9%). According to Kruskal Wallis test, there was no significant differences among the four designs; however, the Mann-Whitney test revealed that there was a significant difference in osseointegration between designs C and A (P=0.021) (Figure 5.4.d), where the highest bone to implant contact ratio was achieved in Design C and the lowest ratio in Design A. Onlays in Design A showed more osseointegration between the infiltrated bone and the lateral surface of the implant compared to the medial surface; however, Design B showed more osseointegration in the medial side where the groove was located. On the other hand, onlays from designs C and D showed almost equal bone to contact ratio in both sides of the implant.

5.6 Discussion

5.6.1 Bone metabolic activity

The bone formation process was monitored by positron emission tomography–computed tomography (PET-CT) (8 weeks) after placement of the onlays. This fused PET-CT method allowed the detection of the activity of mineralized bone formation in a 3D bony architecture reconstructed by the CT scan. Bone metabolism showed a higher activity in the lateral and inferior regions of the onlay compared to the medial region, and showed no activity in the superior region in the early detection of bone formation. These findings were in agreement with our previous studies, where similar heterogeneous bone growth distribution across the onlay was noticed; however, the reason behind it was not clear [9]. Previous studies demonstrated that bone metabolic activity is directly related to

the host bone formation and blood flow [299, 300]; therefore, using PET-CT findings enabled us to provide an accurate picture of bone metabolic activity, bone formation and blood flow in monetite onlays augmented on the calvarial bone. Here we showed that the PET-CT can be a very useful method for surveying the viability of the newly formed bone in synthetic bone grafts.

5.6.2 Bone augmentation with customized onlays

5.6.2.1 Bone augmentation within onlays

All onlay designs shared the same microporosity throughout the materials (pore size <20μm [300]) with a total porosity of 44% [8]. However, the different macroporosity (i.e. pore size >100 μm [300]) of each design effected the augmented bone volume, bone height gained, and Ti implant osseointegration within the onlays.

According to the literature, the minimum pore size required to regenerate mineralized bone is considered to be <100μm [299]. Smaller pores (75–100 μm) resulted in the ingrowth of un-mineralized osteoid tissue, and pores of 10–44 and 44–75 μm were penetrated only by fibrous tissue [299]. However, larger pore sizes of 300–400 μm showed new bone and capillary formation [299]. Therefore, the 1 mm holes and grooves in designs D, B and C were expected to promote the growth of bone and capillaries.

The effect of microporosity and macroporosity in synthetic blocks was already confirmed in the previous studies by increasing or decreasing the micro- or/and the macroporosity in these blocks [8, 301]. However, in this study, macroporosity was designed to facilitate the blood diffusion from areas with higher metabolic rate to areas with lower rate as mentioned earlier in the results section. Therefore, our results

demonstrate that introducing customized macroporous geometry can significantly increase the amount of new bone that is formed within synthetic onlay grafts. The mean average of augmented bone volume gained ranged between 36% (Design A – no macropores) and 47% (Design D – most macropores) of the total onlay area. These results agree with previous studies showing that adding large holes and increasing macroporosity leads to an improvement of bone formation in synthetic biomaterials [302, 303].

Regardless of the design, bone was always more abundant in the lateral and inferior areas of the onlays. This spatially dependant effect was also seen in a previous study in which monolithic monetite onlays were used [304] and was expected to be seen in the PET analysis, indicating that the bone metabolic activity was higher in the lateral and inferior regions of the calvaria probably due to the anatomy of the blood vessels in the calvarial bone.

On the other hand, the distribution of bone formed within the medial and superior areas seemed to be influenced by the onlay design. Our results indicate that the macroporosity seem to have influenced the bone distribution by directing the bone growth from high metabolic areas to the rest of the graft through the holes and grooves. The superior areas of the onlays showed higher bone formation in designs C and D compared to designs A and B. In addition, the medial side showed higher bone formation in designs B, C and D compared to Design A.

Although Design D showed more overall bone formation (47%) compared to Design A (36%), the bone volume achieved in Design D was still lower than the one reported for autologous onlays (55-60%) [9]. However, the bone volume in the

customized monetite onlays reached over 35% of the total graft volume, which could certainly be considered as a successful grafting procedure [305].

Designs B and C had a groove around the implant, on the upper surface facing the periosteum or the lower surface facing the calvarial bone respectively. These two designs were produced to assess the influence of adding macroporosity in different regions of the onlay as mentioned earlier in the results section. The design with a groove facing the calvarial bone (Design C) had higher percentage of bone formation in comparison to the design with the groove facing the periosteum (Design B). These results seem to indicate that bone regeneration might be originating from the calvarial bone but not from the periosteum. This is in agreement with previous studies on bone augmentation in rabbit calvaria [219, 306]. During bone regeneration, stem cells are produced from either the periosteum or the cancellous bone to assist in bone growth [307]. Although the periosteum plays an important role in long bone regeneration [308], previous studies have demonstrated that the periosteum covering the calvarial bone has a minor role in osteogenesis and only enhances bone formation in the areas close to it [219, 306].

5.6.2.2 Bone height gained

The overall bone height gained was significantly higher in Design D compared to the other designs, which was probably due to the presence of high macroporosity in Design D that lead to the increase in bone formation and therefore the increase in bone height. In addition, increasing macroporosity significantly enhanced the distribution of bone height gained in the medial areas for Design D in comparison to the other designs (Figure 5.8).

In this study, customized monetite onlays were able to provide an additional bone height of almost 4 mm when placed on the calvarial bone (2mm). This indicates that augmenting a severely resorbed mandible (< 7.0 mm, Cawood type IV[82]) with these onlays can provide sufficient bone height for the placement of dental implants [82, 103, 309]. Although future studies will have to be done to prove that this is possible in human subjects.

5.6.2.3 Monetite resorption

After 8 weeks of implantation, the percentage of the remaining monetite material in the onlays ranged from 43% to 57% of the total original area of the onlays. This is similar to previous studies in which it was shown that after *in vivo* implantation of the onlays, only 50-66% of monetite remained after a period of 8 weeks [9, 214].

According to the Hixon and Crowell equation, two factors affect the dissolution rate of a given material *in vivo*, the properties of the material itself such as geometry (porosity and surface area) and solubility, and the properties of the dissolving medium such as the volume and temperature [310]. Rabbits have a stable temperature and concentration of ions in serum, in addition to the high rate of water exchange because of their low body mass [219, 305]. Therefore, the resorption rate of the monetite that is mainly due to either passive dissolution or the cellular activity would depend mostly on its solubility and geometry [311]. This explains the significantly lower amount of remaining monetite in Design D compared to the other designs. Since this design had more macroporosity that increased the surface area that is in contact with the body fluids facilitating monetite resorption in these onlays.

The size of the holes and grooves in designs B, C and D were large enough for cells to go through and increase the monetite resorption by cellular activity. However, resorption of monetite in designs B (47.9%), C (51.0%) and D (56.5%) was very similar to Design A (42.2%). This seems to indicate that macropores allowing cellular infiltration had a minor effect on monetite resorption and passive diffusion was the main mechanism affecting the resorption of these onlays.

The volume of macroporosity (including holes and grooves) in each design was 0.31% in Design A, 5.86% in designs B and C, and 14.71% in Design D. Although there was a difference between the ratios of the macroporosity in each design, monetite resorption factor was almost identical among all the designs. This means that the high microporosity in all designs (44%) played a major role in monetite resorption, and the macroporosity only played a minor role.

XRD analysis at the end of the two surgical procedures showed that the crystalline pattern of the onlay consists of three materials, monetite, β-TCP and apatite, confirming our previous observations [9]. The interpolated maps of the XRD analysis demonstrated that monetite was the main constituent of the medial and superior regions of the onlay, and poorly crystalline apatite was found in the inferior and the lateral region of the onlay. Both XRD and histological findings seem to agree in indicating that bone was present in the areas where there was no monetite. In addition, there was no evidence of monetite conversion to hydroxyapatite throughout the onlay.

5.6.2.4 Dental implant osseointegration

In this study, we demonstrated for that bone augmented with synthetic onlays can osseointegrate with Ti dental implants. Four weeks after placing the Ti implants, 21-38% of their surface was osseointegrated with the newly formed bone within the monetite onlays. A previous study stated that 50% of bone to implant contact ratio is needed to provide a stable implant restoration [312]; however, placement of dental implants can be considered successful when the newly formed bone volume reaches 30-40% of the total graft volume [157]. Therefore, the volume of bone infiltration reached in our monetite onlays (36-47%) demonstrates that monetite onlays are probably suitable for a successful Ti dental placement, although future studies should be done to improve the bone to implant contact ratio in monetite onlays.

In addition, the local bone metabolic activity and anatomy affected the bone-implant contact ratio of each side of the dental implant, whereupon the ratio was higher in the lateral side of the implant in the Design A compared to the medial side. On the other hand, the ratio was higher in the medial side of the implant in Design B due to the presence of the groove in that area leading to more bone formation in the medial side and therefore higher osseointegration ratio was achieved. Design C and D, showed almost equal bone to implant contact ratios in both sides, hence the bone infiltration was distributed homogenously in the medial and lateral areas of these designs. Although Design D had higher bone formation percentage among all the designs, Design C had the highest bone to implant contact ratio than all the other designs including Design D. This was probably because the holes in Design D directed bone formation to the sides of the onlays and away from the implant and had less influence over implant osseointegration,

while the groove in Design C was close to the implant, which facilitated the direction of bone growth towards the implant (Figure 5.3.c). Therefore, increasing the complexity of onlay design can compensate for differences due to anatomical features.

5.7 Limitations and future studies

This study was not designed to assess the biodegradation rate of monetite onlays, since the complex geometry of the onlays hindered the calculation of the original onlay volume. Therefore, future studies are needed in order to explore the effects of geometry on onlay resorption. Moreover, this study did not include any mechanical tests for the osseointegrated implants, which should be considered in the future. Even though both the calvarial bone and the mandible form intramembranously, vertical bone augmentation is mostly relevant in the posterior atrophic mandible. Accordingly, future studies should be done for clinical applications in the mandible. Onlays could be designed to direct bone growth toward the implants in future studies, because this will increase the osseointegration in synthetic onlays.

5.8 Conclusion

Our results demonstrate that bone metabolic activity in onlays is anatomy-dependant and correlated with the ability of bone augmentation. In addition, the results demonstrate that it is possible to achieve osseointegration of dental implants in bone augmented with synthetic monetite onlays. Macroporous geometry can enhance bone growth, bone height gained and Ti implant osseointegration within the monetite onlays. Onlays geometry should be designed to facilitate the diffusion of cells and nutrients from

high bone metabolic to low bone metabolic areas. More bone formation was found in onlays with increased porosity facing the calvarial surface compared to onlays with porosity facing the periosteum.

5.9 Acknowledgements

The authors acknowledge financial support from ‘‘Fundacion Espanola para la Ciencia y Tecnologia’’ (FECYT); The Spanish Science and Education Ministry (MAT2006-13646-C03-01); the UCM Program for Research Groups; The Canada Research Chair program, NSERC Discovery Grant (J.E.B.), NSERC Discovery Grant (F.T) and the Québec Ministère des Relations Internationales (Québec-Bavaria Exchange Program) PSR-SIIRI-029 IBI; and the dental implant provider.

Chapter Six: Conclusion

==========

From the results of this thesis we can conclude the following:

- Bone augmented with allograft onlays is comparable to the host native alveolar bone in terms of histological features and bone volume.
- The success rate of implants placed in bone augmented with allograft onlays is comparable to the success rate of implants placed in either bone augmented with autograft onlays or even native alveolar bone.
- Bone metabolic activity in onlays is anatomy-dependant and correlated with the ability of bone augmentation.
- It is possible to achieve osseointegration of dental implants in bone augmented with synthetic monetite onlays.
- Macroporous geometry can enhance bone growth, bone height gained and Ti implant osseointegration within the monetite onlays.
- Onlays geometry should be designed to facilitate the diffusion of cells and nutrients from high bone metabolic to low bone metabolic areas.
- More bone formation was found in onlays with increased porosity facing the calvarial surface compared to onlays with porosity facing the periosteum.

Chapter Seven: References

==========

[1] Clementini M, Morlupi A, Agrestini C, Ottria L. Success rate of dental implants inserted in autologous bone graft regenerated areas: a systematic review. Oral & implantology. 2011;4:3-10.
[2] Esposito M, Grusovin MG, Felice P, Karatzopoulos G, Worthington HV, Coulthard P. Interventions for replacing missing teeth: horizontal and vertical bone augmentation techniques for dental implant treatment. The Cochrane database of systematic reviews. 2009:CD003607.
[3] Bhatt RA, Rozental TD. Bone graft substitutes. Hand clinics. 2012;28:457-68.
[4] Waasdorp J, Reynolds MA. Allogeneic bone onlay grafts for alveolar ridge augmentation: a systematic review. The International journal of oral & maxillofacial implants. 2010;25:525-31.
[5] Araujo PP, Oliveira KP, Montenegro SC, Carreiro AF, Silva JS, Germano AR. Block allograft for reconstruction of alveolar bone ridge in implantology: a systematic review. Implant dentistry. 2013;22:304-8.
[6] Levai JP, Bringer O, Descamps S, Boisgard S. [Xenograft-related complications after filling valgus open wedge tibial osteotomy defects]. Revue de chirurgie orthopedique et reparatrice de l'appareil moteur. 2003;89:707-11.
[7] Lumetti S, Consolo U, Galli C, Multinu A, Piersanti L, Bellini P, et al. Fresh-frozen bone blocks for horizontal ridge augmentation in the upper maxilla: 6-month outcomes of a randomized controlled trial. Clinical implant dentistry and related research. 2014;16:116-23.
[8] Habibovic P, Gbureck U, Doillon CJ, Bassett DC, van Blitterswijk CA, Barralet JE. Osteoconduction and osteoinduction of low-temperature 3D printed bioceramic implants. Biomaterials. 2008;29:944-53.
[9] Tamimi F, Torres J, Gbureck U, Lopez-Cabarcos E, Bassett DC, Alkhraisat MH, et al. Craniofacial vertical bone augmentation: a comparison between 3D printed monolithic monetite blocks and autologous onlay grafts in the rabbit. Biomaterials. 2009;30:6318-26.
[10] Torres J, Tamimi F, Alkhraisat MH, Prados-Frutos JC, Rastikerdar E, Gbureck U, et al. Vertical bone augmentation with 3D-synthetic monetite blocks in the rabbit calvaria. Journal of clinical periodontology. 2011;38:1147-53.
[11] Branemark PI, Adell R, Breine U, Hansson BO, Lindstrom J, Ohlsson A. Intra-osseous anchorage of dental prostheses. I. Experimental studies. Scandinavian journal of plastic and reconstructive surgery. 1969;3:81-100.
[12] Branemark PI, Hansson BO, Adell R, Breine U, Lindstrom J, Hallen O, et al. Osseointegrated implants in the treatment of the edentulous jaw. Experience from a 10-year period. Scandinavian journal of plastic and reconstructive surgery Supplementum. 1977;16:1-132.
[13] Zarb GA, Zarb FL. Tissue integrated dental prostheses. Quintessence international. 1985;16:39-42.

[14] Cochran DL, Morton D, Weber HP. Consensus statements and recommended clinical procedures regarding loading protocols for endosseous dental implants. The International journal of oral & maxillofacial implants. 2004;19 Suppl:109-13.
[15] Weiss CM. A comparative analysis of fibro-osteal and osteal integration and other variables that affect long term bone maintenance around dental implants. The Journal of oral implantology. 1987;13:467-87.
[16] Terheyden H, Lang NP, Bierbaum S, Stadlinger B. Osseointegration--communication of cells. Clinical oral implants research. 2012;23:1127-35.
[17] Abrahamsson I, Berglundh T, Linder E, Lang NP, Lindhe J. Early bone formation adjacent to rough and turned endosseous implant surfaces. An experimental study in the dog. Clinical oral implants research. 2004;15:381-92.
[18] Berglundh T, Abrahamsson I, Lang NP, Lindhe J. De novo alveolar bone formation adjacent to endosseous implants. Clinical oral implants research. 2003;14:251-62.
[19] Bosshardt DD, Salvi GE, Huynh-Ba G, Ivanovski S, Donos N, Lang NP. The role of bone debris in early healing adjacent to hydrophilic and hydrophobic implant surfaces in man. Clinical oral implants research. 2011;22:357-64.
[20] Singhatanadgit W. Biologic responses to new advanced surface modifications of endosseous medical implants. Bone and tissue regeneration inights. 2009:2 1-11.
[21] Shard AG, Tomlins PE. Biocompatibility and the efficacy of medical implants. Regenerative medicine. 2006;1:789-800.
[22] Thevenot P, Hu W, Tang L. Surface chemistry influences implant biocompatibility. Current topics in medicinal chemistry. 2008;8:270-80.
[23] Puleo DA, Nanci A. Understanding and controlling the bone-implant interface. Biomaterials. 1999;20:2311-21.
[24] Ratner BD, Bryant SJ. Biomaterials: where we have been and where we are going. Annual review of biomedical engineering. 2004;6:41-75.
[25] Wilson CJ, Clegg RE, Leavesley DI, Pearcy MJ. Mediation of biomaterial-cell interactions by adsorbed proteins: a review. Tissue engineering. 2005;11:1-18.
[26] Rajpurohit R, Koch CJ, Tao Z, Teixeira CM, Shapiro IM. Adaptation of chondrocytes to low oxygen tension: relationship between hypoxia and cellular metabolism. Journal of cellular physiology. 1996;168:424-32.
[27] Cooper LF. Biologic determinants of bone formation for osseointegration: clues for future clinical improvements. The Journal of prosthetic dentistry. 1998;80:439-49.
[28] Davies JE. Understanding peri-implant endosseous healing. Journal of dental education. 2003;67:932-49.
[29] Depprich R, Zipprich H, Ommerborn M, Mahn E, Lammers L, Handschel J, et al. Osseointegration of zirconia implants: an SEM observation of the bone-implant interface. Head & face medicine. 2008;4:25.
[30] Colnot C, Romero DM, Huang S, Rahman J, Currey JA, Nanci A, et al. Molecular analysis of healing at a bone-implant interface. Journal of dental research. 2007;86:862-7.
[31] Levin L. Dealing with dental implant failures. Refuat Hapeh Vehashinayim. 2010;27:6-12, 60.
[32] Tolman DE. Advanced residual ridge resorption: surgical management. The International journal of prosthodontics. 1993;6:118-25.
[33] Esposito M, Grusovin MG, Polyzos IP, Felice P, Worthington HV. Interventions for replacing missing teeth: dental implants in fresh extraction sockets (immediate,

immediate-delayed and delayed implants). The Cochrane database of systematic reviews. 2010:CD005968.
[34] Albrektsson T, Zarb G, Worthington P, Eriksson AR. The long-term efficacy of currently used dental implants: a review and proposed criteria of success. The International journal of oral & maxillofacial implants. 1986;1:11-25.
[35] Lekholm U, Gunne J, Henry P, Higuchi K, Linden U, Bergstrom C, et al. Survival of the Branemark implant in partially edentulous jaws: a 10-year prospective multicenter study. The International journal of oral & maxillofacial implants. 1999;14:639-45.
[36] van Steenberghe D, Lekholm U, Bolender C, Folmer T, Henry P, Herrmann I, et al. Applicability of osseointegrated oral implants in the rehabilitation of partial edentulism: a prospective multicenter study on 558 fixtures. The International journal of oral & maxillofacial implants. 1990;5:272-81.
[37] Natali AN, Carniel EL, Pavan PG. Investigation of viscoelastoplastic response of bone tissue in oral implants press fit process. Journal of biomedical materials research Part B, Applied biomaterials. 2009;91:868-75.
[38] Lioubavina-Hack N, Lang NP, Karring T. Significance of primary stability for osseointegration of dental implants. Clinical oral implants research. 2006;17:244-50.
[39] Tabassum A, Meijer GJ, Wolke JG, Jansen JA. Influence of the surgical technique and surface roughness on the primary stability of an implant in artificial bone with a density equivalent to maxillary bone: a laboratory study. Clinical oral implants research. 2009;20:327-32.
[40] Atsumi M, Park SH, Wang HL. Methods used to assess implant stability: current status. The International journal of oral & maxillofacial implants. 2007;22:743-54.
[41] Raghavendra S, Wood MC, Taylor TD. Early wound healing around endosseous implants: a review of the literature. The International journal of oral & maxillofacial implants. 2005;20:425-31.
[42] Chiapasco M, Zaniboni M, Boisco M. Augmentation procedures for the rehabilitation of deficient edentulous ridges with oral implants. Clinical oral implants research. 2006;17 Suppl 2:136-59.
[43] Blomqvist JE, Alberius P, Isaksson S. Retrospective analysis of one-stage maxillary sinus augmentation with endosseous implants. The International journal of oral & maxillofacial implants. 1996;11:512-21.
[44] Branemark PI, Adell R, Albrektsson T, Lekholm U, Lindstrom J, Rockler B. An experimental and clinical study of osseointegrated implants penetrating the nasal cavity and maxillary sinus. Journal of oral and maxillofacial surgery : official journal of the American Association of Oral and Maxillofacial Surgeons. 1984;42:497-505.
[45] Jokstad A, Braegger U, Brunski JB, Carr AB, Naert I, Wennerberg A. Quality of dental implants. International dental journal. 2003;53:409-43.
[46] Lemons JE. Dental implant biomaterials. Journal of the American Dental Association. 1990;121:716-9.
[47] Chong L, Khocht A, Suzuki JB, Gaughan J. Effect of implant design on initial stability of tapered implants. The Journal of oral implantology. 2009;35:130-5.
[48] Delaunay CP, Kapandji AI. Acetabular screw rings and surface treatment. Clinical orthopaedics and related research. 1997:130-41.

[49] Romanos GE, Johansson CB. Immediate loading with complete implant-supported restorations in an edentulous heavy smoker: histologic and histomorphometric analyses. The International journal of oral & maxillofacial implants. 2005;20:282-90.
[50] Romanos GE, Toh CG, Siar CH, Wicht H, Yacoob H, Nentwig GH. Bone-implant interface around titanium implants under different loading conditions: a histomorphometrical analysis in the Macaca fascicularis monkey. Journal of periodontology. 2003;74:1483-90.
[51] O'Sullivan D, Sennerby L, Meredith N. Influence of implant taper on the primary and secondary stability of osseointegrated titanium implants. Clinical oral implants research. 2004;15:474-80.
[52] Esposito M, Murray-Curtis L, Grusovin MG, Coulthard P, Worthington HV. Interventions for replacing missing teeth: different types of dental implants. The Cochrane database of systematic reviews. 2007:CD003815.
[53] Louropoulou A, Slot DE, Van der Weijden FA. Titanium surface alterations following the use of different mechanical instruments: a systematic review. Clinical oral implants research. 2012;23:643-58.
[54] Le Guehennec L, Soueidan A, Layrolle P, Amouriq Y. Surface treatments of titanium dental implants for rapid osseointegration. Dental materials : official publication of the Academy of Dental Materials. 2007;23:844-54.
[55] Karoussis IK, Bragger U, Salvi GE, Burgin W, Lang NP. Effect of implant design on survival and success rates of titanium oral implants: a 10-year prospective cohort study of the ITI Dental Implant System. Clinical oral implants research. 2004;15:8-17.
[56] Buser D, Mericske-Stern R, Bernard JP, Behneke A, Behneke N, Hirt HP, et al. Long-term evaluation of non-submerged ITI implants. Part 1: 8-year life table analysis of a prospective multi-center study with 2359 implants. Clinical oral implants research. 1997;8:161-72.
[57] Buser D, Weber HP, Lang NP. Tissue integration of non-submerged implants. 1-year results of a prospective study with 100 ITI hollow-cylinder and hollow-screw implants. Clinical oral implants research. 1990;1:33-40.
[58] Mombelli A, Lang NP. Clinical parameters for the evaluation of dental implants. Periodontology 2000. 1994;4:81-6.
[59] Olszta MJ, Cheng X, Jee SS, Kumar R, Kim Y-Y, Kaufman MJ, et al. Bone structure and formation: A new perspective. Materials Science and Engineering: R: Reports. 2007;58:77-116.
[60] Aszodi A, Bateman JF, Gustafsson E, Boot-Handford R, Fassler R. Mammalian skeletogenesis and extracellular matrix: what can we learn from knockout mice? Cell structure and function. 2000;25:73-84.
[61] Green J. The physicochemical structure of bone: cellular and noncellular elements. Mineral and electrolyte metabolism. 1994;20:7-15.
[62] Rho JY, Kuhn-Spearing L, Zioupos P. Mechanical properties and the hierarchical structure of bone. Medical engineering & physics. 1998;20:92-102.
[63] Fanghanel J, Gedrange T, Proff P. Bone quality, quantity and metabolism in terms of dental implantation. Biomedizinische Technik Biomedical engineering. 2008;53:215-9.
[64] Long MW. Osteogenesis and bone-marrow-derived cells. Blood cells, molecules & diseases. 2001;27:677-90.

[65] Hofbauer LC, Khosla S, Dunstan CR, Lacey DL, Boyle WJ, Riggs BL. The roles of osteoprotegerin and osteoprotegerin ligand in the paracrine regulation of bone resorption. Journal of bone and mineral research : the official journal of the American Society for Bone and Mineral Research. 2000;15:2-12.
[66] Teitelbaum SL. Bone resorption by osteoclasts. Science. 2000;289:1504-8.
[67] Klein-Nulend J, Nijweide PJ, Burger EH. Osteocyte and bone structure. Current osteoporosis reports. 2003;1:5-10.
[68] Roberts WE, Turley PK, Brezniak N, Fielder PJ. Implants: Bone physiology and metabolism. CDA journal California Dental Association. 1987;15:54-61.
[69] Bolander ME. Regulation of fracture repair by growth factors. Proceedings of the society for experimental biology and medicine. 1992;200:165-70.
[70] Einhorn TA. The cell and molecular biology of fracture healing. Clinical orthopaedics and related research. 1998:S7-21.
[71] Gerstenfeld LC, Cullinane DM, Barnes GL, Graves DT, Einhorn TA. Fracture healing as a post-natal developmental process: molecular, spatial, and temporal aspects of its regulation. Journal of cellular biochemistry. 2003;88:873-84.
[72] Ai-Aql ZS, Alagl AS, Graves DT, Gerstenfeld LC, Einhorn TA. Molecular mechanisms controlling bone formation during fracture healing and distraction osteogenesis. Journal of dental research. 2008;87:107-18.
[73] Giannoudis PV, Einhorn TA, Marsh D. Fracture healing: the diamond concept. Injury. 2007;38 Suppl 4:S3-6.
[74] Stone CA. A molecular approach to bone regeneration. British journal of plastic surgery. 1997;50:369-73.
[75] Barnes GL, Kostenuik PJ, Gerstenfeld LC, Einhorn TA. Growth factor regulation of fracture repair. Journal of bone and mineral research : the official journal of the American Society for Bone and Mineral Research. 1999;14:1805-15.
[76] Peng H, Usas A, Olshanski A, Ho AM, Gearhart B, Cooper GM, et al. VEGF improves, whereas sFlt1 inhibits, BMP2-induced bone formation and bone healing through modulation of angiogenesis. Journal of bone and mineral research : the official journal of the American Society for Bone and Mineral Research. 2005;20:2017-27.
[77] Tarkka T, Sipola A, Jamsa T, Soini Y, Yla-Herttuala S, Tuukkanen J, et al. Adenoviral VEGF-A gene transfer induces angiogenesis and promotes bone formation in healing osseous tissues. The journal of gene medicine. 2003;5:560-6.
[78] Mulari MT, Qu Q, Harkonen PL, Vaananen HK. Osteoblast-like cells complete osteoclastic bone resorption and form new mineralized bone matrix in vitro. Calcified tissue international. 2004;75:253-61.
[79] Barber HD, Betts NJ. Rehabilitation of maxillofacial trauma patients with dental implants. Implant dentistry. 1993;2:191-3.
[80] Schropp L, Wenzel A, Kostopoulos L, Karring T. Bone healing and soft tissue contour changes following single-tooth extraction: a clinical and radiographic 12-month prospective study. The International journal of periodontics & restorative dentistry. 2003;23:313-23.
[81] de Wijs FL, Cune MS. Immediate labial contour restoration for improved esthetics: a radiographic study on bone splitting in anterior single-tooth replacement. The International journal of oral & maxillofacial implants. 1997;12:686-96.

[82] Cawood JI, Howell RA. A classification of the edentulous jaws. International journal of oral and maxillofacial surgery. 1988;17:232-6.
[83] van Steenberghe D. A retrospective multicenter evaluation of the survival rate of osseointegrated fixtures supporting fixed partial prostheses in the treatment of partial edentulism. The Journal of prosthetic dentistry. 1989;61:217-23.
[84] Norton MR, Odell EW, Thompson ID, Cook RJ. Efficacy of bovine bone mineral for alveolar augmentation: a human histologic study. Clinical oral implants research. 2003;14:775-83.
[85] Chiapasco M, Casentini P, Zaniboni M. Bone augmentation procedures in implant dentistry. The International journal of oral & maxillofacial implants. 2009;24 Suppl:237-59.
[86] Jensen SS, Terheyden H. Bone augmentation procedures in localized defects in the alveolar ridge: clinical results with different bone grafts and bone-substitute materials. The International journal of oral & maxillofacial implants. 2009;24 Suppl:218-36.
[87] Misch CM. Maxillary autogenous bone grafting. Dental clinics of North America. 2011;55:697-713.
[88] Bianchi A, Felice P, Lizio G, Marchetti C. Alveolar distraction osteogenesis versus inlay bone grafting in posterior mandibular atrophy: a prospective study. Oral surgery, oral medicine, oral pathology, oral radiology, and endodontics. 2008;105:282-92.
[89] Felice P, Marchetti C, Piattelli A, Pellegrino G, Checchi V, Worthington H, et al. Vertical ridge augmentation of the atrophic posterior mandible with interpositional block grafts: bone from the iliac crest versus bovine anorganic bone. European journal of oral implantology. 2008;1:183-98.
[90] Chin M. Distraction osteogenesis for dental implants. Atlas of the oral and maxillofacial surgery clinics of North America. 1999;7:41-63.
[91] Ilizarov GA. The tension-stress effect on the genesis and growth of tissues: Part II. The influence of the rate and frequency of distraction. Clinical orthopaedics and related research. 1989:263-85.
[92] Rocchietta I, Fontana F, Simion M. Clinical outcomes of vertical bone augmentation to enable dental implant placement: a systematic review. Journal of clinical periodontology. 2008;35:203-15.
[93] Enislidis G, Fock N, Millesi-Schobel G, Klug C, Wittwer G, Yerit K, et al. Analysis of complications following alveolar distraction osteogenesis and implant placement in the partially edentulous mandible. Oral surgery, oral medicine, oral pathology, oral radiology, and endodontics. 2005;100:25-30.
[94] Turker N, Basa S, Vural G. Evaluation of osseous regeneration in alveolar distraction osteogenesis with histological and radiological aspects. Journal of oral and maxillofacial surgery : official journal of the American Association of Oral and Maxillofacial Surgeons. 2007;65:608-14.
[95] Bernstein S, Cooke J, Fotek P, Wang HL. Vertical bone augmentation: where are we now? Implant dentistry. 2006;15:219-28.
[96] Marianetti TM, Leuzzi F, Foresta E, Gasparini G, Cervelli D, Amoroso PF, et al. Vertical distraction osteogenesis combined with bilateral 2-step osteotomy for preprosthetic rehabilitation of edentulous mandible. The Journal of craniofacial surgery. 2013;24:1175-8.

[97] Simion M, Trisi P, Piattelli A. Vertical ridge augmentation using a membrane technique associated with osseointegrated implants. The International journal of periodontics & restorative dentistry. 1994;14:496-511.
[98] Chen ST, Darby IB, Adams GG, Reynolds EC. A prospective clinical study of bone augmentation techniques at immediate implants. Clinical oral implants research. 2005;16:176-84.
[99] Milinkovic I, Cordaro L. Are there specific indications for the different alveolar bone augmentation procedures for implant placement? A systematic review. International journal of oral and maxillofacial surgery. 2014.
[100] Stellingsma C, Raghoebar GM, Meijer HJ, Batenburg RH. Reconstruction of the extremely resorbed mandible with interposed bone grafts and placement of endosseous implants. A preliminary report on outcome of treatment and patients' satisfaction. The British journal of oral & maxillofacial surgery. 1998;36:290-5.
[101] Stoelinga PJ, Tideman H, Berger JS, de Koomen HA. Interpositional bone graft augmentation of the atrophic mandible: a preliminary report. Journal of oral surgery. 1978;36:30-2.
[102] Stoelinga PJ, Blijdorp PA, Ross RR, De Koomen HA, Huybers TJ. Augmentation of the atrophic mandible with interposed bone grafts and particulate hydroxylapatite. Journal of oral and maxillofacial surgery : official journal of the American Association of Oral and Maxillofacial Surgeons. 1986;44:353-60.
[103] Felice P, Marchetti C, Iezzi G, Piattelli A, Worthington H, Pellegrino G, et al. Vertical ridge augmentation of the atrophic posterior mandible with interpositional bloc grafts: bone from the iliac crest vs. bovine anorganic bone. Clinical and histological results up to one year after loading from a randomized-controlled clinical trial. Clinical oral implants research. 2009;20:1386-93.
[104] Felice P, Cannizzaro G, Checchi V, Marchetti C, Pellegrino G, Censi P, et al. Vertical bone augmentation versus 7-mm-long implants in posterior atrophic mandibles. Results of a randomised controlled clinical trial of up to 4 months after loading. European journal of oral implantology. 2009;2:7-20.
[105] Isaksson S, Alberius P. Maxillary alveolar ridge augmentation with onlay bone-grafts and immediate endosseous implants. Journal of cranio-maxillo-facial surgery : official publication of the European Association for Cranio-Maxillo-Facial Surgery. 1992;20:2-7.
[106] Kahnberg KE, Nystrom E, Bartholdsson L. Combined use of bone grafts and Branemark fixtures in the treatment of severely resorbed maxillae. The International journal of oral & maxillofacial implants. 1989;4:297-304.
[107] Garcia-Denche JT, Wu X, Martinez PP, Eimar H, Ikbal DJ, Hernandez G, et al. Membranes over the lateral window in sinus augmentation procedures: a two-arm and split-mouth randomized clinical trials. Journal of clinical periodontology. 2013;40:1043-51.
[108] Buser D, Dula K, Hirt HP, Schenk RK. Lateral ridge augmentation using autografts and barrier membranes: a clinical study with 40 partially edentulous patients. Journal of oral and maxillofacial surgery : official journal of the American Association of Oral and Maxillofacial Surgeons. 1996;54:420-32; discussion 32-3.

[109] Chen ST, Wilson TG, Jr., Hammerle CH. Immediate or early placement of implants following tooth extraction: review of biologic basis, clinical procedures, and outcomes. The International journal of oral & maxillofacial implants. 2004;19 Suppl:12-25.
[110] Fugazzotto PA, Vlassis J, Butler B. ITI implant use in private practice: clinical results with 5,526 implants followed up to 72+ months in function. The International journal of oral & maxillofacial implants. 2004;19:408-12.
[111] Chiapasco M, Zaniboni M. Failures in jaw reconstructive surgery with autogenous onlay bone grafts for pre-implant purposes: incidence, prevention and management of complications. Oral and maxillofacial surgery clinics of North America. 2011;23:1-15, v.
[112] Chiapasco M, Zaniboni M, Rimondini L. Autogenous onlay bone grafts vs. alveolar distraction osteogenesis for the correction of vertically deficient edentulous ridges: a 2-4-year prospective study on humans. Clinical oral implants research. 2007;18:432-40.
[113] Cordaro L, Amade DS, Cordaro M. Clinical results of alveolar ridge augmentation with mandibular block bone grafts in partially edentulous patients prior to implant placement. Clinical oral implants research. 2002;13:103-11.
[114] Jensen J, Sindet-Pedersen S. Autogenous mandibular bone grafts and osseointegrated implants for reconstruction of the severely atrophied maxilla: a preliminary report. Journal of oral and maxillofacial surgery : official journal of the American Association of Oral and Maxillofacial Surgeons. 1991;49:1277-87.
[115] Donovan MG, Dickerson NC, Hanson LJ, Gustafson RB. Maxillary and mandibular reconstruction using calvarial bone grafts and Branemark implants: a preliminary report. Journal of oral and maxillofacial surgery : official journal of the American Association of Oral and Maxillofacial Surgeons. 1994;52:588-94.
[116] Elsalanty ME, Genecov DG. Bone grafts in craniofacial surgery. Craniomaxillofacial trauma & reconstruction. 2009;2:125-34.
[117] Kalfas IH. Principles of bone healing. Neurosurgical focus. 2001;10:E1.
[118] Jarcho M. Calcium phosphate ceramics as hard tissue prosthetics. Clinical orthopaedics and related research. 1981:259-78.
[119] Masters DH. Implants. Bone and bone substitutes. CDA journal California Dental Association. 1988;16:56-65.
[120] Rejda BV, Peelen JG, de Groot K. Tri-calcium phosphate as a bone substitute. Journal of bioengineering. 1977;1:93-7.
[121] Misch CE, Dietsh F. Bone-grafting materials in implant dentistry. Implant dentistry. 1993;2:158-67.
[122] Davis WH, Delo RI, Weiner JR, Terry B. Transoral bone graft for atrophy of the mandible. Journal of oral surgery. 1970;28:760-5.
[123] Hjorting-Hansen E. Bone grafting to the jaws with special reference to reconstructive preprosthetic surgery. A historical review. Mund-, Kiefer- und Gesichtschirurgie : MKG. 2002;6:6-14.
[124] Nystrom E, Ahlqvist J, Kahnberg KE, Rosenquist JB. Autogenous onlay bone grafts fixed with screw implants for the treatment of severely resorbed maxillae. Radiographic evaluation of preoperative bone dimensions, postoperative bone loss, and changes in soft-tissue profile. International journal of oral and maxillofacial surgery. 1996;25:351-9.

[125] Greenwald AS, Boden SD, Goldberg VM, Khan Y, Laurencin CT, Rosier RN, et al. Bone-graft substitutes: facts, fictions, and applications. The Journal of bone and joint surgery American volume. 2001;83-A Suppl 2 Pt 2:98-103.
[126] Haas R, Haidvogl D, Dortbudak O, Mailath G. Freeze-dried bone for maxillary sinus augmentation in sheep. Part II: biomechanical findings. Clinical oral implants research. 2002;13:581-6.
[127] Karabuda C, Ozdemir O, Tosun T, Anil A, Olgac V. Histological and clinical evaluation of 3 different grafting materials for sinus lifting procedure based on 8 cases. Journal of periodontology. 2001;72:1436-42.
[128] Buck BE, Malinin TI, Brown MD. Bone transplantation and human immunodeficiency virus. An estimate of risk of acquired immunodeficiency syndrome (AIDS). Clinical orthopaedics and related research. 1989:129-36.
[129] Mellonig JT, Prewett AB, Moyer MP. HIV inactivation in a bone allograft. Journal of periodontology. 1992;63:979-83.
[130] Aichelmann-Reidy ME, Yukna RA. Bone replacement grafts. The bone substitutes. Dental clinics of North America. 1998;42:491-503.
[131] Habibovic P, de Groot K. Osteoinductive biomaterials--properties and relevance in bone repair. Journal of tissue engineering and regenerative medicine. 2007;1:25-32.
[132] Zimmermann G, Moghaddam A. Allograft bone matrix versus synthetic bone graft substitutes. Injury. 2011;42 Suppl 2:S16-21.
[133] Bauer TW, Muschler GF. Bone graft materials. An overview of the basic science. Clinical orthopaedics and related research. 2000:10-27.
[134] Giannoudis PV, Dinopoulos H, Tsiridis E. Bone substitutes: an update. Injury. 2005;36 Suppl 3:S20-7.
[135] Bonfiglio M, Jeter WS. Immunological responses to bone. Clinical orthopaedics and related research. 1972;87:19-27.
[136] Siddiqui SA, Lipton J, Bryk E, Vigorita V, Evangalista J. The pathology of bone allograft. The Journal of bone and joint surgery British volume. 1999;81:935.
[137] Borgonovo AE, Tommasi F, Panigalli A, Bianchi AC, Boninsegna R, Santoro F. Use of fresh frozen bone graft in rehabilitation of maxillar atrophy. Minerva stomatologica. 2012;61:141-54.
[138] Contar CM, Sarot JR, Bordini J, Jr., Galvao GH, Nicolau GV, Machado MA. Maxillary ridge augmentation with fresh-frozen bone allografts. Journal of oral and maxillofacial surgery : official journal of the American Association of Oral and Maxillofacial Surgeons. 2009;67:1280-5.
[139] Albert A, Leemrijse T, Druez V, Delloye C, Cornu O. Are bone autografts still necessary in 2006? A three-year retrospective study of bone grafting. Acta orthopaedica Belgica. 2006;72:734-40.
[140] Palmer SH, Gibbons CL, Athanasou NA. The pathology of bone allograft. The Journal of bone and joint surgery British volume. 1999;81:333-5.
[141] Urist MR, Strates BS. Bone morphogenetic protein. Journal of dental research. 1971;50:1392-406.
[142] Mellonig JT, Bowers GM, Bailey RC. Comparison of bone graft materials. Part I. New bone formation with autografts and allografts determined by Strontium-85. Journal of periodontology. 1981;52:291-6.

[143] Mellonig JT, Bowers GM, Cotton WR. Comparison of bone graft materials. Part II. New bone formation with autografts and allografts: a histological evaluation. Journal of periodontology. 1981;52:297-302.
[144] Dodson SA, Bernard GW, Kenney EB, Carranza FA. In vitro comparison of aged and young osteogenic and hemopoietic bone marrow stem cells and their derivative colonies. Journal of periodontology. 1996;67:184-96.
[145] Syftestad GT, Urist MR. Bone aging. Clinical orthopaedics and related research. 1982:288-97.
[146] Guerrero JS, Al-Jandan BA. Allograft for maxillary sinus floor augmentation: a retrospective study of 90 cases. Implant dentistry. 2012;21:136-40.
[147] Novell J, Novell-Costa F, Ivorra C, Farinas O, Munilla A, Martinez C. Five-year results of implants inserted into freeze-dried block allografts. Implant dentistry. 2012;21:129-35.
[148] Friedlaender GE, Strong DM, Sell KW. Studies on the antigenicity of bone. I. Freeze-dried and deep-frozen bone allografts in rabbits. The Journal of bone and joint surgery American volume. 1976;58:854-8.
[149] Turner DW, Mellonig JT. Antigenicity of freeze-dried bone allograft in periodontal osseous defects. Journal of periodontal research. 1981;16:89-99.
[150] Zmolek JC, Dorr LD. Revision total hip arthroplasty. The use of solid allograft. The Journal of arthroplasty. 1993;8:361-70.
[151] Keith JD, Jr. Localized ridge augmentation with a block allograft followed by secondary implant placement: a case report. The International journal of periodontics & restorative dentistry. 2004;24:11-7.
[152] Leonetti JA, Koup R. Localized maxillary ridge augmentation with a block allograft for dental implant placement: case reports. Implant Dent. 2003;12:217-26.
[153] Lyford RH, Mills MP, Knapp CI, Scheyer ET, Mellonig JT. Clinical evaluation of freeze-dried block allografts for alveolar ridge augmentation: a case series. The International journal of periodontics & restorative dentistry. 2003;23:417-25.
[154] Nissan J, Marilena V, Gross O, Mardinger O, Chaushu G. Histomorphometric analysis following augmentation of the posterior mandible using cancellous bone-block allograft. Journal of biomedical materials research Part A. 2011;97:509-13.
[155] Peleg M, Sawatari Y, Marx RN, Santoro J, Cohen J, Bejarano P, et al. Use of corticocancellous allogeneic bone blocks for augmentation of alveolar bone defects. The International journal of oral & maxillofacial implants. 2010;25:153-62.
[156] Laurencin CT, El-Amin SF. Xenotransplantation in orthopaedic surgery. The Journal of the American Academy of Orthopaedic Surgeons. 2008;16:4-8.
[157] Hallman M, Sennerby L, Lundgren S. A clinical and histologic evaluation of implant integration in the posterior maxilla after sinus floor augmentation with autogenous bone, bovine hydroxyapatite, or a 20:80 mixture. The International journal of oral & maxillofacial implants. 2002;17:635-43.
[158] Valentini P, Abensur DJ. Maxillary sinus grafting with anorganic bovine bone: a clinical report of long-term results. The International journal of oral & maxillofacial implants. 2003;18:556-60.
[159] Yildirim M, Spiekermann H, Biesterfeld S, Edelhoff D. Maxillary sinus augmentation using xenogenic bone substitute material Bio-Oss in combination with

venous blood. A histologic and histomorphometric study in humans. Clinical oral implants research. 2000;11:217-29.
[160] Calvo-Guirado JL, Gomez-Moreno G, Guardia J, Ortiz-Ruiz A, Piatelli A, Barone A, et al. Biological response to porcine xenograft implants: an experimental study in rabbits. Implant dentistry. 2012;21:112-7.
[161] Cohen RE, Mullarky RH, Noble B, Comeau RL, Neiders ME. Phenotypic characterization of mononuclear cells following anorganic bovine bone implantation in rats. Journal of periodontology. 1994;65:1008-15.
[162] Piattelli M, Favero GA, Scarano A, Orsini G, Piattelli A. Bone reactions to anorganic bovine bone (Bio-Oss) used in sinus augmentation procedures: a histologic long-term report of 20 cases in humans. The International journal of oral & maxillofacial implants. 1999;14:835-40.
[163] Rothamel D, Schwarz F, Herten M, Ferrari D, Mischkowski RA, Sager M, et al. Vertical ridge augmentation using xenogenous bone blocks: a histomorphometric study in dogs. The International journal of oral & maxillofacial implants. 2009;24:243-50.
[164] Zitzmann NU, Scharer P, Marinello CP, Schupbach P, Berglundh T. Alveolar ridge augmentation with Bio-Oss: a histologic study in humans. The International journal of periodontics & restorative dentistry. 2001;21:288-95.
[165] Chan HL, Lin GH, Fu JH, Wang HL. Alterations in bone quality after socket preservation with grafting materials: a systematic review. The International journal of oral & maxillofacial implants. 2013;28:710-20.
[166] Emmings FG. Chemically modified osseous material for the restoration of bone defects. Journal of periodontology. 1974;45:385-90.
[167] Melcher AH, Dent HD. The use of heterogenous anorganic bone as an implant material in oral procedures. Oral surgery, oral medicine, and oral pathology. 1962;15:996-1000.
[168] Shue L, Yufeng Z, Mony U. Biomaterials for periodontal regeneration: a review of ceramics and polymers. Biomatter. 2012;2:271-7.
[169] Hutmacher DW. Scaffolds in tissue engineering bone and cartilage. Biomaterials. 2000;21:2529-43.
[170] Kretlow JD, Young S, Klouda L, Wong M, Mikos AG. Injectable biomaterials for regenerating complex craniofacial tissues. Advanced materials. 2009;21:3368-93.
[171] Yukna RA. HTR polymer grafts in human periodontal osseous defects. I. 6-month clinical results. Journal of periodontology. 1990;61:633-42.
[172] Yukna RA. Clinical evaluation of HTR polymer bone replacement grafts in human mandibular Class II molar furcations. Journal of periodontology. 1994;65:342-9.
[173] Rezwan K, Chen QZ, Blaker JJ, Boccaccini AR. Biodegradable and bioactive porous polymer/inorganic composite scaffolds for bone tissue engineering. Biomaterials. 2006;27:3413-31.
[174] Lagoa AL, Wedemeyer C, von Knoch M, Loer F, Epple M. A strut graft substitute consisting of a metal core and a polymer surface. Journal of materials science Materials in medicine. 2008;19:417-24.
[175] Ishaug SL, Crane GM, Miller MJ, Yasko AW, Yaszemski MJ, Mikos AG. Bone formation by three-dimensional stromal osteoblast culture in biodegradable polymer scaffolds. Journal of biomedical materials research. 1997;36:17-28.

[176] Ma PX, Choi JW. Biodegradable polymer scaffolds with well-defined interconnected spherical pore network. Tissue engineering. 2001;7:23-33.
[177] Shen H, Hu X, Bei J, Wang S. The immobilization of basic fibroblast growth factor on plasma-treated poly(lactide-co-glycolide). Biomaterials. 2008;29:2388-99.
[178] Yu L, Chang GT, Zhang H, Ding JD. Injectable block copolymer hydrogels for sustained release of a PEGylated drug. International journal of pharmaceutics. 2008;348:95-106.
[179] Vainionpaa S, Laasonen E, Patiala H, Rusanen M, Rokkannen P. Acute dislocation of the patella. Clinical, radiographic and operative findings in 64 consecutive cases. Acta orthopaedica Scandinavica. 1986;57:331-3.
[180] Simon CG, Jr., Khatri CA, Wight SA, Wang FW. Preliminary report on the biocompatibility of a moldable, resorbable, composite bone graft consisting of calcium phosphate cement and poly(lactide-co-glycolide) microspheres. Journal of orthopaedic research : official publication of the Orthopaedic Research Society. 2002;20:473-82.
[181] Danesh-Meyer MJ, Wikesjo UM. Gingival recession defects and guided tissue regeneration: a review. Journal of periodontal research. 2001;36:341-54.
[182] Polimeni G, Koo KT, Pringle GA, Agelan A, Safadi FF, Wikesjo UM. Histopathological observations of a polylactic acid-based device intended for guided bone/tissue regeneration. Clinical implant dentistry and related research. 2008;10:99-105.
[183] Eschbach L. Nonresorbable polymers in bone surgery. Injury. 2000;31 Suppl 4:22-7.
[184] De Leonardis D, Pecora GE. Augmentation of the maxillary sinus with calcium sulfate: one-year clinical report from a prospective longitudinal study. The International journal of oral & maxillofacial implants. 1999;14:869-78.
[185] Thomas MV, Puleo DA, Al-Sabbagh M. Bioactive glass three decades on. Journal of long-term effects of medical implants. 2005;15:585-97.
[186] Hench LL, Paschall HA. Direct chemical bond of bioactive glass-ceramic materials to bone and muscle. Journal of biomedical materials research. 1973;7:25-42.
[187] el-Ghannam A, Ducheyne P, Shapiro IM. Formation of surface reaction products on bioactive glass and their effects on the expression of the osteoblastic phenotype and the deposition of mineralized extracellular matrix. Biomaterials. 1997;18:295-303.
[188] Schepers E, de Clercq M, Ducheyne P, Kempeneers R. Bioactive glass particulate material as a filler for bone lesions. Journal of oral rehabilitation. 1991;18:439-52.
[189] Nevins ML, Camelo M, Nevins M, King CJ, Oringer RJ, Schenk RK, et al. Human histologic evaluation of bioactive ceramic in the treatment of periodontal osseous defects. The International journal of periodontics & restorative dentistry. 2000;20:458-67.
[190] Sculean A, Windisch P, Keglevich T, Gera I. Clinical and histologic evaluation of an enamel matrix protein derivative combined with a bioactive glass for the treatment of intrabony periodontal defects in humans. The International journal of periodontics & restorative dentistry. 2005;25:139-47.
[191] Dreesman H. Über Knochenplombierung. Beitr Klin Chir. 1892:804-10.
[192] Blaha JD. Calcium sulfate bone-void filler. Orthopedics. 1998;21:1017-9.
[193] Shaffer CD, App GR. The use of plaster of paris in treating infrabony periodontal defects in humans. Journal of periodontology. 1971;42:685-90.
[194] Thomas MV, Puleo DA, Al-Sabbagh M. Calcium sulfate: a review. Journal of long-term effects of medical implants. 2005;15:599-607.

[195] Ricci JL, Blumenthal NC, Spivak JM, Alexander H. Evaluation of a low-temperature calcium phosphate particulate implant material: physical-chemical properties and in vivo bone response. Journal of oral and maxillofacial surgery : official journal of the American Association of Oral and Maxillofacial Surgeons. 1992;50:969-78.
[196] Wagner JR. Clinical and histological case study using resorbable hydroxylapatite for the repair of osseous defects prior to endosseous implant surgery. The Journal of oral implantology. 1989;15:186-92.
[197] Nery EB, Lynch KL. Preliminary clinical studies of bioceramic in periodontal osseous defects. Journal of periodontology. 1978;49:523-7.
[198] Artzi Z, Nemcovsky CE, Tal H, Dayan D. Histopathological morphometric evaluation of 2 different hydroxyapatite-bone derivatives in sinus augmentation procedures: a comparative study in humans. Journal of periodontology. 2001;72:911-20.
[199] Artzi Z, Nemcovsky CE, Dayan D. Nonceramic hydroxyapatite bone derivative in sinus augmentation procedures: clinical and histomorphometric observations in 10 consecutive cases. The International journal of periodontics & restorative dentistry. 2003;23:381-9.
[200] Block MS, Kent JN. Long-term radiographic evaluation of hydroxylapatite-augmented mandibular alveolar ridges. Journal of oral and maxillofacial surgery : official journal of the American Association of Oral and Maxillofacial Surgeons. 1984;42:793-6.
[201] Jensen OT. Combined hydroxylapatite augmentation and lip-switch vestibuloplasty in the mandible. Oral surgery, oral medicine, and oral pathology. 1985;60:349-55.
[202] Shafer SC, Parnell AG. Hydroxylapatite augmentation of the mandible with simultaneous mucosal graft vestibuloplasty. Journal of oral and maxillofacial surgery : official journal of the American Association of Oral and Maxillofacial Surgeons. 1984;42:749-50.
[203] Klein CP, Driessen AA, de Groot K, van den Hooff A. Biodegradation behavior of various calcium phosphate materials in bone tissue. Journal of biomedical materials research. 1983;17:769-84.
[204] Minegishi D, Lin C, Noguchi T, Ishikawa I. Porous hydroxyapatite granule implants in periodontal osseous defects in monkeys. The International journal of periodontics & restorative dentistry. 1988;8:50-63.
[205] Hashimoto-Uoshima M, Ishikawa I, Kinoshita A, Weng HT, Oda S. Clinical and histologic observation of replacement of biphasic calcium phosphate by bone tissue in monkeys. The International journal of periodontics & restorative dentistry. 1995;15:205-13.
[206] LeGeros RZ. Calcium phosphate materials in restorative dentistry: a review. Advances in dental research. 1988;2:164-80.
[207] Amler MH. Osteogenic potential of nonvital tissues and synthetic implant materials. Journal of periodontology. 1987;58:758-61.
[208] Baldock WT, Hutchens LH, Jr., McFall WT, Jr., Simpson DM. An evaluation of tricalcium phosphate implants in human periodontal osseous defects of two patients. Journal of periodontology. 1985;56:1-7.
[209] Bowers GM, Vargo JW, Levy B, Emerson JR, Bergquist JJ. Histologic observations following the placement of tricalcium phosphate implants in human intrabony defects. Journal of periodontology. 1986;57:286-7.

[210] Stahl SS, Froum S. Histological evaluation of human intraosseous healing responses to the placement of tricalcium phosphate ceramic implants. I. Three to eight months. Journal of periodontology. 1986;57:211-7.
[211] Strub JR, Gaberthuel TW, Firestone AR. Comparison of tricalcium phosphate and frozen allogenic bone implants in man. Journal of periodontology. 1979;50:624-9.
[212] Shetty V, Han TJ. Alloplastic materials in reconstructive periodontal surgery. Dental clinics of North America. 1991;35:521-30.
[213] Tamimi F, Torres J, Lopez-Cabarcos E, Bassett DC, Habibovic P, Luceron E, et al. Minimally invasive maxillofacial vertical bone augmentation using brushite based cements. Biomaterials. 2009;30:208-16.
[214] Gbureck U, Hölzel T, Klammert U, Würzler K, Müller FA, Barralet JE. Resorbable dicalcium phosphate bone substitutes prepared by 3D powder printing. Advanced functional materials. 2007;17:3940-5.
[215] Constantz BR, Barr BM, Ison IC, Fulmer MT, Baker J, McKinney L, et al. Histological, chemical, and crystallographic analysis of four calcium phosphate cements in different rabbit osseous sites. Journal of biomedical materials research. 1998;43:451-61.
[216] Bohner M, Gbureck U. Thermal reactions of brushite cements. Journal of biomedical materials research Part B, Applied biomaterials. 2008;84:375-85.
[217] Tamimi F, Torres J, Kathan C, Baca R, Clemente C, Blanco L, et al. Bone regeneration in rabbit calvaria with novel monetite granules. Journal of biomedical materials research Part A. 2008;87:980-5.
[218] Gbureck U, Vorndran E, Muller FA, Barralet JE. Low temperature direct 3D printed bioceramics and biocomposites as drug release matrices. Journal of controlled release : official journal of the Controlled Release Society. 2007;122:173-80.
[219] Tamimi F, Torres J, Bassett D, Barralet J, Cabarcos EL. Resorption of monetite granules in alveolar bone defects in human patients. Biomaterials. 2010;31:2762-9.
[220] Popelut A, Valet F, Fromentin O, Thomas A, Bouchard P. Relationship between sponsorship and failure rate of dental implants: a systematic approach. PLoS One. 2010;5:e10274.
[221] Fu M, Deng R, Wang J, Wang X. Horizontal gene transfer in herpesviruses identified by using support vector machine. Acta virologica. 2011;55:203-17.
[222] Grunder U, Gracis S, Capelli M. Influence of the 3-D bone-to-implant relationship on esthetics. The International journal of periodontics & restorative dentistry. 2005;25:113-9.
[223] Belser UC, Schmid B, Higginbottom F, Buser D. Outcome analysis of implant restorations located in the anterior maxilla: a review of the recent literature. he International journal of oral & maxillofacial implants. 2004;19 Suppl:30-42.
[224] Triplett RG, Schow SR. Autologous bone grafts and endosseous implants: complementary techniques. Journal of maxillofacial and oral surgery. 1996;54:486-94.
[225] Galanis CC, Sfantsikopoulos MM, Koidis PT, Kafantaris NM, Mpikos PG. Computer methods for automating preoperative dental implant planning: implant positioning and size assignment. Computer methods and programs in biomedicine. 2007;86:30-8.

[226] Sahin S, Akagawa Y, Wadamoto M, Sato Y. The three-dimensional bone interface of an osseointegrated implant. II: A morphometric evaluation after three months of loading. The Journal of prosthetic dentistry. 1996;76:176-80.
[227] Akagawa Y, Wadamoto M, Sato Y, Tsuru H. The three-dimensional bone interface of an osseointegrated implant: a method for study. The Journal of prosthetic dentistry. 1992;68:813-6.
[228] Wadamoto M, Akagawa Y, Sato Y, Kubo T. The three-dimensional bone interface of an osseointegrated implant. I: A morphometric evaluation in initial healing. The Journal of prosthetic dentistry. 1996;76:170-5.
[229] McAllister BS, Haghighat K. Bone augmentation techniques. Journal of periodontology. 2007;78:377-96.
[230] Aghaloo TL, Moy PK. Which hard tissue augmentation techniques are the most successful in furnishing bony support for implant placement? he International journal of oral & maxillofacial implants. 2007;22 Suppl:49-70.
[231] Pikos MA. Block autografts for localized ridge augmentation: Part II. The posterior mandible. Implant dentistry. 2000;9:67-75.
[232] Bahat O, Fontanessi RV. Efficacy of implant placement after bone grafting for three-dimensional reconstruction of the posterior jaw. The International journal of periodontics & restorative dentistry. 2001;21:220-31.
[233] Donos N, Mardas N, Chadha V. Clinical outcomes of implants following lateral bone augmentation: systematic assessment of available options (barrier membranes, bone grafts, split osteotomy). Journal of clinical periodontology. 2008;35:173-202.
[234] Proussaefs P, Lozada J. The use of intraorally harvested autogenous block grafts for vertical alveolar ridge augmentation: a human study. The International journal of periodontics & restorative dentistry. 2005;25:351-63.
[235] Kim JW, Cho MH, Kim SJ, Kim MR. Alveolar distraction osteogenesis versus autogenous onlay bone graft for vertical augmentation of severely atrophied alveolar ridges after 12 years of long-term follow-up. Oral surgery, oral medicine, oral pathology and oral radiology. 2013;116:540-9.
[236] Burchardt H. Biology of bone transplantation. The Orthopedic clinics of North America. 1987;18:187-96.
[237] Misch CM. Comparison of intraoral donor sites for onlay grafting prior to implant placement. Int J Oral Maxillofac Implants. 1997;12:767-76.
[238] Narang R, Ruben MP, Harris MH, Wells H. Improved healing of experimental defects in the canine mandible by grafts of decalcified allogenic bone. Oral surgery, oral medicine, and oral pathology. 1970;30:142-50.
[239] Nissan J, Ghelfan O, Mardinger O, Calderon S, Chaushu G. Efficacy of cancellous block allograft augmentation prior to implant placement in the posterior atrophic mandible. Clinical implant dentistry and related research. 2011;13:279-85.
[240] Nissan J, Mardinger O, Calderon S, Romanos GE, Chaushu G. Cancellous bone block allografts for the augmentation of the anterior atrophic maxilla. Clinical implant dentistry and related research. 2011;13:104-11.
[241] Chaushu G, Mardinger O, Calderon S, Moses O, Nissan J. The use of cancellous block allograft for sinus floor augmentation with simultaneous implant placement in the posterior atrophic maxilla. Journal of periodontology. 2009;80:422-8.

[242] Perrott DH, Smith RA, Kaban LB. The use of fresh frozen allogeneic bone for maxillary and mandibular reconstruction. International journal of oral and maxillofacial surgery. 1992;21:260-5.
[243] Gazdag AR, Lane JM, Glaser D, Forster RA. Alternatives to Autogenous Bone Graft: Efficacy and Indications. The Journal of the American Academy of Orthopaedic Surgeons. 1995;3:1-8.
[244] Mizutani A, Fujita T, Watanabe S, Sakakida K, Okada Y. Experiments on antigenicity and osteogenicity in allotransplanted cancellous bone. International orthopaedics. 1990;14:243-8.
[245] Boyan BD, Ranly DM, Schwartz Z. Use of growth factors to modify osteoinductivity of demineralized bone allografts: lessons for tissue engineering of bone. Dental clinics of North America. 2006;50:217-28, viii.
[246] Yuan H, Zou P, Yang Z, Zhang X, De Bruijn JD, De Groot K. Bone morphogenetic protein and ceramic-induced osteogenesis. Journal of materials science Materials in medicine. 1998;9:717-21.
[247] Eppley BL, Pietrzak WS, Blanton MW. Allograft and alloplastic bone substitutes: a review of science and technology for the craniomaxillofacial surgeon. The journal of craniofacial surgery. 2005;16:981-9.
[248] Buser D, Dula K, Belser U, Hirt HP, Berthold H. Localized ridge augmentation using guided bone regeneration. 1. Surgical procedure in the maxilla. The International journal of periodontics & restorative dentistry. 1993;13:29-45.
[249] Haddad FS, Spangehl MJ, Masri BA, Garbuz DS, Duncan CP. Circumferential allograft replacement of the proximal femur. A critical analysis. Clinical orthopaedics and related research. 2000:98-107.
[250] Mnaymneh W, Malinin TI, Makley JT, Dick HM. Massive osteoarticular allografts in the reconstruction of extremities following resection of tumors not requiring chemotherapy and radiation. Clinical orthopaedics and related research. 1985:76-87.
[251] Tomford WW, Mankin HJ. Bone banking. Update on methods and materials. Orthop Clin North Am. 1999;30:565-70.
[252] Zlotolow IM, Huryn JM, Piro JD, Lenchewski E, Hidalgo DA. Osseointegrated implants and functional prosthetic rehabilitation in microvascular fibula free flap reconstructed mandibles. American journal of surgery. 1992;164:677-81.
[253] Petrungaro PS, Amar S. Localized ridge augmentation with allogenic block grafts prior to implant placement: case reports and histologic evaluations. Implant dentistry. 2005;14:139-48.
[254] Nissan J, Gross O, Mardinger O, Ghelfan O, Sacco R, Chaushu G. Post-traumatic implant-supported restoration of the anterior maxillary teeth using cancellous bone block allografts. J Oral Maxillofac Surg. 2011;69:e513-8.
[255] Nissan J, Mardinger O, Strauss M, Peleg M, Sacco R, Chaushu G. Implant-supported restoration of congenitally missing teeth using cancellous bone block-allografts. Oral surgery, oral medicine, oral pathology, oral radiology, and endodontics. 2011;111:286-91.
[256] Nissan J, Marilena V, Gross O, Mardinger O, Chaushu G. Histomorphometric analysis following augmentation of the anterior atrophic maxilla with cancellous bone block allograft. The International journal of oral & maxillofacial implants. 2012;27:84-9.

[257] Chiapasco M, Gatti C, Gatti F. Immediate loading of dental implants placed in severely resorbed edentulous mandibles reconstructed with autogenous calvarial grafts. Clinical oral implants research. 2007;18:13-20.
[258] Roccuzzo M, Ramieri G, Bunino M, Berrone S. Autogenous bone graft alone or associated with titanium mesh for vertical alveolar ridge augmentation: a controlled clinical trial. Clinical oral implants research. 2007;18:286-94.
[259] von Arx T, Cochran DL, Hermann JS, Schenk RK, Buser D. Lateral ridge augmentation using different bone fillers and barrier membrane application - A histologic and histomorphometric pilot study in the canine mandible. Clinical Oral Implants Research. 2001;12:260-9.
[260] Misch CE, Perel ML, Wang HL, Sammartino G, Galindo-Moreno P, Trisi P, et al. Implant success, survival, and failure: the International Congress of Oral Implantologists (ICOI) Pisa Consensus Conference. Implant dentistry. 2008;17:5-15.
[261] Cohen J. Statistical power analysis for the behavioral sciences, 1st edition, Hillsdale: Lawrence Erlbaum Associates. (2nd Edition, 1988). 1969.
[262] Contar CMM, Sarot JR, Bordini J, Galvao GH, Nicolau GV, Machado MAN. Maxillary Ridge Augmentation With Fresh-Frozen Bone Allografts. Journal of Oral and Maxillofacial Surgery. 2009;67:1280-5.
[263] Waasdorp J, Reynolds MA. Allogeneic Bone Onlay Grafts for Alveolar Ridge Augmentation: A Systematic Review. International Journal of Oral & Maxillofacial Implants. 2010;25:525-31.
[264] Graham SM, Leonidou A, Aslam-Pervez N, Hamza A, Panteliadis P, Heliotis M, et al. Biological therapy of bone defects: the immunology of bone allo-transplantation. Expert opinion on biological therapy. 2010;10:885-901.
[265] Leniz P, Ripalda P, Forriol F. The incorporation of different sorts of cancellous bone graft and the reaction of the host bone. A histomorphometric study in sheep. International orthopaedics. 2004;28:2-6.
[266] Eriksson AR, Albrektsson T, Albrektsson B. Heat caused by drilling cortical bone. Temperature measured in vivo in patients and animals. Acta orthopaedica Scandinavica. 1984;55:629-31.
[267] Gapski R, Wang HL, Mascarenhas P, Lang NP. Critical review of immediate implant loading. Clinical oral implants research. 2003;14:515-27.
[268] NIH Consensus Conference Statement: dental implants. The International journal of oral & maxillofacial implants. 1988;3:290-3.
[269] Widmark G, Andersson B, Ivanoff CJ. Mandibular bone graft in the anterior maxilla for single-tooth implants. Presentation of surgical method. International journal of oral and maxillofacial surgery. 1997;26:106-9.
[270] Raghoebar GM, Batenburg RH, Vissink A, Reintsema H. Augmentation of localized defects of the anterior maxillary ridge with autogenous bone before insertion of implants. Journal of oral and maxillofacial surgery : official journal of the American Association of Oral and Maxillofacial Surgeons. 1996;54:1180-5; discussion 5-6.
[271] McCarthy C, Patel RR, Wragg PF, Brook IM. Dental implants and onlay bone grafts in the anterior maxilla: analysis of clinical outcome. The International journal of oral & maxillofacial implants. 2003;18:238-41.
[272] Renouard F, Nisand D. Impact of implant length and diameter on survival rates. Clinical oral implants research. 2006;17 Suppl 2:35-51.

[273] Dasmah A, Thor A, Ekestubbe A, Sennerby L, Rasmusson L. Marginal bone-level alterations at implants installed in block versus particulate onlay bone grafts mixed with platelet-rich plasma in atrophic maxilla. a prospective 5-year follow-up study of 15 patients. Clinical implant dentistry and related research. 2013;15:7-14.
[274] Carinci F, Guidi R, Franco M, Viscioni A, Rigo L, De Santis B, et al. Implants inserted in fresh-frozen bone: a retrospective analysis of 88 implants loaded 4 months after insertion. Quintessence international. 2009;40:413-9.
[275] Carlsson GE, Bergman B, Hedegard B. Changes in contour of the maxillary alveolar process under immediate dentures. A longitudinal clinical and x-ray cephalometric study covering 5 years. Acta odontologica Scandinavica. 1967;25:45-75.
[276] Rudy RJ, Levi PA, Bonacci FJ, Weisgold AS, Engler-Hamm D. Intraosseous anchorage of dental prostheses: an early 20th century contribution. Compendium of continuing education in dentistry. 2008;29:220-2, 4, 6-8 passim.
[277] Aloy-Prosper A, Maestre-Ferrin L, Penarrocha-Oltra D, Penarrocha-Diago M. Bone regeneration using particulate grafts: an update. Medicina oral, patologia oral y cirugia bucal. 2011;16:e210-4.
[278] Maestre-Ferrin L, Boronat-Lopez A, Penarrocha-Diago M. Augmentation procedures for deficient edentulous ridges, using onlay autologous grafts: an update. Medicina oral, patología oral y cirugía bucal. 2009;14:e402-7.
[279] Esposito M, Grusovin MG, Willings M, Coulthard P, Worthington HV. The effectiveness of immediate, early, and conventional loading of dental implants: a Cochrane systematic review of randomized controlled clinical trials. The International journal of oral & maxillofacial implants. 2007;22:893-904.
[280] Esposito M, Worthington HV, Thomsen P, Coulthard P. Interventions for replacing missing teeth: different times for loading dental implants. The Cochrane database of systematic reviews. 2004:CD003878.
[281] Johansson B, Back T, Hirsch JM. Cutting torque measurements in conjunction with implant placement in grafted and nongrafted maxillas as an objective evaluation of bone density: a possible method for identifying early implant failures? Clinical implant dentistry and related research. 2004;6:9-15.
[282] Consolo U, Travaglini D, Todisco M, Trisi P, Galli S. Histologic and biomechanical evaluation of the effects of implant insertion torque on peri-implant bone healing. The Journal of craniofacial surgery. 2013;24:860-5.
[283] Pithon MM, Figueiredo DS, Oliveira DD. Mechanical evaluation of orthodontic mini-implants of different lengths. Journal of oral and maxillofacial surgery : official journal of the American Association of Oral and Maxillofacial Surgeons. 2013;71:479-86.
[284] Anitua E, Alkhraisat MH, Pinas L, Orive G. Efficacy of biologically guided implant site preparation to obtain adequate primary implant stability. Annals of anatomy = Anatomischer Anzeiger : official organ of the Anatomische Gesellschaft. 2014.
[285] Esposito M, Grusovin MG, Felice P, Karatzopoulos G, Worthington HV, Coulthard P. The efficacy of horizontal and vertical bone augmentation procedures for dental implants - a Cochrane systematic review. European journal of oral implantology. 2009;2:167-84.
[286] Hill NM, Horne JG, Devane PA. Donor site morbidity in the iliac crest bone graft. The Australian and New Zealand journal of surgery. 1999;69:726-8.

[287] Wang X, Ni Q. Determination of cortical bone porosity and pore size distribution using a low field pulsed NMR approach. Journal of orthopaedic research : official publication of the Orthopaedic Research Society. 2003;21:312-9.
[288] Lecomte A, Gautier H, Bouler JM, Gouyette A, Pegon Y, Daculsi G, et al. Biphasic calcium phosphate: a comparative study of interconnected porosity in two ceramics. Journal of biomedical materials research Part B, Applied biomaterials. 2008;84:1-6.
[289] Gendler E. Perforated demineralized bone matrix: a new form of osteoinductive biomaterial. Journal of biomedical materials research. 1986;20:687-97.
[290] Habibovic P, Yuan H, van der Valk CM, Meijer G, van Blitterswijk CA, de Groot K. 3D microenvironment as essential element for osteoinduction by biomaterials. Biomaterials. 2005;26:3565-75.
[291] Park JW, Kim ES, Jang JH, Suh JY, Park KB, Hanawa T. Healing of rabbit calvarial bone defects using biphasic calcium phosphate ceramics made of submicron-sized grains with a hierarchical pore structure. Clinical oral implants research. 2010;21:268-76.
[292] Walsh WR, Vizesi F, Michael D, Auld J, Langdown A, Oliver R, et al. Beta-TCP bone graft substitutes in a bilateral rabbit tibial defect model. Biomaterials. 2008;29:266-71.
[293] Xu S, Li D, Wang C, Wang Z, Lu B. Cell proliferation in CPC scaffold with a central channel. Bio-medical materials and engineering. 2007;17:1-8.
[294] Berding G, Burchert W, van den Hoff J, Pytlik C, Neukam FW, Meyer GJ, et al. Evaluation of the incorporation of bone grafts used in maxillofacial surgery with [18F]fluoride ion and dynamic positron emission tomography. European journal of nuclear medicine. 1995;22:1133-40.
[295] Piert M, Winter E, Becker GA, Bilger K, Machulla H, Muller-Schauenburg W, et al. Allogenic bone graft viability after hip revision arthroplasty assessed by dynamic [18F]fluoride ion positron emission tomography. European journal of nuclear medicine. 1999;26:615-24.
[296] Hsu WK, Feeley BT, Krenek L, Stout DB, Chatziioannou AF, Lieberman JR. The use of 18F-fluoride and 18F-FDG PET scans to assess fracture healing in a rat femur model. European journal of nuclear medicine and molecular imaging. 2007;34:1291-301.
[297] Even-Sapir E, Mishani E, Flusser G, Metser U. 18F-Fluoride positron emission tomography and positron emission tomography/computed tomography. Seminars in nuclear medicine. 2007;37:462-9.
[298] Renka RJ, Cline AK. A triangle-based C1interpolation method. Journal of mathematics. 1984;14.
[299] McInnis JC, Robb RA, Kelly PJ. The relationship of bone blood flow, bone tracer deposition, and endosteal new bone formation. The Journal of laboratory and clinical medicine. 1980;96:511-22.
[300] Messa C, Goodman WG, Hoh CK, Choi Y, Nissenson AR, Salusky IB, et al. Bone metabolic activity measured with positron emission tomography and [18F]fluoride ion in renal osteodystrophy: correlation with bone histomorphometry. The Journal of clinical endocrinology and metabolism. 1993;77:949-55.
[301] von Doernberg MC, von Rechenberg B, Bohner M, Grunenfelder S, van Lenthe GH, Muller R, et al. In vivo behavior of calcium phosphate scaffolds with four different pore sizes. Biomaterials. 2006;27:5186-98.

[302] Bose S, Roy M, Bandyopadhyay A. Recent advances in bone tissue engineering scaffolds. Trends in biotechnology. 2012;30:546-54.
[303] Hulbert SF, Young FA, Mathews RS, Klawitter JJ, Talbert CD, Stelling FH. Potential of ceramic materials as permanently implantable skeletal prostheses. Journal of biomedical materials research. 1970;4:433-56.
[304] Dutta Roy T, Simon JL, Ricci JL, Rekow ED, Thompson VP, Parsons JR. Performance of hydroxyapatite bone repair scaffolds created via three-dimensional fabrication techniques. Journal of biomedical materials research Part A. 2003;67:1228-37.
[305] Yeo A, Wong WJ, Khoo HH, Teoh SH. Surface modification of PCL-TCP scaffolds improve interfacial mechanical interlock and enhance early bone formation: an in vitro and in vivo characterization. Journal of biomedical materials research Part A. 2010;92:311-21.
[306] Marino FT, Torres J, Tresguerres I, Jerez LB, Cabarcos EL. Vertical bone augmentation with granulated brushite cement set in glycolic acid. Journal of biomedical materials research Part A. 2007;81:93-102.
[307] Gosain AK, Gosain SA, Sweeney WM, Song LS, Amarante MT. Regulation of osteogenesis and survival within bone grafts to the calvaria: the effect of the dura versus the pericranium. Plastic and reconstructive surgery. 2011;128:85-94.
[308] Tamura K, Sato S, Kishida M, Asano S, Murai M, Ito K. The use of porous beta-tricalcium phosphate blocks with platelet-rich plasma as an onlay bone graft biomaterial. Journal of periodontology. 2007;78:315-21.
[309] Stellingsma C, Vissink A, Meijer HJ, Kuiper C, Raghoebar GM. Implantology and the severely resorbed edentulous mandible. Critical reviews in oral biology and medicine : an official publication of the American Association of Oral Biologists. 2004;15:240-8.
[310] Hixson AW, Crowell JH. Dependence of reaction velocity upon surface and agitation. Industrial and Engineering Chemsitry. 1931;23:923-31.
[311] Grossardt C, Ewald A, Grover LM, Barralet JE, Gbureck U. Passive and active in vitro resorption of calcium and magnesium phosphate cements by osteoclastic cells. Tissue engineering Part A. 2010;16:3687-95.
[312] Albrektsson T, Jansson T, Lekholm U. Osseointegrated dental implants. Dental clinics of North America. 1986;30:151-74.

Appendices

==========

1. Published Articles

2. Journal Permission

Biomaterials xxx (2014) 1–10

Contents lists available at ScienceDirect

Biomaterials

journal homepage: www.elsevier.com/locate/biomaterials

Osseointegration of dental implants in 3D-printed synthetic onlay grafts customized according to bone metabolic activity in recipient site

Faleh Tamimi [a,*], Jesus Torres [b], Khadijeh Al-Abedalla [a], Enrique Lopez-Cabarcos [c], Mohammad H. Alkhraisat [c], David C. Bassett [d], Uwe Gbureck [e], Jake E. Barralet [a]

[a] Faculty of Dentistry, McGill University, 3640 University Street, Montreal, H3A 2B2 QC, Canada
[b] Faculty of Dentistry, Universidad Complutense de Madrid, Spain
[c] Department of Physical Chemistry II, Universidad Complutense de Madrid, Spain
[d] Department of Physics, Norwegian University of Science and Technology, Trondheim, Norway
[e] Department of Functional Materials in Medicine and Dentistry, University of Würzburg, Würzburg, Germany

ARTICLE INFO

Article history:
Received 25 February 2014
Accepted 20 March 2014
Available online xxx

Keywords:
Bone graft
Dental implant
Calcium phosphate
Osseointegration
Porosity

ABSTRACT

Onlay grafts made of monolithic microporous monetite bioresorbable bioceramics have the capacity to conduct bone augmentation. However, there is heterogeneity in the graft behaviour *in vivo* that seems to correlate with the host anatomy. In this study, we sought to investigate the metabolic activity of the regenerated bone in monolithic monetite onlays by using positron emission tomography–computed tomography (PET-CT) in rats. This information was used to optimize the design of monetite onlays with different macroporous architecture that were then fabricated using a 3D-printing technique. *In vivo*, bone augmentation was attempted with these customized onlays in rabbits. PET-CT findings demonstrated that bone metabolism in the calvarial bone showed higher activity in the inferior and lateral areas of the onlays. Histological observations revealed higher bone volume (up to 47%), less heterogeneity and more implant osseointegration (up to 38%) in the augmented bone with the customized monetite onlays. Our results demonstrated for the first time that it is possible to achieve osseointegration of dental implants in bone augmented with 3D-printed synthetic onlays. It was also observed that designing the macropore geometry according to the bone metabolic activity was a key parameter in increasing the volume of bone augmented within monetite onlays.

1. Introduction

Dental implants are currently the preferred treatment option for replacement of teeth lost due to disease, trauma, surgery or congenital problems, because they are highly successful and maintain the integrity of the surrounding tissues [1,2]. Successful implant placement requires sufficient alveolar bone volume in order to ensure implant stability and osseointegration [1,3]. In severe cases of disease or trauma, alveolar bone must be restored before or in combination with implant placement. Although established procedures are highly successful for horizontal bone, vertical bone augmentation remains a major challenge due to anatomical limitations and technical difficulties [3,4].

There are three major surgical approaches for alveolar ridge restoration: guided bone regeneration, bone augmentation and distraction osteogenesis [4]; however, each of these techniques has its own limitations when used in cases with severe alveolar bone loss [5]. Bone augmentation using onlay bone grafts, harvested from either intraoral or extraoral sites is currently the most reliable technique with the highest success rate [6,7]. However, the use of autografts as onlays has many drawbacks such as the high morbidity and blood loss at the donor site, the need for multiple surgical sites, high resorption rate of the graft, and limited bone availability [6,8,9]. Not surprisingly, previous studies have reported that patients prefer a bone substitute block over an autograft block harvested from the iliac crest [5].

Synthetic bone substitutes, such as calcium phosphates, are being developed to eliminate the need of autologous grafts and to

* Corresponding author. Faculty of Dentistry, Room M60C, Strathcona Anatomy & Dent, 3640 University Street, Montreal, QC H3A 0C7, Canada. Tel.: +1 514 398 7203x09654; fax: +1 514 398 8900.
E-mail addresses: faleh.tamimimarino@mcgill.ca, fdamimim@farm.ucm.es (F. Tamimi).

http://dx.doi.org/10.1016/j.biomaterials.2014.03.050
0142-9612/

overcome their limitations [10]. Among these materials, dicalcium phosphate anhydrous (monetite) is of special interest because it is a resorbable, osteoconductive and osteoinductive biomaterial [10,11]. Moreover, monetite onlays could be suitable for vertical bone augmentation, and can be produced in customized designs using 3D-printing [12,13].

The *in vivo* osteoconductivity of synthetic bone substitutes is dependent on several properties including morphology, chemical composition and geometry at both the macro- and micro-scale. Biomaterials pore size, distribution and interconnectivity can significantly influence the exchange of fluids and hence the delivery of ions, nutrients and cells within and through the bone substitute [14–19]. On the other hand, porosity can increase the biodegradation of the implant material by increasing the surface area in contact with body fluids, which may enhance the osteoinductive potential of the material [16], but may also mechanically weaken the material, so a fine balance must be found.

Dental implants can be successfully placed in onlays when the newly formed bone occupies 30–40% of the total volume of the onlay [20]. Previously we have shown that monetite onlays used for vertical bone augmentation could be infiltrated by new bone *in vivo*, occupying up to 43% of the graft volume after 8 weeks implantation [21]. However, these onlays were still inferior to autologous grafts and featured heterogeneous bone growth distribution across their medial-lateral and inferior–superior axes, where higher bone volume was observed in the lateral and inferior areas of the onlays, which matches the distribution of blood vessels in the recipient site.

Therefore, we hypothesized that the anatomy of the recipient site could influence the bone metabolism within moneite onlays, and therefore accordingly, modifying the design of the synthetic onlays using 3D-printing technique by adding geometrical features that would facilitate and enhance the blood perfusion within the onlays could improve the bone growth in these onlays *in vivo*.

Previous studies proved that PET analysis could be used as a tool to assess bone viability in autogenous and allogeneic bone grafts [22,23]. Compared to other techniques, PET can detect early-mineralized bone formation and provide insight into the bone metabolic activity that occurs at specific sites of the skeleton [24,25].

Accordingly, the first aim of this study was to evaluate bone metabolic activity within monolithic monetite onlays *in vivo* using positron emission tomography-computed tomography (PET-CT). The second aim was to assess to what extent the customization of the onlay designed according to the anatomy and metabolic activity of the recipient site could affect the amount of bone formed in monetite onlays and its ability to osseointegrate with Ti dental implants.

2. Materials and methods

2.1. Ethical approval

In vivo experiments were approved by the ethical committee for animal experiments of the Rey Juan Carlos University of Madrid, Spain. Experiments were performed according to the guidelines described by the European Community Council Directive of 24 November 1986 (86/609/EEC), and adequate measures were taken to minimize pain and discomfort to the animals.

2.2. Assessment of bone metabolic activity in onlays

The aim of this part was to evaluate the metabolic activity within monolithic monetite onlays using PET analysis.

2.2.1. Onlays fabrication and three dimensional-printing (3D-printing)

A previously described 3D-printing technique (Z-Corporation, Rock Hill, SC) was used to prepare dicalcium phosphate dihydrate (DCPD) onlays [26]. Briefly, a 2:1 M ratio mixture of dicalcium phosphate anhydrous ($CaHPO_4$, monetite) (Merck, Darmstadt, Germany) and calcium carbonate ($CaCO_3$, calcite) (Merck, Darmstadt, Germany) was heated at 1400 °C for 7 h to synthesize α/β-tricalcium phosphate (α/β-TCP). After quenching to room temperature, the sintered mixture was crushed using a pestle and mortar, and then passed through a 160 μm sieve. Finally, a planetary ball mill (PM400, Retsch, Germany) was used for milling β-TCP for 10 min. Brushite onlays were printed with a 3D-powder printing system (Z-Corporation, Rock Hill, S.C) using 20% of diluted phosphoric acid (H_3PO_4) and β-TCP powder (Merck, Darmstadt, Germany).

After being printed, the samples were retrieved from the powder bed, and cleaned from residual unreacted β-TCP powder. To increase the degree of reaction to DCPD, the samples were stored in 20% H_3PO_4 for 3 × 60 s, and the onlays were then concurrently dehydrated into monetite and sterilized by autoclaving (121 °C; humidity 100%; 30 min). The final onlays were composed of the samples was approximately 63% monetite and 37% unreacted β-TCP with a total porosity of 44% [10,21]. Monetite monolithic blocks were prepared without any geometrical modifications using CAD software (Alibre design Xpress 10.0, Alibre Inc., Rock Hill, S.C). These blocks were cylindrical in shape (Ø 5.0 mm, 5.0 mm thick), and had a central hole (Ø 1.0 mm) for fixation with osteosynthesis screws (Mozo Gar, Valladolid; Spain).

2.2.2. Surgical procedure

Six monolithic onlays were placed on the calvarial bone of 6 female Wistar rats (0.2–0.4 kg weight). The rats were anaesthetized and the head was shaved. The cutaneous surface was disinfected with povidone iodine solution prior to the operation. A ~2 cm long full depth incision was made on the linea media of the calvaria and the periosteum was separated from the bone surface with a periosteal elevator. The monolithic monetite blocks were secured with osseosynthesis titanium screws. The incision was closed with a silk 4-o suture and the animals were left to heal for 8 weeks before being sacrificed with an overdose of sodium pentobarbital (Dolethal; Vetoquinol, France).

2.2.3. Computed tomography (CT) and positron emission tomography (PET)

Computed tomography (CT) and positron emission tomography (PET) scanning were performed after 8 weeks of healing period using PET-CT Albira Ars machine (Oncovision, Valencia; Spain). The live animals were anesthetized and placed in a supine position. Consequently, they received an injection of 18F–NaF tracer (the dose was 15MSv per rat), and simultaneously they were introduced into the PET-CT scanning machine for 20 min. PET and CT images were taken in three sections (coronal, sagittal and horizontal) and processed by using the software PMOD 2.95 (PMOD technologies, Zurich University, Zurich; Switzerland) (Fig. 1a–i).

2.3. Customizing onlays with different designs

2.3.1. Designs fabrication

According to the findings of PET analysis for bone metabolic activity, onlays were designed to allow blood flow and bone formation from areas of high metabolic rate to areas of low metabolic rate. Therefore, different designs were created using CAD software (Alibre design Xpress 10.0, Alibre Inc., Rock Hill, S.C). All designs were cylindrical in shape (Ø 9.0 mm, 4.0 mm thick), and had a central hole (Ø 0.5 mm) for fixation with osteosynthesis screws (AO/ASIF 4.0 self-drilling screws, Synthes GmbH&Co, Umkirch, Germany) (Fig. 2a–c). The onlays were then printed as described earlier.

2.3.2. Surgical procedure

Sixteen New Zealand rabbits (3.5–4.0 kg) were used to test the customized onlays *in vivo*. The animals were anesthetized and their heads were shaved before disinfecting the cutaneous surface with povidone iodine solution prior to the surgery. A full depth incision (~5 cm) was made on the linea media of the calvaria, and then the periosteum was separated from the bone using a periosteal elevator. Onlays were placed on the calvarial bone and fixed with osteosynthesis titanium screws. After a healing period of 8 weeks, a second surgery was performed to expose the onlays and place the Ti dental implants after four weeks from the initial placement of the onlays (3.35 mm Ø, 8.5 mm length; NobelBiocare, Kloten, Switzerland) (Fig. 2e–h) and then the incisions were closed with a silk 3-0 suture. Computed tomography (CT scan) and Cone beam images were taken in a lateral view of the rabbits' skull 4 weeks after Ti-implant placement, followed by sacrificing the rabbits. After that, implant samples from surgical sites were collected for histological analysis (Fig. 2i and j).

2.3.3. Histological preparation

Histological examinations were performed on dehydrated and resin embedded sections as described previously [12,21]. Shortly, the explants were fixed in 2.5% glutaraldehyde solution followed by dehydration in ascending concentrations of ethanol. The samples were then infiltrated and embedded in resin for 24 h before final polymerization (Technovit, Leica Microsystems GmbH, Wetzlar, Germany). Coronal histological sections crossing the centre of the onlays were taken using a micro saw (SP1600 Leica Microsystems GmbH, Wetzlar, Germany), and the samples were stained with methylene blue (MB) and basic fuchsine (BF).

Pictures of histological sections were taken by Bioquant Nova Prime software (BIOQUANT Image Analysis Corporation, Nashville, TN) using a ProgRes C14 digital camera (Jenoptik, Jena, Germany) installed on a Leica DMR light and fluorescence microscope (Leica DMR microscope type 020-525.024, Leica Microsystems, Wetzlar,

Please cite this article in press as: Tamimi F, et al., Osseointegration of dental implants in 3D-printed synthetic onlay grafts customized according to bone metabolic activity in recipient site, Biomaterials (2014), http://dx.doi.org/10.1016/j.biomaterials.2014.03.050

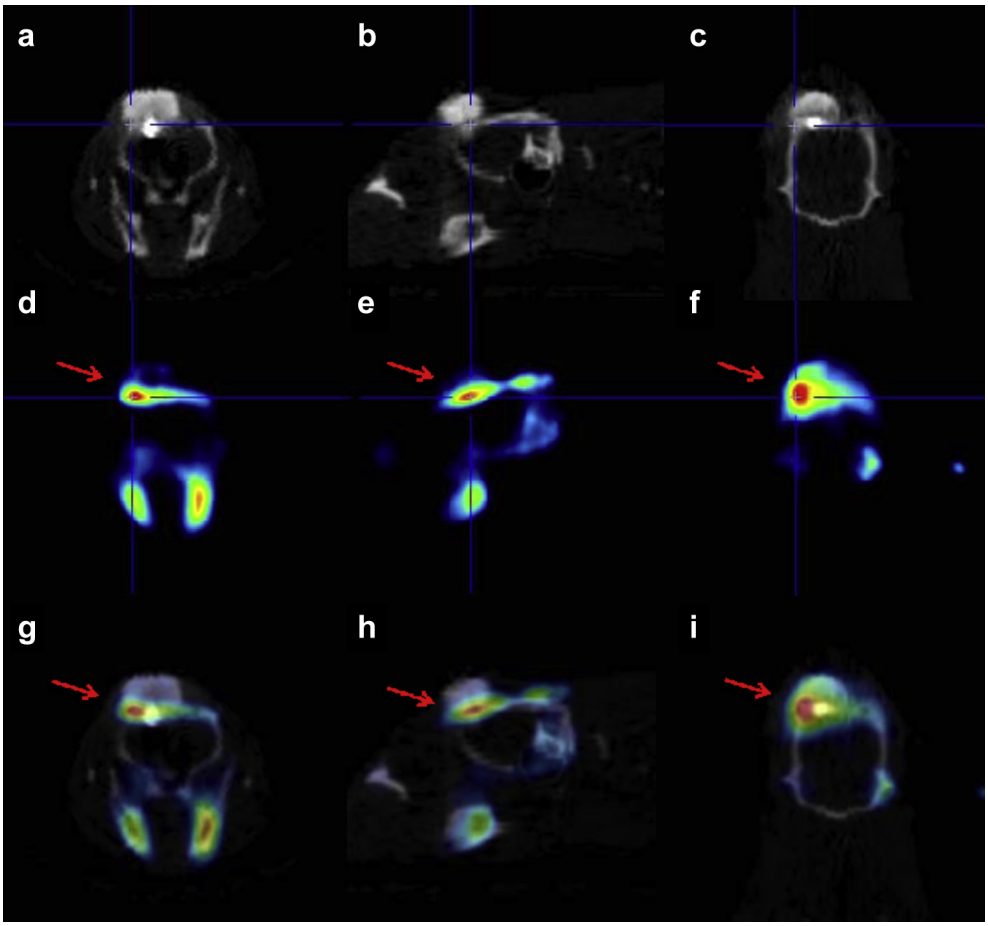

Fig. 1. (a–c) CT scans of the onlays fixed with screws on the rats' calvaria bone in a coronal, sagittal and horizontal sections respectively. **(d–f)** PET images, taken in a coronal, sagittal and horizontal sections respectively, demonstrating the low and high (red arrows) regions of bone metabolic activity. **(g–i)** Superimposed images of PET and CT scans, demonstrating that the high bone metabolic activity was in the lateral region of the onlays (red arrows) compared to the medial region. (For interpretation of the references to colour in this figure legend, the reader is referred to the web version of this article.)

Germany). Prior to analysis, the individual pictures were stitched using the software PTGui (New House Internet Services B.V., Rotterdam; The Netherlands) (Fig. 3).

2.3.4. Histomorphometrical analysis

Images of the histological coronal sections crossing the centre of the blocks were used to perform the histomorphometrical analysis of the implanted area [12,21]. For each histological section, the area occupied by the remaining unresorbed graft material, as well as the bone growing around and within the onlays was identified and measured. These values were used to calculate the percentage of bone volume, and remaining material within the onlay, as well as the bone height and Ti implant osseointegration (Fig. 4).

In each image section, the augmented bone area was divided into 24 smaller squares (1 mm × 1 mm) using a 6 column × 4 row computer generated grid which was adjusted to cover the entire onlay in the image, and localized histomorphometrical analysis was performed for each square (Supplementary) [12,21]. The localized histomorphometrical values of each square were interpolated in order to generate a statistical map of the distribution of bone and remaining monetite within the onlays using the Renka-Kline model [27] (Origin 7.0; Origin Lab Co., Northampton, MA) (Fig. 5). The monetite resorption was quantified by subtracting the area of remaining monetite in the histological sections (after 8 weeks) from the original cross-sectional area of each onlay divided by the original cross-sectional area of each onlay adjusted to the original microporosity (44%).

To evaluate the bone height gained within the onlays during implantation, histological sections crossing through the dental implants at the centre of the onlays were evaluated. Vertical bone height was measured by calculating the distance between the original calvarial surface and the maximum bone height gained in the onlays. To assess the maximum bone height distribution within the onlays, the augmented bone area was divided into 8 smaller columns (1 mm × 4 mm) using the same computer generated grid described above, and maximum bone height in each column was measured (Supplementary). The software Image J (ImageJ 1.46r; Wayne Rasband, National Institutes of Health, Maryland) was used to assess the percentage of bone-to-implant contact ratio.

Kruskal–Wallis one-way analysis was used to evaluate any significant differences among the four designs, and Mann–Whitney test was used to evaluate head-to-head differences between the designs (SPSS 19, IBM Corp.; New York; USA). The statistical significance was set at a value of $P < 0.05$.

2.3.5. X-ray diffraction analysis

X-ray diffraction (XRD) was used to analyze the crystallographic composition of the implanted onlays in the polymerized blocks using the X-ray diffraction spectroscopic machine (D8 DISCOVER/GADDS, Bruker, Karlsruhe, Germany) with a two-dimensional detector (50 mm, HI–STAR, Bruker, Karlsruhe, Germany). XRD patterns were collected at 40 kV and 40 mA Cu Kα monochromatic radiation, and from $2\theta = 20°–45°$ scanning angle with a step size of 0.02° and a normalized count time of 1s/step. The International Centre for Diffraction Data references were used to check for α-TCP (PDF Ref. 09–0348), β-TCP (PDF Ref. 09–0169), monetite (PDF Ref. 09–0080), brushite (PDF Ref. 09–0077) and hydroxyapatite (PDF Ref. 09–0432) using a DIFFRACplus EVA software (AXS, Bruker, Karlsruhe, Germany) that analyzes the data obtained from each XRD spectrum (Fig. 6a and b). To demonstrate the distribution of the HA and monetite crystals within the onlays, multi-target scan was run to record patterns of different points across the onlay. This multi-target scan was used to generate interpolated maps of the XRD patterns by using Origin program (Origin 7.0; Origin Lab Co., Northampton, MA).

3. Results

3.1. Bone metabolic activity

3.1.1. PET-CT Analysis

None of the monolithic onlays grafted on rats calvaria were lost or showed any signs of inflammation. CT and PET imaging were performed 8 weeks after the grafting procedures, and CT images of

Please cite this article in press as: Tamimi F, et al., Osseointegration of dental implants in 3D-printed synthetic onlay grafts customized according to bone metabolic activity in recipient site, Biomaterials (2014), http://dx.doi.org/10.1016/j.biomaterials.2014.03.050

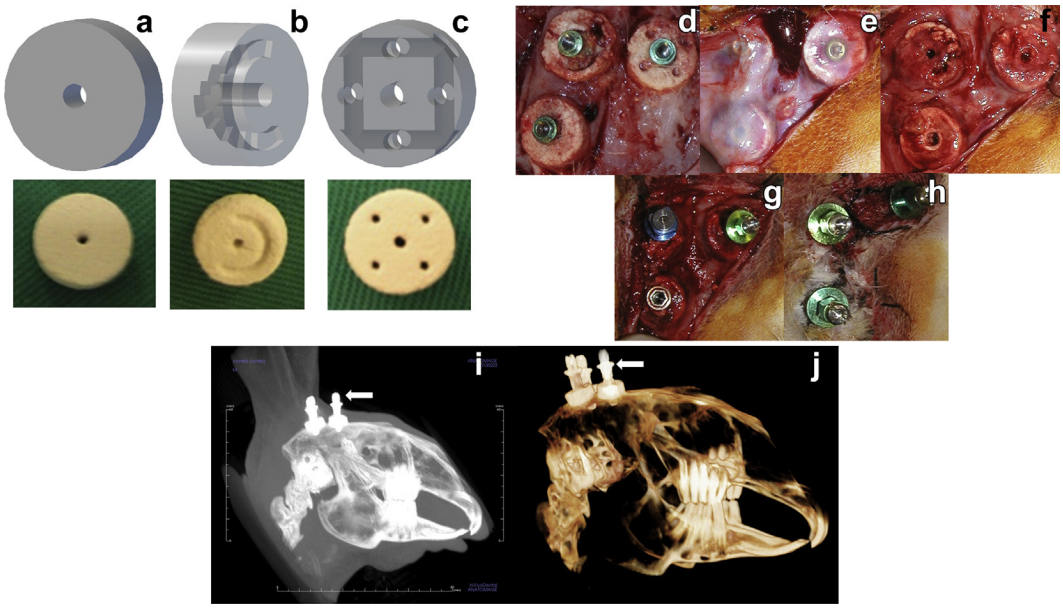

Fig. 2. **(a–c)** CAD images of the onlay designs (top) compared with photographs of the 3D-printed monetite bioceramics (bottom): **(a)** Design A, monolithic without any surface modifications; **(b)** Designs B and C had a C-shaped groove either on the superior surface of the onlay facing the periosteum (Design B) or on the inferior surface of the onlay facing the bone (Design C); **(c)** Design D had 8 interconnected channels (4 vertical and 4 horizontal) opened into all the surfaces of the onlay. All designs possessed a central hole to allow placement of osteosynthesis screws. **(d–h)** Photographs depicting the surgical procedure: **(d)** onlay placement fixation with osteosynthesis screws; **(e)** Opening of the surgical sites after 4 weeks, **(f)** and removal of the osteosynthesis screws; **(g)** Implant placement in the holes left be the removed screws; **(h)** Suturing of the surgical site. **(i,j)** CT scan and cone beam in a lateral view of the skull showing the Ti implants (arrows) in the monetite onlays following placement on the rabbit calvaria respectively.

the onlay in different sections showed that the onlays were well integrated to the calvarial bone (Fig. 1a–c). PET analyses showed that the bone metabolism was significantly higher in the lateral and inferior areas of the onlay compared to other areas (Fig. 1d–f). PET and CT scan were superimposed on each other to display the increase of bone metabolic activity that is shown in the PET images on the anatomical structure that could be seen in the CT images (Fig. 1g–i).

These results were used to construct the second objective of the study, where onlays with different geometry were designed to facilitate an equal distribution of the bone metabolic activity across the onlay.

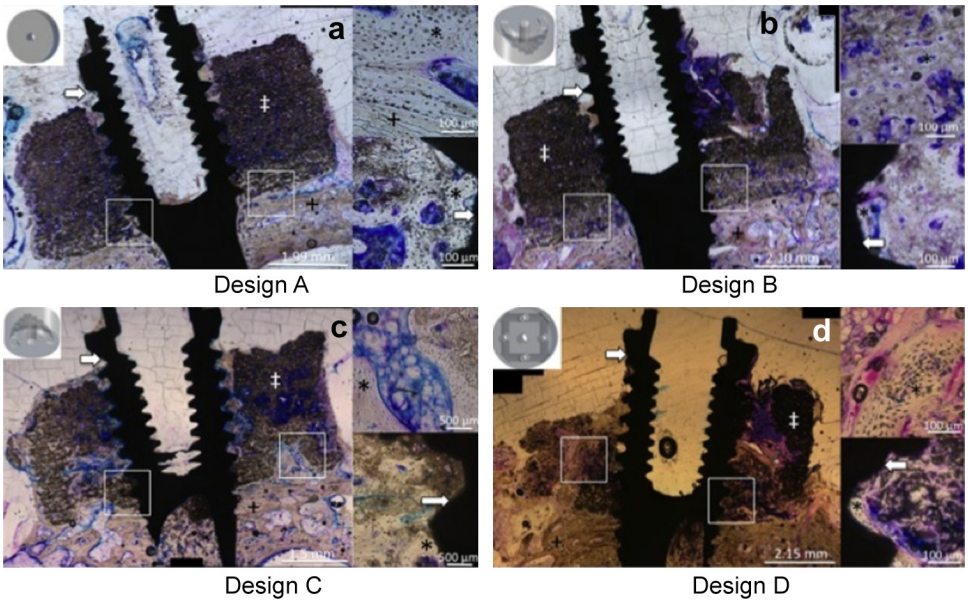

Fig. 3. Histological micrograph sections taken from: Design A **(a)**, Design B **(b)**, Design C **(c)**, and Design D **(d)** showing bone infiltration within the monetite onlays (‡) grafted on the calvarial bone in rabbits (+), and Ti dental implant (arrow). Original magnification ×2.5. Inserts show magnified sections of images (a, b, c and d) showing the osseointegration interface between the newly formed bone (*) in the onlays and the Ti implants (arrow), and the integrated area between the calvarial bone (+) and the bone infiltrated in the onlays (*), original magnification ×20.

Please cite this article in press as: Tamimi F, et al., Osseointegration of dental implants in 3D-printed synthetic onlay grafts customized according to bone metabolic activity in recipient site, Biomaterials (2014), http://dx.doi.org/10.1016/j.biomaterials.2014.03.050

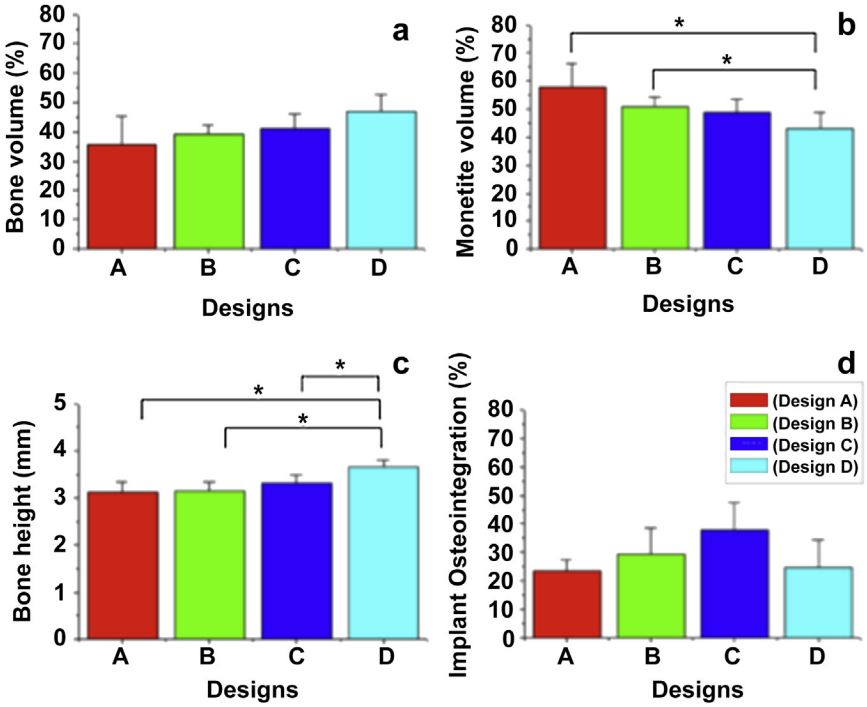

Fig. 4. Graphs of the histomorphometrical analysis representing: **(a)** Bone volume percentages and **(b)** monetite percentage in the different onlay designs. **(c)** Ti implant osseointegration, **(d)** bone height gained in the different onlay designs (*) Indicates that there is significant difference between the designs (P value < 0.05).

3.1.2. Monetite onlays with different designs

The geometrical modification of the onlays was aimed to increase bone formation and blood flow in the medial and superior areas, hence they showed low bone metabolic activity according to the PET-CT analysis. Therefore, four designs were fabricated: Design A, monolithic without any modifications as a control group (Fig. 2a). Design B included a C-shaped groove with a hill-like depth profile on the superior surface of the onlay facing the overlain periosteum. The length of the groove equals half the circumference of the cylinder's surface, where the groove sloped inside the onlay (Fig. 2b). When implanted, the deepest part of the groove is the most inferior surface of the slope facing the midline suture of the calvarial bone, and the shallowest part is at the ends of the groove (Fig. 2d).

Design C was the same as Design B, but the C-shaped groove was placed on the inferior surface of the onlay facing the periosteally stripped bone, where the deepest part of the groove would be the most superior surface of the slope (Fig. 2b). Designs B and C were fabricated to assess the influence of adding macroporosity in different regions of the onlay.

Design D included 8 interconnected channels open at all the surfaces of the onlay. Four vertical channels open on the superior and inferior surfaces of the cylinder, and four horizontal channels open on the sides of the cylinder (Fig. 2c) to allow blood diffusion from the high metabolic areas (lateral and inferior) to low metabolic areas (medial and superior). The final phase composition of the samples was approximately 63% monetite and 37% unreacted β-TCP. All design features were discernable at the resolution of printing with a total microporosity of 44% and a micropore diameter of 10–20 μm [10].

3.2. Bone augmentation with customized onlays

3.2.1. Surgical observation

During the two surgical procedures and the post-operative phase, no complications were noticed. Upon implant retrieval, no signs of rejection were observed in all the onlays and they all appeared to be integrated and vascularized. Moreover, no loosening of the Ti implants or onlays was observed (Fig. 2i and j).

3.2.2. Histological observation

Histological observations revealed that the onlays were well integrated with the calvarial bone (Fig. 3). In addition, no inflammatory cell infiltration was found around or within the onlays (Fig. 3). Bone infiltration and blood vessels formation occurred throughout the monetite onlays of all designs (Fig. 3), although it was more pronounced inside the holes of Design D and grooves of Design C (Fig. 3c and d).

Abundant soft tissue formation and scarce bone infiltration was observed on the superior areas of the groove in Design B; however, the inferior part of the groove showed more bone formation in comparison to the other parts of the same groove (Fig. 3c). The Ti implants appeared to be osseointegrated with the new bone formed in the onlays, as it can be inferred from the close contact observed between the infiltrated bone and the surface of the Ti implants (Fig. 3).

3.2.3. Histomorphometrical analysis

3.2.3.1. Bone augmentation within onlays. Histomorphometric analysis revealed that the percentage of new bone formed in the onlays ranged between 35.7 ± 9.8% (Design A) to 46.9 ± 5.7% (Design D) of the total onlay area (Fig. 4a). Although Kruskal–Wallis test did not show any significant differences among the designs, Mann–Whitney test showed that there was a significant head-to-head difference between designs A and D ($P = 0.047$), as well as between designs B and D ($P = 0.028$) (Fig. 4a). The interpolated maps of the histomorphometrical analysis for the distribution of augmented bone within the onlays revealed that more bone formed in the lateral and inferior areas of all the onlays as well as inside the holes and grooves, and less bone formed in the superior and medial areas (Fig. 5a and Supplementary).

Please cite this article in press as: Tamimi F, et al., Osseointegration of dental implants in 3D-printed synthetic onlay grafts customized according to bone metabolic activity in recipient site, Biomaterials (2014), http://dx.doi.org/10.1016/j.biomaterials.2014.03.050

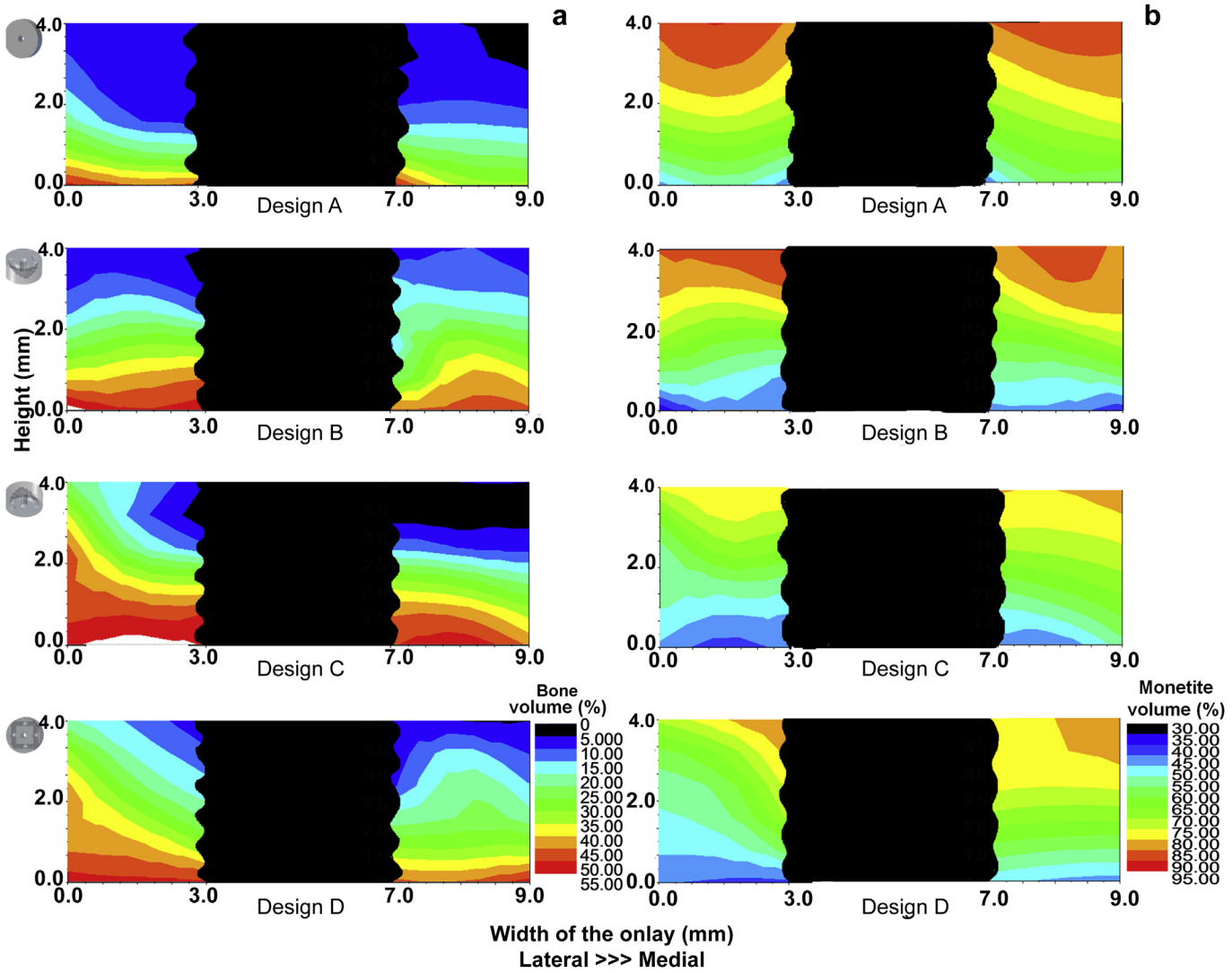

Fig. 5. Interpolated maps of the histomorphometrical results in (Fig. 1 Supplementary): **(a)** the averaged distribution of the newly formed bone in the onlays of the four designs. Red and orange colours show intense bone growth. Yellow and greens colours indicate moderate new bone formation, while blue and black indicate low bone formation in the onlays. **(b)** Distribution of the remained material within the onlays of the different designs. Red and orange colours show concentrated remaining material. Yellow and greens colours indicate moderate material, while blue and black indicate low material left in the onlays. (For interpretation of the references to colour in this figure legend, the reader is referred to the web version of this article.)

In the areas close to the calvarial bone (inferiorly), designs A and C showed more bone formation in the lateral side compared to the medial side. However, designs B and D showed almost equal amount of bone infiltration in both sides (Fig. 5a and Supplementary). In the superior areas close to the periosteum, all designs showed more bone formation in the lateral areas than the medial areas (Fig. 5a and Supplementary).

The groove in both designs B and C showed more bone formation in the inferior and lateral areas compared to the superior and medial ones (Fig. 5a and Supplementary). In addition, Design D showed more bone formation inside the holes compared to the other areas (Fig. 5a and Supplementary), and more bone formation was observed in the inferior areas of the holes compared to the superior areas (Fig. 5a and Supplementary).

3.2.3.2. Effect of customized macroporous geometry on bone formation. Although the heterogeneity of bone distribution was noticeable in Design A, the other designs showed more uniformly bone distribution along the medial-lateral and superior–inferior axes. In areas close to the periosteum, designs C and D showed higher bone formation in the lateral side compared to designs A and B (Fig. 5a and Supplementary). However, all designs showed little or no bone formation in the most superior-medial area.

The groove in Design C showed more bone formation and no soft tissue infiltration compared to Design B (Fig. 5a and Supplementary). In addition, designs B and C showed high bone formation in the area around the implant compared to designs A and D, where Design D showed more bone formation in the sides of the onlay compared to the centre area (Fig. 5a and Supplementary).

3.2.3.3. Bone height gained. The average bone height gained in the monetite onlays ranged from 3.1 ± 0.2 mm in Design A to 3.7 ± 0.1 mm in Design D. The Mann–Whitney test showed that there were significant differences between the designs A and D ($P = 0.021$), B and D ($P = 0.021$), C and D ($P = 0.021$) (Fig. 4c). All onlays gained more bone height in the lateral area compared to the medial area (Supplementary). According to the Kruskal Wallis test, there were no significant differences between the medial areas of

Please cite this article in press as: Tamimi F, et al., Osseointegration of dental implants in 3D-printed synthetic onlay grafts customized according to bone metabolic activity in recipient site, Biomaterials (2014), http://dx.doi.org/10.1016/j.biomaterials.2014.03.050

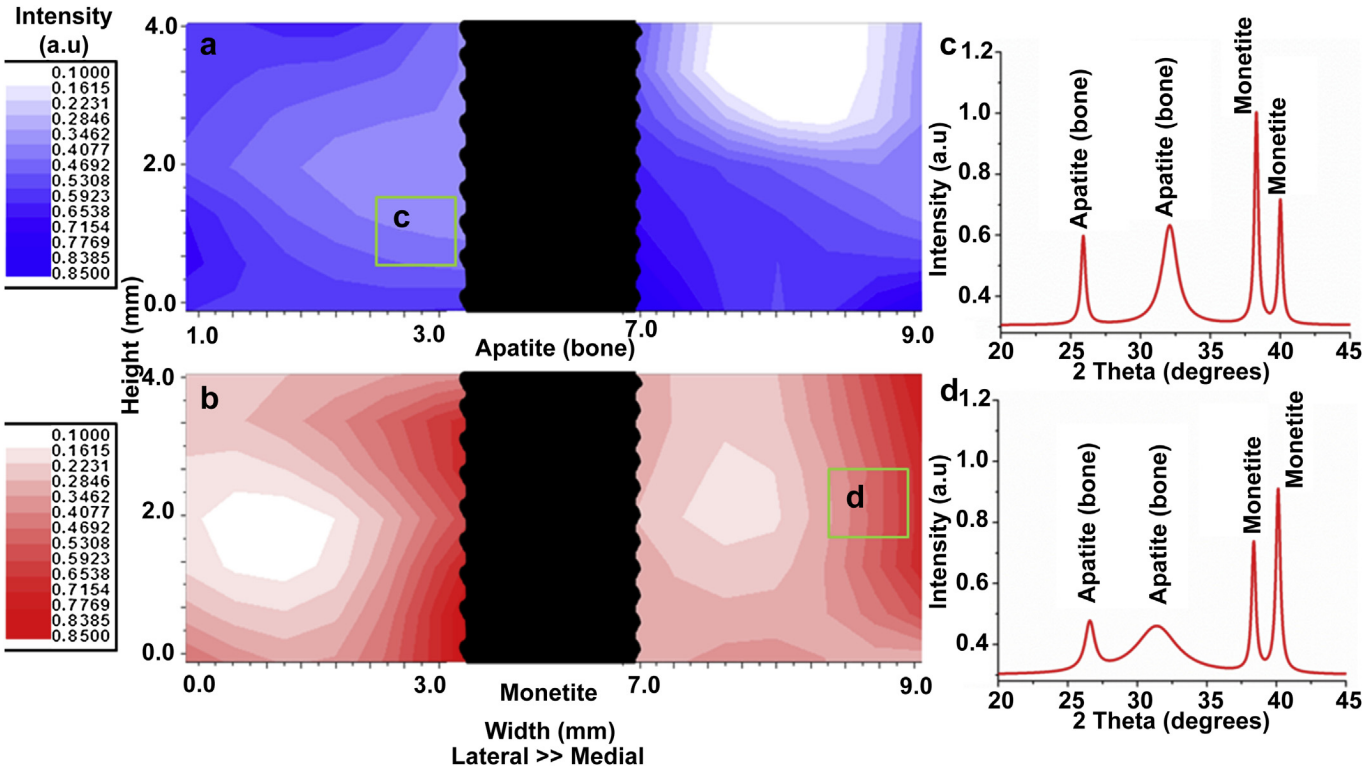

Fig. 6. Interpolated maps of the XRD phase analysis demonstrating the distribution of **(a)** apatite crystals (bone) and **(b)** monetite crystals across the onlays. The red and blue colours indicate high concentrations of material crystals, while the white colour indicates low concentration of both materials. **(c,d)** XRD patterns of the remaining material (apatite (bone) and monetite) within the onlay, demonstrating the materials intensity according to the diffraction angle 2θ. (For interpretation of the references to colour in this figure legend, the reader is referred to the web version of this article.)

the designs. However, the Mann–Whitney test showed that designs C and D gained significantly more bone height in comparison to the other designs.

In the medial area close to the implant, a significant difference in bone height was found between designs D and B ($P = 0.021$), as well as designs D and C ($P = 0.021$) (Supplementary). In the centre of the medial area, there were significant differences between designs D and A ($P = 0.021$), designs D and B ($P = 0.021$), designs D and C ($P = 0.043$), as well as between designs A and C ($P = 0.021$), and designs B and C ($P = 0.021$) (Supplementary). In addition, the most medial side of the onlay showed a significant difference between designs A and C ($P = 0.043$), as well as designs A and D ($P = 0.021$).

3.2.3.4. Monetite resorption. The percentage of remaining unresorbed monetite ranged between 43.1 ± 5.7% (in Design D) and 57.7 ± 8.5% (in Design A) of the total onlay area, with significant differences between designs A and D ($P = 0.037$), as well as between designs B and D ($P = 0.037$) (Fig. 4b). The interpolated maps of the remaining monetite distribution showed that a scarce amount of monetite remained in the inferior areas of all the onlays, and a greater amount remained in the medial and upper areas of designs A and B compared to designs C and D (Fig. 5b. and Supplementary). The monetite resorption in Design A reached 42.2 ± 8.9%, and reached 47.9 ± 6.9% and 51.0 ± 8.1% in designs B and C respectively, and 56.5 ± 7.4% in Design D. The monetite resorption in Design D was significantly higher than in Design A, with a significant difference between Design A and D ($P = 0.047$).

XRD pattern analysis confirmed the histological observations and demonstrated that the crystals of the remaining material were composed of monetite and β-TCP only (Fig. 6c and d). XRD interpolated maps of Design B demonstrated that bone (apatite crystals) was more concentrated in the lateral and inferior regions of the onlay compared to the medial and superior ones where monetite crystals were more concentrated (Fig. 6a and b).

3.2.3.5. Implant osseointegration. The surface of the Ti-implants placed in the onlays was partially osseointegrated (20.9 ± 9.7% – 37.8 ± 9.9%). According to Kruskal Wallis test, there was no significant differences among the four designs; however, the Mann–Whitney test revealed that there was a significant difference in osseointegration between designs C and A ($P = 0.021$) (Fig. 4d), where the highest bone to implant contact ratio was achieved in Design C and the lowest ratio in Design A. Onlays in Design A showed more osseointegration between the infiltrated bone and the lateral surface of the implant compared to the medial surface; however, Design B showed more osseointegration in the medial side where the groove was located. On the other hand, onlays from designs C and D showed almost equal bone to contact ratio in both sides of the implant.

4. Discussion

4.1. Bone metabolic activity

The bone formation process was monitored by positron emission tomography–computed tomography (PET-CT) (8 weeks) after placement of the onlays. This fused PET-CT method allowed the detection of the activity of mineralized bone formation in a 3D bony architecture reconstructed by the CT scan. Bone metabolism showed a higher activity in the lateral and inferior regions of the onlay compared to the medial region, and showed no activity in the superior region in the early detection of bone formation.

Please cite this article in press as: Tamimi F, et al., Osseointegration of dental implants in 3D-printed synthetic onlay grafts customized according to bone metabolic activity in recipient site, Biomaterials (2014), http://dx.doi.org/10.1016/j.biomaterials.2014.03.050

These findings were in agreement with our previous studies, where similar heterogeneous bone growth distribution across the onlay was noticed; however, the reason behind it was not clear [21]. Previous studies demonstrated that bone metabolic activity is directly related to the host bone formation and blood flow [28,29]; therefore, using PET-CT findings enabled us to provide an accurate picture of bone metabolic activity, bone formation and blood flow in monetite onlays augmented on the calvarial bone. Here we showed that the PET-CT can be a very useful method for surveying the viability of the newly formed bone in synthetic bone grafts.

4.2. Bone augmentation with customized onlays

4.2.1. Bone augmentation within onlays

All onlay designs shared the same microporosity throughout the materials (pore size <20 μm [29]) with a total porosity of 44% [10]. However, the different macroporosity (i.e. pore size >100 μm [29]) of each design effected the augmented bone volume, bone height gained, and Ti implant osseointegration within the onlays.

According to the literature, the minimum pore size required to regenerate mineralized bone is considered to be <100 μm [28]. Smaller pores (75–100 μm) resulted in the ingrowth of unmineralized osteoid tissue, and pores of 10–44 and 44–75 μm were penetrated only by fibrous tissue [28]. However, larger pore sizes of 300–400 μm showed new bone and capillary formation [28]. Therefore, the 1 mm holes and grooves in designs D, B and C were expected to promote the growth of bone and capillaries.

The effect of microporosity and macroporosity in synthetic blocks was already confirmed in the previous studies by increasing or decreasing the micro- or/and the macroporosity in these blocks [10,30]. However, in this study, macroporosity was designed to facilitate the blood diffusion from areas with higher metabolic rate to areas with lower rate as mentioned earlier in the results section. Therefore, our results demonstrate that introducing customized macroporous geometry can significantly increase the amount of new bone that is formed within synthetic onlay grafts. The mean average of augmented bone volume gained ranged between 36% (Design A – no macropores) and 47% (Design D – most macropores) of the total onlay area. These results agree with previous studies showing that adding large holes and increasing macroporosity leads to an improvement of bone formation in synthetic biomaterials [31,32].

Regardless of the design, bone was always more abundant in the lateral and inferior areas of the onlays. This spatially dependant effect was also seen in a previous study in which monolithic monetite onlays were used [33] and was expected to be seen in the PET analysis, indicating that the bone metabolic activity was higher in the lateral and inferior regions of the calvaria probably due to the anatomy of the blood vessels in the calvarial bone.

On the other hand, the distribution of bone formed within the medial and superior areas seemed to be influenced by the onlay design. Our results indicate that the macroporosity seem to have influenced the bone distribution by directing the bone growth from high metabolic areas to the rest of the graft through the holes and grooves. The superior areas of the onlays showed higher bone formation in designs C and D compared to designs A and B. In addition, the medial side showed higher bone formation in designs B, C and D compared to Design A.

Although Design D showed more overall bone formation (47%) compared to Design A (36%), the bone volume achieved in Design D was still lower than the one reported for autologous onlays (55–60%) [21]. However, the bone volume in the customized monetite onlays reached over 35% of the total graft volume, which could certainly be considered as a successful grafting procedure [34].

Designs B and C had a groove around the implant, on the upper surface facing the periosteum or the lower surface facing the calvarial bone respectively. These two designs were produced to assess the influence of adding macroporosity in different regions of the onlay as mentioned earlier in the results section. The design with a groove facing the calvarial bone (Design C) had higher percentage of bone formation in comparison to the design with the groove facing the periosteum (Design B). These results seem to indicate that bone regeneration might be originating from the calvarial bone but not from the periosteum. This is in agreement with previous studies on bone augmentation in rabbit calvaria [35,36]. During bone regeneration, stem cells are produced from either the periosteum or the cancellous bone to assist in bone growth [37]. Although the periosteum plays an important role in long bone regeneration [38], previous studies have demonstrated that the periosteum covering the calvarial bone has a minor role in osteogenesis and only enhances bone formation in the areas close to it [35,36].

4.2.2. Bone height gained

The overall bone height gained was significantly higher in Design D compared to the other designs, which was probably due to the presence of high macroporosity in Design D that lead to the increase in bone formation and therefore the increase in bone height. In addition, increasing macroporosity significantly enhanced the distribution of bone height gained in the medial areas for Design D in comparison to the other designs (Supplementary).

In this study, customized monetite onlays were able to provide an additional bone height of almost 4 mm when placed on the calvarial bone (2 mm). This indicates that augmenting a severely resorbed mandible (<7.0 mm, Cawood type IV [39]) with these onlays can provide sufficient bone height for the placement of dental implants [9,39,40]. Although future studies will have to be done to prove that this is possible in human subjects.

4.2.3. Monetite resorption

After 8 weeks of implantation, the percentage of the remaining monetite material in the onlays ranged from 43% to 57% of the total original area of the onlays. This is similar to previous studies in which it was shown that after *in vivo* implantation of the onlays, only 50–66% of moentite remained after a period of 8 weeks [21,26].

According to the Hixon and Crowell equation, two factors affect the dissolution rate of a given material *in vivo*, the properties of the material itself such as geometry (porosity and surface area) and solubility, and the properties of the dissolving medium such as the volume and temperature [41]. Rabbits have a stable temperature and concentration of ions in serum, in addition to the high rate of water exchange because of their low body mass [34,36]. Therefore, the resorption rate of the monetite that is mainly due to either passive dissolution or the cellular activity would depend mostly on its solubility and geometry [42]. This explains the significantly lower amount of remaining monetite in Design D compared to the other designs. Since this design had more macroporosity that increased the surface area that is in contact with the body fluids facilitating monetite resorption in these onlays.

The size of the holes and grooves in designs B, C and D were large enough for cells to go through and increase the monetite resorption by cellular activity. However, resorption of monetite in designs B (47.9%), C (51.0%) and D (56.5%) was very similar to Design A (42.2%). This seems to indicate that macrospores allowing cellular infiltration had a minor effect on monetite resorption and passive diffusion was the main mechanism affecting the resorption of these onlays.

Please cite this article in press as: Tamimi F, et al., Osseointegration of dental implants in 3D-printed synthetic onlay grafts customized according to bone metabolic activity in recipient site, Biomaterials (2014), http://dx.doi.org/10.1016/j.biomaterials.2014.03.050

The volume of macroporosity (including holes and grooves) in each design was 0.31% in Design A, 5.86% in designs B and C, and 14.71% in Design D. Although there was a difference between the ratios of the macroporosity in each design, monetite resorption factor was almost identical among all the designs. This means that the high microporosity in all designs (44%) played a major role in moentite resorption, and the macroporosity only played a minor role.

XRD analysis at the end of the two surgical procedures showed that the crystalline pattern of the onlay consists of three materials, monetite, β-TCP and apatite, confirming our previous observations [21]. The interpolated maps of the XRD analysis demonstrated that monetite was the main constituent of the medial and superior regions of the onlay, and poorly crystalline apatite was found in the inferior and the lateral region of the onlay. Both XRD and histological findings seem to agree in indicating that bone was present in the areas where there was no monetite. In addition, there was no evidence of monetite conversion to hydroxyapatite throughout the onlay.

4.2.4. Dental implant osseointegration

In this study, we demonstrated for that bone augmented with synthetic onlays can osseointegrate with Ti dental implants. Four weeks after placing the Ti implants, 21–38% of their surface was osseointegrated with the newly formed bone within the monetite onlays.

A previous study stated that 50% of bone to implant contact ratio is needed to provide a stable implant restoration [43]; however, placement of dental implants can be considered successful when the newly formed bone volume reaches 30–40% of the total graft volume [20]. Therefore, the volume of bone infiltration reached in our monetite onlays (36–47%) demonstrates that monetite onlays are probably suitable for a successful Ti dental placement, although future studies should be done to improve the bone to implant contact ratio in monetite onlays.

In addition, the local bone metabolic activity and anatomy affected the bone-implant contact ratio of each side of the dental implant, whereupon the ratio was higher in the lateral side of the implant in the Design A compared to the medial side. On the other hand, the ratio was higher in the medial side of the implant in Design B due to the presence of the groove in that area leading to more bone formation in the medial side and therefore higher osseointegration ratio was achieved. Design C and D, showed almost equal bone to implant contact ratios in both sides, hence the bone infiltration was distributed homogenously in the medial and lateral areas of these designs. Although Design D had higher bone formation percentage among all the designs, Design C had the highest bone to implant contact ratio than all the other designs including Design D. This was probably because the holes in Design D directed bone formation to the sides of the onlays and away from the implant and had less influence over implant osseointegration, while the groove in Design C was close to the implant, which facilitated the direction of bone growth towards the implant (Fig. 3c). Therefore, increasing the complexity of onlay design can compensate for differences due to anatomical features.

5. Limitations and future studies

This study was not designed to assess the biodegradation rate of monetite onlays, since the complex geometry of the onlays hindered the calculation of the original onlay volume. Therefore, future studies are needed in order to explore the effects of geometry on onlay resorption. Moreover, this study did not include any mechanical tests for the osseointegrated implants, which should be considered in the future. Even though both the calvarial bone and the mandible form intramembranously, vertical bone augmentation is mostly relevant in the posterior atrophic mandible. Accordingly, future studies should be done for clinical applications in the mandible. Onlays could be designed to direct bone growth toward the implants in future studies, because this will increase the osseointegration in synthetic onlays.

6. Conclusion

Our results demonstrate that bone metabolic activity in onlays is anatomy-dependant and correlated with the ability of bone augmentation. In addition, the results demonstrate that it is possible to achieve osseointegration of dental implants in bone augmented with synthetic monetite onlays. Macroporuos geometry can enhance bone growth, bone height gained and Ti implant osseointegration within the monetite onlays. Onlays geometry should be designed to facilitate the diffusion of cells and nutrients from high bone metabolic to low bone metabolic areas. More bone formation was found in onlays with increased porosity facing the calvarial surface compared to onlays with porosity facing the periosteum.

Acknowledgements

The authors acknowledge financial support from “Fundacion Espanola para la Ciencia y Tecnologia” (FECYT); The Spanish Science and Education Ministry (MAT2006-13646-C03-01); the UCM Program for Research Groups; The Canada Research Chair program, NSERC Discovery Grant (RGPIN 418617-12) (J.E.B.), NSERC Discovery Grant (F.T) and the Québec Ministère des Relations Internationales (Québec-Bavaria Exchange Program) PSR-SIIRI-029 IBI; and the dental implant provider.

Appendix A. Supplementary data

Supplementary data related to this article can be found at http://dx.doi.org/10.1016/j.biomaterials.2014.03.050.

References

[1] Levin L. Dealing with dental implant failures. J Appl Oral Sci 2008;16(3):171–5.
[2] Tolman DE. Advanced residual ridge resorption: surgical management. Int J Prosthodont 1993;6(2):118–25.
[3] Rocchietta I, Fontana F, Simion M. Clinical outcomes of vertical bone augmentation to enable dental implant placement: a systematic review. J Clin Periodontol 2008;35(8 Suppl.):203–15.
[4] McAllister BS, Haghighat K. Bone augmentation techniques. J Periodontol 2007;78(3):377–96.
[5] Esposito M, Grusovin MG, Felice P, Karatzopoulos G, Worthington HV, Coulthard P. The efficacy of horizontal and vertical bone augmentation procedures for dental implants – a Cochrane systematic review. Eur J Oral Implantol 2009;2(3):167–84.
[6] Hill NM, Horne JG, Devane PA. Donor site morbidity in the iliac crest bone graft. Aust N Z J Surg 1999;69(10):726–8.
[7] Isaksson S, Alberius P. Maxillary alveolar ridge augmentation with onlay bone-grafts and immediate endosseous implants. J Craniomaxillofac Surg 1992;20(1):2–7.
[8] Chiapasco M, Zaniboni M, Rimondini L. Autogenous onlay bone grafts vs. alveolar distraction osteogenesis for the correction of vertically deficient edentulous ridges: a 2-4-year prospective study on humans. Clin Oral Implants Res 2007;18(4):432–40.
[9] Felice P, Marchetti C, Iezzi G, Piattelli A, Worthington H, Pellegrino G, et al. Vertical ridge augmentation of the atrophic posterior mandible with interpositional bloc grafts: bone from the iliac crest vs. bovine an organic bone. Clinical and histological results up to one year after loading from a randomized-controlled clinical trial. Clin Oral Implants Res 2009;20(12):1386–93.
[10] Habibovic P, Gbureck U, Doillon CJ, Bassett DC, van Blitterswijk CA, Barralet JE. Osteoconduction and osteoinduction of low-temperature 3D printed bioceramic implants. Biomaterials 2008;29(7):944–53.
[11] Tamimi F, Torres J, Kathan C, Baca R, Clemente C, Blanco L, et al. Bone regeneration in rabbit calvaria with novel monetite granules. J Biomed Mater Res A 2008;87(4):980–5.

[12] Torres J, Tamimi F, Alkhraisat MH, Prados-Frutos JC, Rastikerdar E, Gbureck U, et al. Vertical bone augmentation with 3D-synthetic monetite blocks in the rabbit calvaria. J Clin Periodontol 2011;38(12):1147–53.
[13] Gbureck U, Vorndran E, Muller FA, Barralet JE. Low temperature direct 3D printed bioceramics and biocomposites as drug release matrices. J Control Release 2007;122(2):173–80.
[14] Lecomte A, Gautier H, Bouler JM, Gouyette A, Pegon Y, Daculsi G, et al. Biphasic calcium phosphate: a comparative study of interconnected porosity in two ceramics. J Biomed Mater Res B Appl Biomater 2008;84(1):1–6.
[15] Gendler E. Perforated demineralized bone matrix: a new form of osteoinductive biomaterial. J Biomed Mater Res 1986;20(6):687–97.
[16] Habibovic P, Yuan H, van der Valk CM, Meijer G, van Blitterswijk CA, de Groot K. 3D microenvironment as essential element for osteoinduction by biomaterials. Biomaterials 2005;26(17):3565–75.
[17] Park JW, Kim ES, Jang JH, Suh JY, Park KB, Hanawa T. Healing of rabbit calvarial bone defects using biphasic calcium phosphate ceramics made of submicron-sized grains with a hierarchical pore structure. Clin Oral Implants Res 2010;21(3):268–76.
[18] Walsh WR, Vizesi F, Michael D, Auld J, Langdown A, Oliver R, et al. Beta-TCP bone graft substitutes in a bilateral rabbit tibial defect model. Biomaterials 2008;29(3):266–71.
[19] Xu S, Li D, Wang C, Wang Z, Lu B. Cell proliferation in CPC scaffold with a central channel. Biomed Mater Eng 2007;17(1):1–8.
[20] Hallman M, Sennerby L, Lundgren S. A clinical and histologic evaluation of implant integration in the posterior maxilla after sinus floor augmentation with autogenous bone, bovine hydroxyapatite, or a 20:80 mixture. Int J Oral Maxillofac Implants 2002;17(5):635–43.
[21] Tamimi F, Torres J, Gbureck U, Lopez-Cabarcos E, Bassett DC, Alkhraisat MH, et al. Craniofacial vertical bone augmentation: a comparison between 3D printed monolithic monetite blocks and autologous onlay grafts in the rabbit. Biomaterials 2009;30(31):6318–26.
[22] Berding G, Burchert W, van den Hoff J, Pytlik C, Neukam FW, Meyer GJ, et al. Evaluation of the incorporation of bone grafts used in maxillofacial surgery with [18F]fluoride ion and dynamic positron emission tomography. Eur J Nucl Med 1995;22(10):1133–40.
[23] Piert M, Winter E, Becker GA, Bilger K, Machulla H, Muller-Schauenburg W, et al. Allogenic bone graft viability after hip revision arthroplasty assessed by dynamic [18F]fluoride ion positron emission tomography. Eur J Nucl Med 1999;26(6):615–24.
[24] Hsu WK, Feeley BT, Krenek L, Stout DB, Chatziioannou AF, Lieberman JR. The use of 18F-fluoride and 18F-FDG PET scans to assess fracture healing in a rat femur model. Eur J Nucl Med Mol Imaging 2007;34(8):1291–301.
[25] Even-Sapir E, Mishani E, Flusser G, Metser U. 18F-Fluoride positron emission tomography and positron emission tomography/computed tomography. Semin Nucl Med 2007;37(6):462–9.
[26] Gbureck U, Hölzel T, Klammert U, Würzler K, Müller FA, Barralet JE. Resorbable dicalcium phosphate bone substitutes prepared by 3D powder printing. Adv Funct Mater 2007;17(18):3940–5.
[27] Renka RJ, Cline AK. A triangle-based C1 interpolation method. Rocky Mt J Math 1984;14(1):223–37.
[28] McInnis JC, Robb RA, Kelly PJ. The relationship of bone blood flow, bone tracer deposition, and endosteal new bone formation. J Lab Clin Med 1980;96(3):511–22.
[29] Messa C, Goodman WG, Hoh CK, Choi Y, Nissenson AR, Salusky IB, et al. Bone metabolic activity measured with positron emission tomography and [18F] fluoride ion in renal osteodystrophy: correlation with bone histomorphometry. J Clin Endocrinol Metab 1993;77(4):949–55.
[30] von Doernberg MC, von Rechenberg B, Bohner M, Grunenfelder S, van Lenthe GH, Muller R, et al. In vivo behavior of calcium phosphate scaffolds with four different pore sizes. Biomaterials 2006;27(30):5186–98.
[31] Bose S, Roy M, Bandyopadhyay A. Recent advances in bone tissue engineering scaffolds. Trends Biotechnol 2012;30(10):546–54.
[32] Hulbert SF, Young FA, Mathews RS, Klawitter JJ, Talbert CD, Stelling FH. Potential of ceramic materials as permanently implantable skeletal prostheses. J Biomed Mater Res 1970;4(3):433–56.
[33] Dutta Roy T, Simon JL, Ricci JL, Rekow ED, Thompson VP, Parsons JR. Performance of hydroxyapatite bone repair scaffolds created via three-dimensional fabrication techniques. J Biomed Mater Res A 2003;67(4):1228–37.
[34] Yeo A, Wong WJ, Khoo HH, Teoh SH. Surface modification of PCL-TCP scaffolds improve interfacial mechanical interlock and enhance early bone formation: an in vitro and in vivo characterization. J Biomed Mater Res A 2010;92(1):311–21.
[35] Marino FT, Torres J, Tresguerres I, Jerez LB, Cabarcos EL. Vertical bone augmentation with granulated brushite cement set in glycolic acid. J Biomed Mater Res A 2007;81(1):93–102.
[36] Tamimi F, Torres J, Bassett D, Barralet J, Cabarcos EL. Resorption of monetite granules in alveolar bone defects in human patients. Biomaterials 2010;31(10):2762–9.
[37] Gosain AK, Gosain SA, Sweeney WM, Song LS, Amarante MT. Regulation of osteogenesis and survival within bone grafts to the calvaria: the effect of the dura versus the pericranium. Plast Reconstr Surg 2011;128(1):85–94.
[38] Tamura K, Sato S, Kishida M, Asano S, Murai M, Ito K. The use of porous beta-tricalcium phosphate blocks with platelet-rich plasma as an onlay bone graft biomaterial. J Periodontol 2007;78(2):315–21.
[39] Cawood JI, Howell RA. A classification of the edentulous jaws. Int J Oral Maxillofac Surg 1988;17(4):232–6.
[40] Stellingsma C, Vissink A, Meijer HJ, Kuiper C, Raghoebar GM. Implantology and the severely resorbed edentulous mandible. Crit Rev Oral Biol Med 2004;15(4):240–8.
[41] Hixson AW, Crowell JH. Dependence of reaction velocity upon surface and agitation. Ind Eng Chem 1931;23(8):923–31.
[42] Grossardt C, Ewald A, Grover LM, Barralet JE, Gbureck U. Passive and active in vitro resorption of calcium and magnesium phosphate cements by osteoclastic cells. Tissue Eng Part A 2010;16(12):3687–95.
[43] Albrektsson T, Jansson T, Lekholm U. Osseointegrated dental implants. Dent Clin North Am 1986;30(1):151–74.

Please cite this article in press as: Tamimi F, et al., Osseointegration of dental implants in 3D-printed synthetic onlay grafts customized according to bone metabolic activity in recipient site, Biomaterials (2014), http://dx.doi.org/10.1016/j.biomaterials.2014.03.050

ELSEVIER LICENSE
TERMS AND CONDITIONS

Apr 15, 2014

This is a License Agreement between khadijeh al-abedalla ("You") and Elsevier ("Elsevier") provided by Copyright Clearance Center ("CCC"). The license consists of your order details, the terms and conditions provided by Elsevier, and the payment terms and conditions.

All payments must be made in full to CCC. For payment instructions, please see information listed at the bottom of this form.

Supplier	Elsevier Limited The Boulevard,Langford Lane Kidlington,Oxford,OX5 1GB,UK
Registered Company Number	1982084
Customer name	khadijeh al-abedalla
Customer address	3512 Rue Durocher, apt 207 Montreal, QC H2X 2E6
License number	3370301390524
License date	Apr 15, 2014
Licensed content publisher	Elsevier
Licensed content publication	Biomaterials
Licensed content title	Osseointegration of dental implants in 3D-printed synthetic onlay grafts customized according to bone metabolic activity in recipient site
Licensed content author	Faleh Tamimi,Jesus Torres,Khadijeh Al-Abedalla,Enrique Lopez-Cabarcos,Mohammad H. Alkhraisat,David C. Bassett,Uwe Gbureck,Jake E. Barralet
Licensed content date	13 April 2014
Licensed content volume number	
Licensed content issue number	
Number of pages	1
Start Page	0
End Page	0
Type of Use	reuse in a thesis/dissertation
Portion	full article
Format	electronic
Are you the author of this Elsevier article?	Yes

Will you be translating?	No
Title of your thesis/dissertation	Onlay grafts for alveolar bone augmentation
Expected completion date	Apr 2014
Estimated size (number of pages)	130
Elsevier VAT number	GB 494 6272 12
Permissions price	0.00 USD
VAT/Local Sales Tax	0.00 USD / 0.00 GBP
Total	0.00 USD
Terms and Conditions	

INTRODUCTION

1. The publisher for this copyrighted material is Elsevier. Byclicking "accept" in connection with completing this licensingtransaction, you agree that the following terms and conditions apply to thistransaction (along with the Billing and Payment terms and conditionsestablished by Copyright Clearance Center, Inc. ("CCC"), at the timethat you opened your Rightslink account and that are available at any time at http://myaccount.copyright.com).

GENERAL TERMS

2. Elsevier hereby grants you permission to reproduce the aforementionedmaterial subject to the terms and conditions indicated.

3. Acknowledgement: If any part of the material to be used (for example,figures) has appeared in our publication with credit or acknowledgement toanother source, permission must also be sought from that source. If suchpermission is not obtained then that material may not be included in yourpublication/copies. Suitable acknowledgement to the source must be made, eitheras a footnote or in a reference list at the end of your publication, asfollows:

"Reprinted from Publication title, Vol /edition number, Author(s), Title ofarticle / title of chapter, Pages No., Copyright (Year), with permission fromElsevier [OR APPLICABLE SOCIETY COPYRIGHT OWNER]." Also Lancet special credit -"Reprinted from The Lancet, Vol. number, Author(s), Title of article, PagesNo., Copyright (Year), with permission from Elsevier."

4. Reproduction of this material is confined to the purpose and/or media forwhich permission is hereby given.

5. Altering/Modifying Material: Not Permitted. However figures andillustrations may be altered/adapted minimally to serve your work. Any otherabbreviations, additions, deletions and/or any other alterations shall be madeonly with prior written authorization of Elsevier Ltd. (Please contact Elsevierat permissions@elsevier.com)

6. If the permission fee for the requested use of our material is waived inthis instance, please be advised that your future requests for Elseviermaterials may attract a fee.

7. Reservation of Rights: Publisher reserves all rights not specificallygranted in the combination of (i) the license details provided by you andaccepted in the course of this licensing transaction, (ii) these terms andconditions and (iii) CCC's Billing and Payment terms and conditions.

8. License Contingent Upon Payment: While you may exercise the rightslicensed immediately upon issuance of the license at the end of the licensingprocess for the transaction, provided that you have disclosed complete andaccurate details of your proposed use, no license is finally effective unlessand until full payment is received from you (either by publisher or by CCC) asprovided in CCC's Billing and Payment terms and conditions. If fullpayment is not received on a timely basis, then any license preliminarilygranted shall be deemed automatically revoked and shall be void as if nevergranted. Further, in the event that you breach any of these terms andconditions or any of CCC's Billing and Payment terms and conditions, thelicense is automatically revoked and shall be void as if never granted. Use of materials as described in a revoked license, as well as any use of thematerials beyond the scope of an unrevoked license, may constitute copyrightinfringement and publisher reserves the right to take any and all action toprotect its copyright in the materials.

9. Warranties: Publisher makes no representations or warranties with respectto the licensed material.

10. Indemnity: You hereby indemnify and agree to hold harmless publisher andCCC, and their respective officers, directors, employees and agents, from andagainst any and all claims arising out of your use of the licensed materialother than as specifically authorized pursuant to this license.

11. No Transfer of License: This license is personal to you and may not besublicensed, assigned, or transferred by you to any other person withoutpublisher's written permission.

12. No Amendment Except in Writing: This license may not be amended exceptin a writing signed by both parties (or, in the case of publisher, by CCC onpublisher's behalf).

13. Objection to Contrary Terms: Publisher hereby objects to any termscontained in any purchase order, acknowledgment, check endorsement or otherwriting prepared by you, which terms are inconsistent with these terms andconditions or CCC's Billing and Payment terms and conditions. These termsand conditions, together with CCC's Billing and Payment terms and conditions(which are incorporated herein), comprise the entire agreement between you andpublisher (and CCC) concerning this licensing transaction. In the eventof any conflict between your obligations established by these terms andconditions and those established by CCC's Billing and Payment terms andconditions, these terms and conditions shall control.

14. Revocation: Elsevier or Copyright Clearance Center may deny thepermissions described in this License at their sole discretion, for any reasonor no reason, with a full refund payable to you. Notice of such denialwill be made using the contact information provided by you. Failure toreceive such notice will not alter or invalidate the denial. In no eventwill Elsevier or Copyright Clearance Center be responsible or liable for anycosts, expenses or damage incurred by you as a result of a denial of yourpermission request, other than a refund of the amount(s) paid by you toElsevier and/or Copyright Clearance Center for denied permissions.

LIMITED LICENSE

The following terms and conditions apply only to specific license types:

15. **Translation**: This permission is granted fornon-exclusive world **English** rights only unless yourlicense was granted for translation rights. If you licensed translation rightsyou may only translate this content into the languages you requested. Aprofessional translator must perform all translations and reproduce the contentword for word preserving the integrity of the article. If this license is tore-use 1 or 2 figures then permission is granted for non-exclusive world rightsin all languages.

16. **Posting licensed content on any Website**: The followingterms and conditions apply as follows: Licensing material from an Elsevierjournal: All content posted to the web site must maintain the copyright informationline on the bottom of each image; A hyper-text must be included to the Homepageof the journal from which you are licensing at http://www.sciencedirect.com/science/journal/xxxxx orthe Elsevier homepage for books at http://www.elsevier.com; CentralStorage: This license does not include permission for a scanned version of thematerial to be stored in a central repository such as that provided byHeron/XanEdu.

Licensing material from an Elsevier book: A hyper-text link must be includedto the Elsevier homepage at http://www.elsevier.com . Allcontent posted to the web site must maintain the copyright information line onthe bottom of each image.

Posting licensed content on Electronic reserve: In addition to the above the following clausesare applicable: The web site must be password-protected and made available onlyto bona fide students registered on a relevant course. This permission isgranted for 1 year only. You may obtain a new license for future websiteposting.

For journal authors: the following clauses are applicable inaddition to the above: Permission granted is limited to the author acceptedmanuscript version* of your paper.

***Accepted Author Manuscript (AAM) Definition:** An accepted authormanuscript (AAM) is the author's version of the manuscript of an article thathas been accepted for publication and which may include any author-incorporatedchanges suggested through the processes of submission processing, peer review,and editor-author communications. AAMs do not include other publishervalue-added contributions such as copy-editing, formatting, technicalenhancements and (if relevant) pagination.

You are not allowed to download and post the published journal article (whetherPDF or HTML, proof or final version), nor may you scan the printed edition tocreate an electronic version. A hyper-text must be included to the Homepage ofthe journal from which you are licensing at http://www.sciencedirect.com/science/journal/xxxxx. As part of our normal production process, you will receive an e-mail noticewhen your article appears on Elsevier's online service ScienceDirect(www.sciencedirect.com). That e-mail will include the article's Digital ObjectIdentifier (DOI). This number provides the electronic link to the publishedarticle and should be included in the posting of your personal version. We askthat you wait until you receive this e-mail and have the DOI to do any posting.

Posting to a repository: Authorsmay post their AAM immediately to their employer's institutional repository forinternal use only and may make their manuscript publically available after thejournal-

specific embargo period has ended.

Please also refer to Elsevier'sArticle Posting Policy for further information.

18. **For book authors** the following clauses are applicable in addition tothe above: Authors are permitted to place a briefsummary of their work online only.. You are notallowed to download and post the published electronic version of your chapter,nor may you scan the printed edition to create an electronic version. Posting to a repository: Authors arepermitted to post a summary of their chapter only in their institution'srepository.

20. **Thesis/Dissertation**: If your license is for use in athesis/dissertation your thesis may be submitted to your institution in eitherprint or electronic form. Should your thesis be published commercially, pleasereapply for permission. These requirements include permission for the Libraryand Archives of Canada to supply single copies, on demand, of the completethesis and include permission for UMI to supply single copies, on demand, ofthe complete thesis. Should your thesis be published commercially, pleasereapply for permission.

Elsevier Open Access Terms andConditions

Elsevier publishes Open Access articles in both its Open Access journals andvia its Open Access articles option in subscription journals.

Authors publishing in an Open Access journal or who choose to make theirarticle Open Access in an Elsevier subscription journal select one of thefollowing Creative Commons user licenses, which define how a reader may reusetheir work: Creative Commons Attribution License (CC BY), Creative CommonsAttribution – Non Commercial - ShareAlike (CC BY NCSA) and Creative Commons Attribution – Non Commercial – No Derivatives (CC BYNC ND)

Terms & Conditions applicable toall Elsevier Open Access articles:

Any reuse of the article must not represent the author as endorsing theadaptation of the article nor should the article be modified in such a way asto damage the author's honour or reputation.

The author(s) must be appropriately credited.

If any part of the material to be used (for example, figures) has appearedin our publication with credit or acknowledgement to another source it is theresponsibility of the user to ensure their reuse complies with the terms andconditions determined by the rights holder.

Additional Terms & Conditionsapplicable to each Creative Commons user license:

CC BY: You may distribute andcopy the article, create extracts, abstracts, and other revised versions,adaptations or derivative works of or from an article (such as a translation),to include in a collective work (such as an anthology), to text or data minethe article, including for commercial purposes without permission from Elsevier

CC BY NC SA: For non-commercialpurposes you may distribute and copy the article, create extracts, abstractsand other revised versions, adaptations or derivative works of or from anarticle (such as a translation), to include in a collective work (such as ananthology), to text and data mine the article and license new adaptations or creationsunder identical terms without permission from Elsevier

CC BY NC ND: For non-commercialpurposes you may distribute and copy the article and include it in a collectivework (such as an anthology), provided you do not alter or modify the article,without permission from Elsevier

Any commercial reuse of Open Access articles published with a CC BY NC SA or CC BY NC NDlicense requires permission from Elsevier and will be subject to a fee.

Commercial reuse includes:

- Promotional purposes (advertising or marketing)
- Commercial exploitation (e.g. a product forsale or loan)
- Systematic distribution (for a fee or free ofcharge)

Please refer to Elsevier'sOpen Access Policy for further information.

21. **Other Conditions**:

v1.7

If you would like to pay for this license now, please remit this license along with your payment made payable to "COPYRIGHT CLEARANCE CENTER" otherwise you will be invoiced within 48 hours of the license date. Payment should be in the form of a check or money order referencing your account number and this invoice number RLNK501278809. Once you receive your invoice for this order, you may pay your invoice by credit card. Please follow instructions provided at that time.

Make Payment To:
Copyright Clearance Center
Dept 001
P.O. Box 843006
Boston, MA 02284-3006

For suggestions or comments regarding this order, contact RightsLink Customer Support: customercare@copyright.com or +1-877-622-5543 (toll free in the US) or +1-978-646-2777.

Gratis licenses (referencing $0 in the Total field) are free. Please retain this printable license for your reference. No payment is required.